Functional analysis of multiple activities associated with the herpes simplex virus-1 DNA polymerase

Functional analysis of multiple activities associated with the herpes simplex virus-1 DNA polymerase

A dissertation presented

by

Jessica Leigh Lawler

to

The Division of Medical Sciences

in partial fulfillment of the requirements

for the degree of

Doctor of Philosophy

in the subject of

Virology

Harvard University

Cambridge, Massachusetts

March 2018

Dissertation Advisor: Dr. Donald M. Coen Jessica Leigh Lawler

Functional analysis of multiple activities associated
with the herpes simplex virus-1 DNA polymerase

Abstract

Of the DNA replication proteins required for herpes simplex virus-1 (HSV-1) viral replication, the catalytic subunit of the DNA polymerase (Pol) has been the most extensively studied, both as a model for Family B polymerases and as a successful antiviral target. Despite decades of work, however, there are still questions regarding the enzyme and its functions that have not been fully resolved, especially related to the RNase H activity, the 3'-5' exonuclease activity, and a putative RNA-binding motif with no defined activity. We set out to answer some of these questions and further define the activities associated with HSV Pol.

There has been a controversy regarding whether an RNase H activity intrinsic to HSV-1 Pol is due to the 3'-5' exonuclease of Pol or whether it is a separate activity, possibly acting on 5' RNA termini. We found that the RNase H activity of HSV Pol exclusively degrades RNA:DNA hybrids with 3' RNA ends, and that this activity is dependent upon the 3'-5' exonuclease active site. Next, we set out to study a 3'-5' exonuclease-deficient mutant that had been previously studied *in vitro* but not characterized in cell culture. We confirmed that this mutant was incapable of replicating in non-complementing cells and determined that this substitution severely affected expression of the protein during infection. Finally, we made substitutions within the putative RNA-binding (RNP) motif within the NH_2-terminal domain of

Pol. We identified that this mutant was incapable of viral replication and viral DNA synthesis, with no defects in expression, localization, or polymerase activity, suggesting that this motif plays a role in viral DNA synthesis separate from the polymerase activity.

Together, these data answered several unresolved questions related to the HSV-1 DNA polymerase and identified the RNP motif as crucial for viral DNA synthesis. Our results argue that the RNP motif's function during viral DNA synthesis is not a 5'-3' RNase H. Additionally, we were able to provide evidence that the defects in replication associated with a well-studied 3'-5' exonuclease mutant were due to expression and not the exonuclease per se.

Table of Contents

Acknowledgements

I would like to thank my parents, Kevin and Cheryl Lawler, my sister, Anna Lawler, my grandparents, Carolyn and Ray Dawson, my late grandparents, James and Anna Lawler, and my extended family too numerous to mention here. Their support, love, advice, and funny anecdotes have been invaluable for both making me the person that I am today and helping me continue to grow.

I would also like to thank my friends who have been there for me through this time from Dallas, Boston, and the Virology Program. We've shared a lot of good times, and their support has been important to me.

I would like to thank my advisor, Don Coen, for his guidance and support. The things I've learned from him, including scientific theory, experimental design, logical thinking, writing, etc. have been, and will continue to be, valuable tools both professionally and personally.

I would like to thank current and former Coen lab members for their support, advice, and friendship, especially Purba Mukherjee, Adrian Wilkie, Han Chen, Mayuri Sharma, and Jean Pesola for their mentorship.

I would like to thank the administrators of the Virology Program, the Division of Medical Sciences, and the Department of Biological Chemistry and Molecular Pharmacology, including Maria Bollinger, Lora Maurer, Bob Bridges, Lisa Rossini, Steve Obuchowski, David Cardozo, and Kristen Parker. They've always made themselves available whenever I've needed help.

I would like to thank my dissertation advisory committee members: Max Nibert (Chair), David Knipe, and Sean Whelan. Their advice and support have been immensely helpful.

I would also like to thank my fellow students and peers in the Virology Program, Immunology Program, BBS, and the Department of Biological Chemistry and Molecular Pharmacology. Their input, friendship, and support have given me many insights and helped to make me a better scientist.

Finally, I'd like to thank my defense committee, David Knipe (Chair), Frederick Wang, Samuel Rabkin, and Timothy Kowalik (University of Massachusetts Medical School) for their willingness to serve on the committee.

Attributions

Chapter 2. Primer/templates, substrates, and assays were designed in collaboration between Jessica Lawler and Purba Mukherjee, with hairpin design help from Han Chen. Purba Mukherjee helped optimize the baculovirus expression and protein purification protocols. Assays were run and data was analyzed by Jessica Lawler with some of the purified protein provided by Shariya Terrell. Jean Pesola helped with analysis using GraphPad Prism software. Charles Knopf generously provided the α-Pol mouse monoclonal 1051c antibody used in this study.

Chapter 3. Viruses were recombined and produced by Jessica Lawler, with troubleshooting help from Adrian Wilkie. Jessica Lawler ran and analyzed all assays. Jean Pesola helped troubleshoot and analyze qPCR assays and aided with statistical analyses. Han Chen and Jessica Lawler collaborated in optimizing the lysate polymerase assays. Charles Hwang generously provided the PolB3 cells used in this study. Additionally, William Summers kindly provided the α-TK goat polyclonal antibody, and Charles Knopf generously provided the α-Pol mouse monoclonal 1051c antibody used in this study.

Chapter 4. Mutations were designed by both Shariya Terrell and Jessica Lawler, and the viruses were recombined and produced by Jessica Lawler, with troubleshooting help from Adrian Wilkie. Jessica Lawler ran and analyzed all assays. Jean Pesola helped troubleshoot and analyze qPCR assays and aided with statistical analyses. Han Chen and Jessica Lawler collaborated in optimizing the lysate polymerase assays. Adrian Wilkie helped design and image the

immunofluorescence microscopy. Purba Mukherjee helped optimize the baculovirus expression and protein purification protocols. Charles Hwang generously provided the PolB3 cells used in this study. Additionally, William Summers kindly provided the α-TK goat polyclonal antibody, Charles Knopf generously provided the α-Pol mouse monoclonal 1051c antibody, and David Knipe kindly provided the α-ICP8 383 rabbit polyclonal used in this study. The Nikon Imaging Center at Harvard Medical School generously provided the equipment and assistance for the immunofluorescence microscopy.

Appendix C. Seamus McCarron located, propagated, and purified viral DNA from the temperature sensitive viruses in this study. Jessica Lawler and Seamus McCarron sequenced the viral DNA. Jessica Lawler compiled and analyzed the data.

Chapter 1

Introduction

DNA Replication

DNA replication is a fundamental process utilized across all organisms required to transfer the genetic material maintained as dsDNA to each divided cell with substantial fidelity. Copying DNA is a highly complicated process that requires numerous subprocesses, enzymes, and regulation to coordinate these components. Due to the stringent constraints and requirements associated with this process, many of the mechanisms used to effect DNA replication have a prominent level of conservation among different organisms. However, the regulation of these processes and the enzymes therein are variable based on the evolutionary constraints placed on different organisms (Kornberg & Baker, 1992; M. O'Donnell, Langston, & Stillman, 2013).

Overall, DNA replication requires a method and location for the initiation of the reaction, a helicase that can overcome the interactions holding the DNA strands together, a mechanism for generating RNA primers from which a catalytic DNA polymerase can copy the template DNA strand, a factor increasing the processivity of this reaction to keep the catalytic subunit from falling off of the DNA, a method for replacing the primers used to initiate the reaction with DNA, mechanisms to deal with potential DNA damage or incorporation errors, and a method for spatially and temporally regulating these multiple processes. Errors associated with any of these mechanisms can cause problems ranging from increased mutagenesis to cell death. Additionally, knowing the conserved and variable mechanisms used in DNA replication help us to determine the specific requirements for survival of different organisms and help to tease apart the processes that may be altered for either fixing or disrupting this essential activity (M. O'Donnell et al., 2013).

Viruses have long served as crucial models for learning more about the mechanisms of eukaryotic DNA replication (reviewed in Challberg & Kelly, 1982; M. O'Donnell et al., 2013). In general, viruses serve as relatively easily manipulatable systems that allow us to quickly and quantifiably detect effects on replication by assessing the ability of the virus to propagate in host cells. Also, since viruses generally require less regulation than their host and prioritize speed over fidelity, determining the crucial aspects of DNA replication is simpler than in most other systems. Furthermore, many viruses make use of cellular systems to replicate their own DNA, so identifying how the cellular environment changes can teach us much about these enzymes. As the similarities between viral and eukaryotic systems can teach us about the crucial aspects of DNA replication, the differences also inform us of the regulation of these mechanisms and how they have evolved to match the needs of the organism. For example, biochemical analysis of the core DNA replication machinery in eukaryotes was first identified based on the replication of SV40 DNA in human cell extracts (reviewed in Fanning & Zhao, 2009).

Despite extensive work over the decades since the identification of DNA as the primary genetic material, there are still many unanswered questions surrounding this process of copying DNA in general and in relation to specific organisms. In this dissertation, we have utilized the herpes simplex virus-1 (HSV-1) model of DNA replication. This system is ideal for the following studies for several reasons: 1) HSV-1 requires fewer components than most other DNA replication systems. 2) Origin-independent replication using a rolling circle mechanism has been reconstituted *in vitro*, making biochemical analysis of the crucial aspects of this system easier. 3) Herpesviruses encode their own replication machinery, allowing us to analyze differences from the eukaryotic components. 4) HSV-1 is the only virus that has been shown to utilize both leading and lagging strand synthesis using its own machinery. 5) The catalytic

subunit of the HSV-1 DNA polymerase has been the target of antiviral treatment, so the identification of novel functions may shed light on potential drug targets. 6) Genetic perturbation of this system using an available reverse genetic system and complementing cell lines has been a useful tool for identifying the contribution of different activities and mechanisms associated with DNA replication (reviewed in Weller & Coen, 2006, 2012).

In my dissertation work, I have tried to shed light on the mechanism by which HSV-1, and possibly other eukaryotic polymerases, removes RNA primers during lagging strand synthesis, clarify the importance of the 3'-5' exonuclease activity on viral DNA replication, and identify novel conserved functions that play important roles in DNA replication. Using the HSV-1 DNA polymerase as a model, I hoped to identify more crucial similarities and differences between this viral polymerase and homologous eukaryotic DNA polymerases that could be isolated either as a potential antiviral target or to increase our knowledge about conserved mechanisms of DNA replication.

Herpesviridae

Herpesviridae comprise a family of viruses that replicate their linear, double-stranded DNA (dsDNA) genomes within the nucleus of the host. The genome is encased within an icosahedral capsid coated in a separate protein layer known as tegument, and this structure is contained within a lipid bilayer envelope (reviewed in F. Liu & Zhou, 2007). Herpesviruses encode a substantial number of proteins that aid in all steps of viral replication, including nucleotide metabolism, viral DNA replication, packaging, release, etc. (Pellett & Roizman, 2013).

Despite many similarities in this family, the host cell range, specificity, efficiency, and rate of progression are all highly variable among human herpesviruses. To delineate some of these differences, three subfamilies of herpesviruses have been defined, known as the *alphaherpesvirinae* (including herpes simplex virus-1 (HSV-1 or HHV-1), herpes simplex virus-2 (HSV-2 or HHV-2), and varicella-zoster virus (VZV or HHV-3)), *betaherpesvirinae* (including human cytomegalovirus (HCMV or HHV-5) and roseoloviruses (HHV-6A, HHV-6B, or HHV-7)), and *gammaherpesvirinae* (Epstein-Barr virus (EBV or HHV-4) and Kaposi's sarcoma-associated herpesvirus (KSHV or HHV-8)) (Pellett & Roizman, 2013).

Herpesviruses are distinctive for their lytic and latent infection cycles, which occur in different cell types across the family. Whereas lytic infection releases progeny virions and propagates spread of the virus to new cells and hosts, latency restricts viral expression for all but a very small subset of genes and the virus is largely dormant, shutting off most replicative functions and allowing herpesviruses to establish lifelong infections. Upon reactivation, the lytic gene products are fully expressed, including the DNA replication machinery, triggering the production of virions, death of the infected cell, viral spread, and detectable symptoms in the host (reviewed in Grinde, 2013; Pellett & Roizman, 2013).

During lytic replication, herpesviruses cause significant alterations in cellular function and structure to facilitate their own replication. Upon infection, the cellular motor machinery is hijacked for transport of the viral DNA to the nucleus (Lyman & Enquist, 2009), and viral proteins almost immediately halt the transcription of all but a few cellular genes, creating an environment that prioritizes production of the viral machinery (Rivas, Schmaling, & Gaglia, 2016). The cytoskeleton of the host is significantly disrupted, with the cellular cytoskeleton and transport systems playing a large part in capsid transport and the reorganization of cellular and

viral components (Lyman & Enquist, 2009). Within the nucleus, striking nuclear structures known as replication compartments (RCs) are formed, which serve as the location of viral DNA replication, transcription, and packaging into capsids (Schmid, Speiseder, Dobner, & Gonzalez, 2014). Host proteins are widely redistributed, and some cellular proteins, including some of the cellular DNA-damage machinery, are recruited to the replication compartments (Tavalai & Stamminger, 2009; Weitzman & Weller, 2011; Xiaofei & Kowalik, 2014). Disruption of the nuclear lamina allows the packaged capsids to undergo egress from the nucleus to the cytoplasm (Lye, Wilkie, Filman, Hogle, & Coen, 2017). In the cytoplasm, more viral proteins (tegument) interact with the capsid and the virion goes through the final packaging steps for envelopment and budding from the host membrane (Henaff, Radtke, & Lippe, 2012; Mettenleiter, 2002).

To correctly time and efficiently structure the steps required for viral replication, herpesviruses have generated a tiered temporal system for the expression of virally-encoded genes during infection (Pellett & Roizman, 2013). The first genes expressed during infection are known as the immediate-early (IE or α) genes. These genes mainly serve roles associated with host transcriptional shutoff, inhibition of the host antiviral immune machinery, and initiation of the next round of viral gene expression, the early (E or β) genes. Early genes mainly encode the viral proteins required for viral DNA replication, and viral DNA synthesis activates the late genes through a mechanism that is still unknown. Additionally, expression of a gene class known as the leaky late (γ1) genes occurs at low levels early and then at elevated levels at late times post infection through a mechanism that is also unknown. The "true" late (L or γ2) genes that are expressed following the start of viral DNA replication encode proteins required for assembly, packaging, and egress of the virus. Furthermore, inhibition of any of these gene classes will inhibit expression of the subsequent gene classes.

Herpesviruses are known to cause morbidity and mortality in humans, particularly in immunocompromised individuals and infants (reviewed in Roizman, Knipe, & Whitley, 2013; Whitley, Kimberlin, & Prober, 2007). The diseases caused by herpesviruses include but are not limited to cold sores, genital herpes, lymphomas, pneumonia, meningitis, encephalitis, chickenpox, shingles, roseola, hepatitis, and Karposi's sarcoma. The generation of antivirals has served to lessen the burden of some of these viruses. Most of these drugs are nucleoside analogs when in phosphorylated form target the catalytic subunit of the viral DNA polymerase. However, poor efficacy, the appearance of resistance mutations, and significant side effects associated with these drugs have prompted attempts to identify novel viral targets and compounds that could be used separately or in combination with the current therapies (reviewed in Coen & Schaffer, 2003; Villarreal, 2003). The catalytic subunit of the DNA polymerase contains multiple regions outside of the polymerase active site that show strong conservation across human herpesviruses. Some of these regions of conservation lie in the NH_2-terminal domain and 3'-5' exonuclease domain, which are structurally conserved among many Family B polymerases but have few stretches of sequence conservation, suggesting that antivirals targeting these domains may have efficacy in several human herpesviruses with fewer side effects on cellular polymerases.

Herpesviruses have also proved to be a valuable tool for learning about basic cellular functions. Many of the replication proteins encoded by herpesviruses, including the catalytic subunit of the DNA polymerase, are conserved and serve as functional homologs for the human DNA replication machinery (Boehmer & Lehman, 1997; Mocarski Jr, 2007; Weller & Coen, 2012). The viral DNA replication machinery requires fewer components and is significantly less complicated than eukaryotic DNA replication, so it serves as a useful model to learn more about

the basic mechanisms of DNA replication involved in other species as well as specific differences. Furthermore, DNA polymerases encoded by herpesviruses are classified within the Family B polymerases that share substantial structural homology among a wide range of species. So, determining more about this enzyme is informative for framing future research on polymerases from other species and their functions.

Herpes Simplex Virus-1

Health Significance

Herpes simplex virus-1 (HSV-1) is an infectious virus that is highly prevalent throughout the world. Most of these infections are transmitted by oral-oral contact, and lytic infection generally causes symptoms of orolabial herpes, or "cold sores," but genital infections also occur (Roizman et al., 2013). HSV-1 infections tend to occur during childhood, and, due to the establishment of latency in the host, this infection is never cleared. Reactivation can lead to viral shedding, either symptomatically or asymptomatically, which leads to transmission of the virus. Occasionally, serious complications such as encephalitis can occur, especially in the immunocompromised patients such as neonates, transplant patients, HIV-infected individuals, etc. (reviewed in Roizman et al., 2013; Wald & Corey, 2007).

Most of the antivirals developed and all of the drugs approved for the treatment of HSV-1 infection have targeted the viral DNA polymerase. The three main classes of drugs that have shown efficacy against HSV-1 are acyclic guanosine analogues (acyclovir (approved for treatment), ganciclovir, valaciclovir (approved for treatment), valganciclovir, and famciclovir (approved for treatment)), acyclic nucleotide analogues (cifofovir and adefovir dipivoxil), and pyrophosphate analogues (foscarnet (approved for treatment)) (reviewed in Coen, 2009; Y. C.

Jiang, Feng, Lin, & Guo, 2016; Weller & Coen, 2006). Nucleoside analogues are selectively phosphorylated by the viral thymidine kinase (TK) in infected cells, and this monophosphate derivative of the drug can be further phosphorylated by cellular kinases to the diphosphate and triphosphate (TP) active derivative. The triphosphate derivative of the drug is a competitive viral DNA polymerase inhibitor, and ACV-TP has been shown to be incorporated into replicating viral DNA and terminate the reaction due to the absence of a 3' hydroxyl (De Clercq, 2008; De Clercq & Holy, 2005; Gilbert, Bestman-Smith, & Boivin, 2002).

Despite the successes associated with these drugs, several drawbacks have also limited their use, including limited potency, limited efficacy, and the development of resistance mutations within immunocompromised patients (Gilbert et al., 2002; Piret & Boivin, 2011). So, recent efforts have focused primarily on discovering novel druggable targets in viral proteins for antivirals that can be used in combination or separately from the currently-available treatments (reviewed in Y. C. Jiang et al., 2016), such as the helicase/primase complex (Weller & Kuchta, 2013), the terminase complex (Heming, Huffman, Jones, & Homa, 2014), and the nuclear egress complex (Bigalke, Heuser, Nicastro, & Heldwein, 2014). As described later in the introduction, there are subtle differences between the structures and functions of the HSV-1 catalytic subunit of the DNA polymerase and eukaryotic polymerases that may be utilized in the design of novel potent inhibitors targeting crucial steps in viral DNA synthesis.

General Information

HSV-1 is a member of the alphaherpesviruses, known for their wide range of permissive host cells, shorter replication cycle, latent infection primarily within sensory ganglia, and efficient replication and spread in cell culture (Pellett & Roizman, 2013). The HSV-1 virion is a spherical particle ~190 nm in diameter containing a 152 kb linear dsDNA genome, icosahedral

capsid consisting of 162 viral capsomers, a highly variable and unstructured viral protein layer known as tegument, and a lipid envelope including as many as 13 distinct viral glycoproteins (Haarr & Skulstad, 1994; Roizman et al., 2013). There is fairly limited sequence diversity among HSV isolates, and there is evidence of high levels of recombination associated with HSV-1 genome evolution, suggesting that this recombination is decreasing genetic diversity (Roizman et al., 2013). Viral DNA recombination is associated with DNA replication and is stimulated by UL12 through the cellular single strand annealing pathway and a single-stranded DNA binding protein (Schumacher et al., 2012; Wilkinson & Weller, 2003).

Remodeling of the Infected Cell Nucleus

Upon infection, HSV-1 causes quick and dramatic changes within the nucleus of infected cells, including but not limited to: mitigating host innate immune systems, controlling histone deposition and modification on HSV-1 genomes, recruitment of host DNA damage machinery, the formation and merging of replication compartments, marginalization of the host chromatin, modifications to the nucleolus, and disruption of the nuclear lamina (Roizman et al., 2013). Upon entry into the nucleus, complexes containing the immediate early proteins can be detected on viral genomes (Everett & Murray, 2005) and the viral genome is populated with nucleosomes (reviewed in Placek & Berger, 2010). PML and ND10 components are recruited adjacent to the viral genomes at the sites containing the immediate early protein ICP4 (Everett & Murray, 2005), and another immediate early protein, a ubiquitin ligase, ICP0, degrades some ND10 proteins that could potentially silence viral transcription and DNA synthesis (Chelbi-Alix & de The, 1999; Everett et al., 1998; Gu & Roizman, 2003). Additionally, all of the immediate early proteins with the exception of US12 (ICP0, ICP4, ICP22, ICP27, and US1.5) are crucial for initiating translation of the early proteins within the nucleus. Early proteins required for viral DNA

synthesis, including single-stranded DNA-binding protein (SSB) ICP8, followed by UL8, UL5, and UL52 (the helicase/primase complex), the processivity subunit UL42, and the catalytic subunit of the DNA polymerase, Pol, localize to multiple punctate foci termed prereplicative sites adjacent to the ICP4 nucleoprotein complexes (Liptak, Uprichard, & Knipe, 1996; Livingston, DeLuca, Wilkinson, & Weller, 2008; Lukonis & Weller, 1997). ICP8 localization has generally been used as a marker to detect prereplicative sites and replication compartments within infected nuclei.

Some of the cellular DNA damage machinery is recruited to these prereplicative sites and others are degraded in a complicated balancing act to control cell cycle progression, genome silencing, and apoptosis, while also mediating viral DNA synthesis, processing, recombination, and repair (Everett, 2006; Lilley, Chaurushiya, & Weitzman, 2010; Weitzman & Weller, 2011; Weller, 2010; Wilkinson & Weller, 2003; Xiaofei & Kowalik, 2014). Additionally, host proteins associated with the protein quality control machinery, including molecular chaperone proteins and components of the 20s proteasome, are recruited to separate virus-induced chaperone-enriched (VICE) domains adjacent to the ICP4 nucleoprotein complexes and prereplicative sites (reviewed in Livingston, Ifrim, Cowan, & Weller, 2009; Weller, 2010).

Later, during times of active DNA replication, these prereplicative sites enlarge and merge to form much larger replication compartments, which occupy a majority of the nuclear space and marginalize host chromatin towards the exterior of the nucleus (de Bruyn Kops & Knipe, 1988; de Bruyn Kops, Uprichard, Chen, & Knipe, 1998; Liptak et al., 1996; Monier, Armas, Etteldorf, Ghazal, & Sullivan, 2000; Simpson-Holley, Colgrove, Nalepa, Harper, & Knipe, 2005; Taylor, McNamee, Day, & Knipe, 2003). Transcription of late genes, DNA replication, capsid packaging, and termination are thought to occur on replication compartments.

However, upon inhibition of viral DNA synthesis through any number of mechanisms including DNA synthesis inhibitor treatment and infection with a replication protein-null virus, these large replication compartments either break up into small, punctate structures resembling prereplicative sites or never merge into the large structures, depending on the nature of the inhibition (Liptak et al., 1996; Lukonis & Weller, 1996; Quinlan, Chen, & Knipe, 1984). The exact mechanisms and interactions forming and holding these structures in place are so far unclear, but they serve as a solid indicator for active viral DNA synthesis during infection.

Initiation of Viral DNA Replication

The HSV-1 genome is both large (152 kb) and complex, containing two unique sequences flanked by inverted repeats and a high GC-content (68%) (Kieff, Bachenheimer, & Roizman, 1971; Roizman et al., 2013; Wadsworth, Hayward, & Roizman, 1976). Upon entry into the nucleus, the linear genome is circularized (Garber, Beverley, & Coen, 1993; Poffenberger & Roizman, 1985; Strang & Stow, 2005), and though an origin of replication is required for the initiation of viral DNA synthesis, there is eventually a switch to an origin-independent mechanism (Blumel & Matz, 1995; Chattopadhyay & Weller, 2006; Skaliter & Lehman, 1994). HSV-1 requires seven virally-encoded proteins to effect DNA replication: the origin-binding protein (UL9), the single-stranded DNA binding protein (ICP8), the helicase-primase complex (UL5, UL8, and UL52), and the DNA polymerase holoenzyme (the catalytic subunit UL30 (Pol) and processivity factor UL42) (McGeoch et al., 1988; Wu, Nelson, McGeoch, & Challberg, 1988). These viral proteins all colocalize at replication compartments by 3 hours post infection (hpi) and reach peak expression at the time of peak viral DNA synthesis around 6-12 hours post infection (Liptak et al., 1996; Roizman et al., 2013).

There are three origins of replication present within the HSV-1 genome, all within the promoter-regulatory regions of transcribed genes. Two, both known as OriS, are present within a repeated region, and the third, OriL, within the unique long (UL) region (Stow, 1982; Weller et al., 1985). All three of these sites contain an A/T-rich region to stimulate dsDNA melting and helicase and SSB binding, surrounded by recognition sites for the origin-binding protein, UL9, and contain palindromes that could potentially form hairpins (Elias & Lehman, 1988; He & Lehman, 2001; Makhov, Boehmer, Lehman, & Griffith, 1996). It is thought that a UL9 dimer interacts with these binding sites and ICP8, the single-stranded DNA (ssDNA) binding protein (Boehmer & Lehman, 1993a, 1993b; Makhov et al., 1996), causing large conformational changes that separate the DNA strands for binding by ICP8 and recruitment of the helicase/primase (H/P) complex (Aslani, Olsson, & Elias, 2002; Macao, Olsson, & Elias, 2004; Olsson et al., 2009). ICP8 (the SSB) has been shown to form filaments *in vitro* (Darwish, Grady, Bai, & Weller, 2015*)*, cooperatively binds ssDNA (Lee & Knipe, 1985; Ruyechan & Weir, 1984), and is important for stimulation of the polymerase activity (Hernandez & Lehman, 1990; Ruyechan & Weir, 1984).

The heterotrimeric H/P complex is recruited to unwind the DNA genome and synthesize short RNA primers about 8-13 nucleotides in length for the initiation of DNA replication (Cavanaugh & Kuchta, 2009; Crute & Lehman, 1991; Crute, Mocarski, & Lehman, 1988; Crute et al., 1989). UL5 and UL52 exhibit the helicase and primase activities crucial for DNA replication (Dracheva, Koonin, & Crute, 1995; Klinedinst & Challberg, 1994; L. A. Zhu & Weller, 1992a, 1992b). The third subunit, UL8, has not been shown to exhibit any catalytic activity but is necessary for recruitment and stimulation of the H/P complex *in vitro* (Barnard, Brown, & Stow, 1997; Marsden et al., 1996; Tanguy Le Gac, Villani, Hoffmann, & Boehmer,

1996; Tenney, Hurlburt, Micheletti, Bifano, & Hamatake, 1994; Tenney, Sheaffer, Hurlburt, Bifano, & Hamatake, 1995). UL8 also interacts with UL9, forms a strong interaction with the single-stranded binding protein, ICP8, and stimulates helicase DNA unwinding (Falkenberg, Bushnell, Elias, & Lehman, 1997; Hamatake, Bifano, Hurlburt, & Tenney, 1997; McLean, Abbotts, Parry, Marsden, & Stow, 1994; Sherman, Gottlieb, & Challberg, 1992; Tanguy Le Gac et al., 1996; Tenney et al., 1994), suggesting that it may play a role in recruitment of the components of the HSV-1 replication fork.

The last viral DNA replication proteins to be recruited are the components of the DNA polymerase, including the catalytic subunit (Pol) and the processivity subunit (UL42) (Liptak et al., 1996). The specific interactions and mechanisms mediating this recruitment are unclear, though a tentative interaction between Pol and UL8 of the H/P complex *in vitro* has been reported (Marsden et al., 1996), and an active primase is required for Pol recruitment (Carrington-Lawrence & Weller, 2003).

UL42, the processivity subunit, is a structural homologue to processivity subunits in other species (Zuccola, Filman, Coen, & Hogle, 2000), namely T4 bacteriophage gp45 (Jarvis, Paul, Hockensmith, & von Hippel, 1989), E. coli Pol III β subunit (Kong, Onrust, O'Donnell, & Kuriyan, 1992), and the eukaryotic proliferating cell nuclear antigen (PCNA) (Krishna, Kong, Gary, Burgers, & Kuriyan, 1994). However, unlike the other proteins listed, UL42 acts as a monomer (Randell & Coen, 2004), forming an interaction with the C-terminus UL30 on one face and an association with DNA on the opposite face (Komazin-Meredith, Santos, et al., 2008; Randell, Komazin, Jiang, Hwang, & Coen, 2005; Zuccola et al., 2000). In contrast to other processivity factors, UL42 has been shown to interact with and hop on DNA (Digard, Chow, Pirrit, & Coen, 1993; Komazin-Meredith, Mirchev, Golan, van Oijen, & Coen, 2008; Komazin-

Meredith, Santos, et al., 2008). UL42 plays crucial roles in viral replication, DNA synthesis, fidelity, and processivity of HSV Pol (Gottlieb, Marcy, Coen, & Challberg, 1990; Hernandez & Lehman, 1990; C. Jiang, Hwang, Randell, Coen, & Hwang, 2007; C. Jiang, Hwang, Wang, et al., 2007; Randell et al., 2005). This increase in processivity has also shown to stimulate HSV Pol-mediated strand displacement synthesis *in vitro* (Y. Zhu, Trego, Song, & Parris, 2003).

Viral DNA Synthesis

HSV-1 DNA replication is thought to initiate through a θ structure and elongate through a rolling circle, recombinational, or some combination of both mechanisms, producing head-to-tail concatemers of the full-length viral genome (Jacob, Morse, & Roizman, 1979). While circular, endless DNA is present until very late stages of DNA replication that suggests a rolling circle mechanism of DNA replication (Becker, Asher, Friedmann, & Kessler, 1978; Davison & Wilkie, 1983; Jacob et al., 1979; Jacob & Roizman, 1977; Jongeneel & Bachenheimer, 1981; Poffenberger & Roizman, 1985), extensive loops, forks, ssDNA, and branched structures have been observed that suggest more complex replication forks and recombination intermediates are present during infection (Friedmann, Shlomai, & Becker, 1977; Hirsch, Cabral, Patterson, & Biswal, 1977; Severini, Scraba, & Tyrrell, 1996; Shlomai, Friedmann, & Becker, 1976). The viral genome concatemers are cleaved upon encapsidation by the terminase complex (Homa & Brown, 1997; Lamberti & Weller, 1998; Salmon & Baines, 1998) by recognition of a packaging sequence (Spaete & Frenkel, 1982; Stow, McMonagle, & Davison, 1983), producing linear dsDNA genomes packaged into capsids for egress to the cytoplasm.

Origin-independent rolling circle replication has been replicated *in vitro* using the HSV-1 replication machinery. The first reported instance showed HSV-1 infected Vero cell lysates could reconstitute DNA synthesis *in vitro* on a preformed replication fork formed from a nicked,

circular dsDNA molecule with a 5' ssDNA tail (Rabkin & Hanlon, 1990). The next study utilized extracts from baculovirus-infected insect cells, characterizing the sufficient viral replication enzymes for rolling circle replication and showing that rolling circle replication was inhibited in the presence of the HSV-1 origin of replication and the origin binding protein (Skaliter & Lehman, 1994). Then, the authors showed that semiconservative rolling circle amplification was possible on circular plasmids lacking the HSV-1 origin of replication with infected 293T cell lysates (Skaliter, Makhov, Griffith, & Lehman, 1996). *In vitro* reconstituted rolling circle amplification was not detected in the absence of mock-infected cell lysates, though, suggesting that a cellular factor is required in this reaction (Skaliter & Lehman, 1994). Whether this cellular factor aids in initiation, lagging strand synthesis, the transition from θ to rolling circle amplification, or another aspect of viral DNA replication is unclear.

HSV-1 replication has been shown to utilize both leading and lagging strand DNA replication *in vitro* on minicircle templates (Falkenberg, Lehman, & Elias, 2000; Stengel & Kuchta, 2011), and "trombone" and ssDNA intermediate structures have been visualized by electron microscopy analysis during replication of these templates (Bermek, Willcox, & Griffith, 2015). The length and comparable efficiency of the strands and the conditions required to visualize effective lagging strand synthesis, including the magnesium concentration and necessity of the single-stranded DNA binding protein ICP8, were variable among the three of these assays, though. The presence of ICP8 was stimulatory for lagging strand synthesis in general, improving the efficiency to match that of the leading strand, and high concentrations of the H/P complex and of magnesium or magnesium acetate also improved the rate of coordinated synthesis (Bermek et al., 2015; Stengel & Kuchta, 2011). In all cases, leading and lagging strand synthesis were linked, and the recruitment of multiple H/P complexes for the activation of

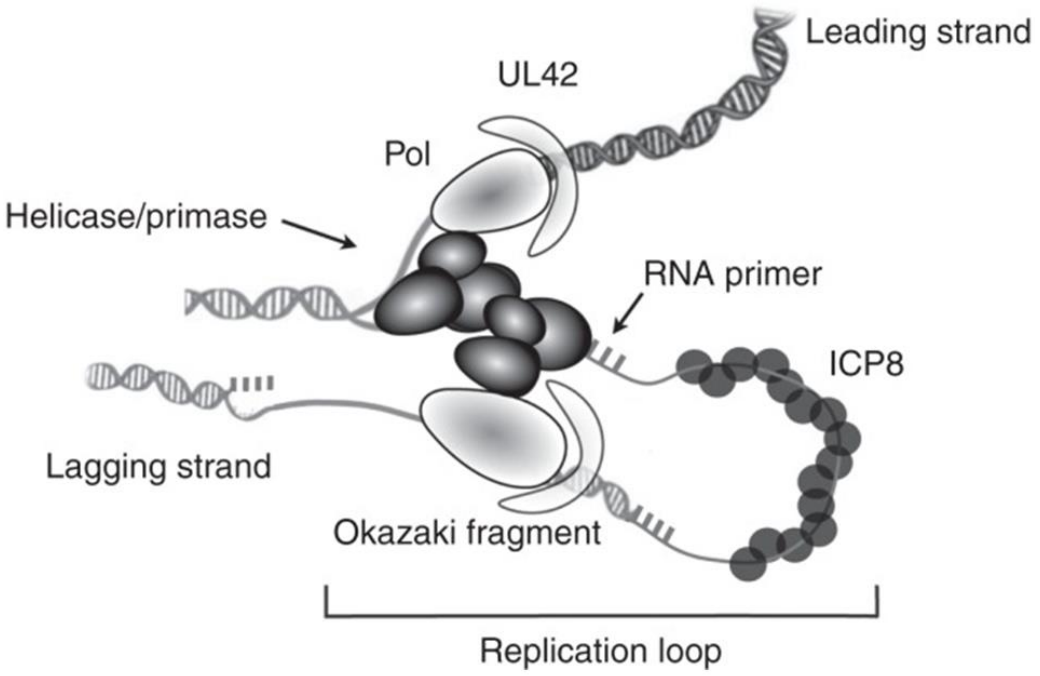

Figure 1.1. Model of coupled leading and lagging strand synthesis during HSV-1 DNA replication and organization of the replication fork (Weller & Coen, 2012). Each of the required viral proteins for origin-independent minicircle replication *in vitro* are shown and labeled, with the leading and lagging strands labeled and RNA primers shown as hatched lines.

primase activity is preferred (Y. Chen et al., 2011), suggesting a mechanism where coupled leading and lagging strand synthesis forms a loop aligning both strands (Figure 1.1) (Weller & Coen, 2012). Whereas coordinated leading and lagging strand synthesis has been shown to be stimulated by ICP8 (Bermek et al., 2015; Stengel & Kuchta, 2011), strand displacement synthesis is not stimulated by this protein *in vitro* (Y. Zhu et al., 2003), a finding that differs from other SSB-polymerase combinations (Fuentes, Rodriguez-Rodriguez, Palaniappan, Fay, & Bambara, 1996; Kornberg & Baker, 1992).

HSV-1 also encodes a thymidine kinase (TK), ribonucleotide reductase (RR), uracil DNA glycosylase (UDG), deoxyuridine triphosphatase (dUTPase), and an alkaline nuclease that are not essential for viral replication in cell culture but play auxiliary roles in viral DNA replication. TK (UL23) can phosphorylate nucleosides to create deoxynucleotide triphosphates (dNTPs) for incorporation by the 5'-3' polymerase activity of HSV Pol (Brown et al., 1995; M. S. Chen, Summers, Walker, Summers, & Prusoff, 1979). The RR (UL39 and UL40) is also associated with dNTP metabolism and increases the pool of dNTPs available for use during DNA synthesis (Averett, Lubbers, Elion, & Spector, 1983; Huszar & Bacchetti, 1981; Ponce de Leon, Eisenberg, & Cohen, 1977). The UDG (UL2) catalyzes the removal of misincorporated uracil from DNA, forming an abasic site that can be repaired by either the viral or cellular base excision repair (BER) pathways (Caradonna & Cheng, 1981). The dUTPase (UL50) hydrolyzes dUTP to dUMP and pyrophosphate, reducing the presence of uracil that can be incorporated and generating a nucleotide precursor (Bjornberg et al., 1993; Caradonna & Adamkiewicz, 1984; Kornberg & Baker, 1992; Williams, 1984). Finally, UL12, the alkaline nuclease, is predicted to stimulate recombination, act as a recombinase that resolves branched structures formed during DNA replication and recombination, and interacts with the host DNA repair machinery

(Balasubramanian, Bai, Buchek, Korza, & Weller, 2010; Goldstein & Weller, 1998; Schumacher et al., 2012).

Despite decades of work and the small number of proteins directly involved in HSV-1 DNA replication, it has become clear that there is still much to uncover about the mechanisms of DNA synthesis. HSV-1 displays intricacy in the timing and control of the expression, function, and localization of both viral and cellular components within the host, and it has become clear that HSV-1 DNA replication is more complicated than was originally thought.

Leading and Lagging Strand Synthesis

The current model of HSV-1 DNA synthesis features a "trombone" structure at the replication fork with coordinated leading and lagging strand synthesis occurring on either strand; this model is also predicted for prokaryotes and eukaryotes (Alberts et al., 1983; Pandey et al., 2009). Whereas leading strand synthesis can proceed continuously in the 5'-3' direction at the replication fork with a single RNA primer to begin the highly processive reaction, lagging strand synthesis is discontinuous and requires the synthesis of short, temporary RNA primers annealed to the template DNA from which 5'-3' DNA polymerization can initiate (Hubscher, Maga, & Spadari, 2002; Kornberg & Baker, 1992). These shorter polymerized fragments between RNA primers complementary to the lagging strand are termed Okazaki fragments (R. Okazaki, Okazaki, Sakabe, Sugimoto, & Sugino, 1968; Sakabe & Okazaki, 1966). RNA primers produced by the H/P complex must be removed and replaced with a gap-filling DNA synthesis reaction and ligation for the completion of DNA replication (Balakrishnan & Bambara, 2013). So far, it is unclear how HSV-1 removes RNA primers for the completion of lagging strand DNA

replication. Potential mechanisms of RNA primer removal and supporting evidence for these mechanisms in HSV-1 are discussed below.

Okazaki Fragment Maturation in Prokaryotes

A simple method for removing RNA primers is utilized by prokaryotes, as modeled by *E. coli* (Kornberg & Baker, 1992). *E. coli* Pol I has been shown to contain an intrinsic 5'-3' RNase H activity, and the organism also encodes two cellular RNase H proteins, RNase H1 and H2 (reviewed in Tadokoro & Kanaya, 2009). While neither of the separate RNase H enzymes are required for cellular viability (Itaya et al., 1999), loss of RNase H1 causes initiation at sites other than the replication initiation site (Hong & Kogoma, 1993). A Pol I mutant retaining its 5'-3' RNase H activity but lacking polymerase activity, on the other hand, exhibited accumulation of Okazaki fragments but was still viable (De Lucia & Cairns, 1969; T. Okazaki, 2002). Additionally, Pol I mutants lacking 5'-3' RNase H activity at high temperature (Kornberg & Baker, 1992) or lacking the entire Pol I enzyme (Fukushima, Itaya, Kato, Ogasawara, & Yoshikawa, 2007) were both inviable, suggesting that the RNase H associated with Pol I is crucial for replication.

Pol I can bind to RNA:DNA and use its 5'-3' RNase H activity to remove RNA primers during synthesis of a replication fork *in vitro*. This allows Pol I to complete maturation of the Okazaki strand without requiring a separate nuclease and leaves a nick that can be ligated by DNA ligase I (Kornberg & Baker, 1992). Since HSV-1 DNA replication is innately simpler and requires fewer components than eukaryotic DNA replication, and HSV Pol contains an RNase H activity (discussed later), it has been suggested that herpesviruses may utilize a mechanism like *E. coli* for Okazaki fragment maturation, whereby a 5'-3' RNase H associated with HSV Pol removes RNA primers.

Okazaki Fragment Maturation in Eukaryotes

Eukaryotic RNA primer removal has been best characterized in the *Saccharomyces cerevisiae* system so far (reviewed in Balakrishnan & Bambara, 2013; Zheng & Shen, 2011). Eukaryotes utilize a mechanism for completing lagging strand synthesis that requires two separate polymerases. The first, Pol α, binds to the RNA primer and begins 5'-3' polymerization on the Okazaki fragment (Lehman & Kaguni, 1989). Pol α is error-prone and not highly processive, though, so it quickly dissociates from the lagging strand to be replaced by Pol δ. Pol δ is more processive and exhibits higher fidelity than Pol α and is utilized to complete extension of the daughter strand on the Okazaki fragment (Jin, Ayyagari, Resnick, Gordenin, & Burgers, 2003; Maga et al., 2001). After reaching the subsequent RNA primer, Pol δ goes through rounds of idling (switching between the 3'-5' exonuclease and the 5'-3' polymerase active sites) until the polymerase successfully proceeds with strand displacement synthesis to the end of the RNA primer (Koc, Stodola, Burgers, & Galletto, 2015). This process generates a 5' displaced "flap" that is removed through recruitment of a separate cellular endonuclease.

Eukaryotes have developed several complementary processes for the removal of the RNA "flap". The displaced RNA strand is removed through successively shorter 5' flap cleavages by Fen1 or through longer flap removal by Dna2 and Pif1, and the nicked dsDNA is ligated by DNA ligase I (Ayyagari, Gomes, Gordenin, & Burgers, 2003; Maga et al., 2001). An exonuclease-deficient HSV Pol mutant has been shown to stimulate strand displacement synthesis and produce 5' "flaps" that can be processed by human Fen1 and ligated *in vitro* (Y. Zhu et al., 2003; Y. Zhu, Wu, Cardoso, & Parris, 2010). Similarly, Pol δ has been shown to have a more processive strand displacement activity when the 3'-5' exonuclease domain is inactive (Jin et al., 2003). Additionally, HSV Pol strand displacement synthesis, like Pol δ, is stimulated

through interactions with its processivity factor (Jin et al., 2003; Y. Zhu et al., 2003). However, unlike Pol δ, HSV Pol strand displacement synthesis is not stimulated by the addition of the single-stranded DNA binding protein (SSB) (Maga et al., 2001; Y. Zhu et al., 2003).

Prior to the studies carried out in this dissertation, there were still many questions regarding the method used by HSV-1 for the removal of RNA primers during lagging strand synthesis. So, we were interested in identifying whether the RNase H activity associated with HSV Pol could degrade RNA:DNA in a 5'-3' direction, as this would aid in determining whether HSV-1 utilizes a mechanism like Pol I for degrading RNA primers or may require a separate viral or cellular nuclease to perform this activity.

The Catalytic Subunit of the HSV-1 DNA Polymerase (HSV Pol)

Structure

The catalytic subunit of the HSV-1 DNA Polymerase (Pol) is a large (~135kD) protein classified within the Family B polymerases (C. W. Knopf & Weisshart, 1988; S. Liu et al., 2006; T. S. Wang, Wong, & Korn, 1989). The Family B polymerases encompass a large number of polymerases from a wide range of species including: eukaryotic polymerases Pol α, δ, and ε (Doublie & Zahn, 2014); prokaryotic *E. coli* Pol II (Iwasaki, Ishino, Toh, Nakata, & Shinagawa, 1991); bacteriophage RB69 and T4 Pol (Spicer et al., 1988; Xia & Konigsberg, 2014); and archaeal *Thermococcus gorgonarius* (Tgo) Pol (Jozwiakowski, Keith, Gilroy, Doherty, & Connolly, 2014). The crystal structure of HSV Pol has been solved, and this protein contains four domains: the pre-NH_2-terminal domain, NH_2-terminal domain, 3'-5' exonuclease domain, and the polymerase domain, composed of the palm, finger, and thumb subdomains (Figure 1.2) (S. Liu et al., 2006). Despite sharing limited stretches of high sequence homology with other

Family B polymerases, HSV Pol has a very similar structural architecture overall, forming a disk-like structure where, based on crystal structures of other Family B polymerases bound to primer-template (Swan, Johnson, Prakash, Prakash, & Aggarwal, 2009; J. Wang et al., 1997), dsDNA binds near the C-terminus and threads ssDNA through the center hole towards the N-terminus (S. Liu et al., 2006; J. Wang et al., 1997). In the well-documented structure of the RB69 Pol, an HSV Pol homologue, three different grooves have been identified within this disk structure: The first groove is between the NH_2-terminal and exonuclease domains and has a basic surface that interacts with the ssDNA strand. The second forms the exonuclease active site and binds the unwound primer strand; this groove lies between the exonuclease domain and the tip of the thumb. The last of these grooves binds dsDNA and is formed by the thumb and palm subdomains (Franklin, Wang, & Steitz, 2001; Shamoo & Steitz, 1999; J. Wang et al., 1997). Additionally, interactions with the processivity subunit, UL42, have been mapped to the extreme C-terminus of HSV Pol (Figure 1.2) (Bridges et al., 2000; Digard, Bebrin, Weisshart, & Coen, 1993; Zuccola et al., 2000).

Part of the NH_2-terminal domain (NTD) and the entire pre-NH_2-terminal domain are produced by an N-terminal extension compared to some other Family B polymerases that is conserved among herpesvirus polymerases, extending 250-amino acids longer than RB69 Pol (S. Liu et al., 2006). An FYNPYL motif has been identified in the pre-NH_2-terminal domain that plays an important but unknown role during infection in cell culture and *in vivo* (S. Liu et al., 2006; Terrell & Coen, 2012; Terrell, Pesola, & Coen, 2014), and the lack of structure in this region suggests that it may be mediating protein interactions with other components of the DNA replication machinery rather than catalyzing an enzymatic activity.

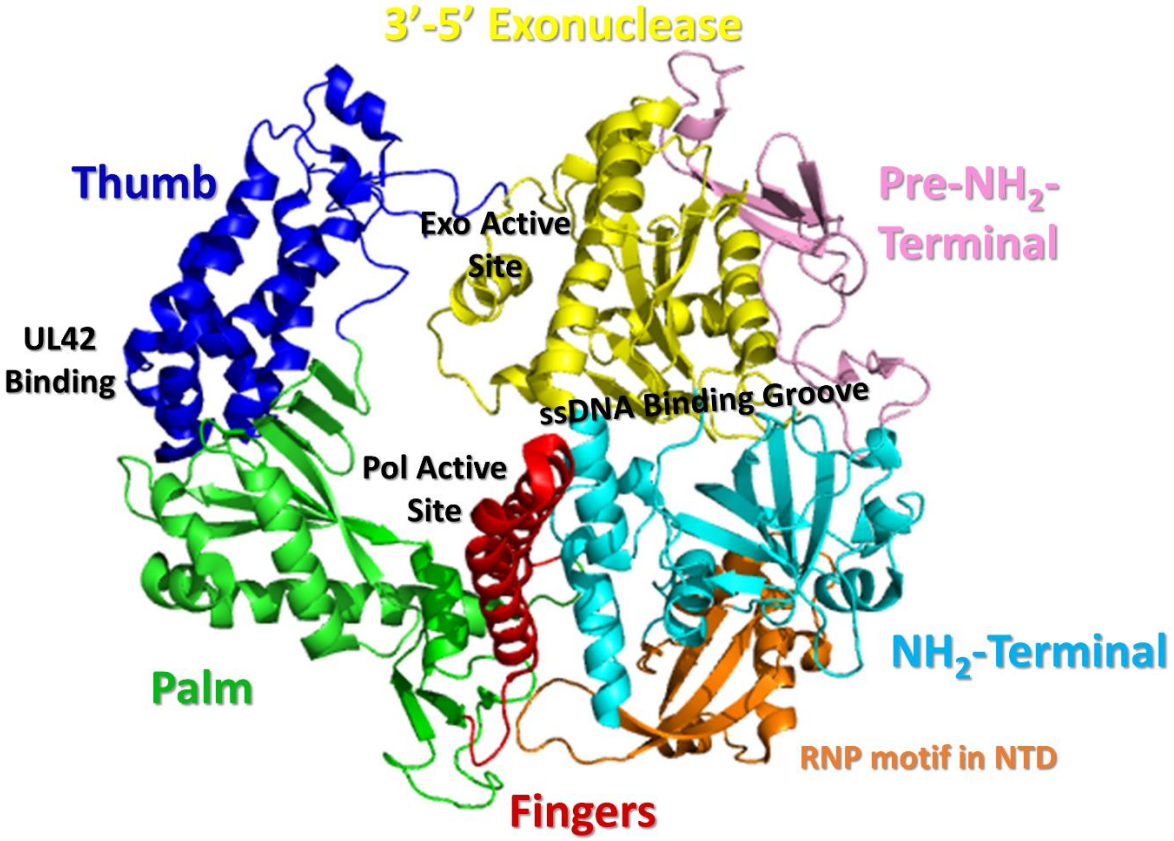

Figure 1.2. Structure of the HSV Pol (S. Liu et al., 2006) (PDB ID: 2GV9). Each of the domains of the protein and the RNP motif within the NH_2-terminal domain are labeled by name and color. Additionally, approximations for the position of the ssDNA-binding groove in RB69 Pol, the 5’-3’ polymerase active site, the C-terminus where UL42 binding has been mapped, and the 3’-5’ exonuclease active site are labeled in black.

The NTD contains three structural motifs that are conserved among some PolB3 polymerases (S. Liu et al., 2006; Swan et al., 2009; J. Wang et al., 1997). The first of these motifs (motif I) forms the putative ssDNA groove with the exonuclease domain (S. Liu et al., 2006). The second (motif II) resembles an RNA-binding motif present within many ribonucleoproteins (RNP motif) (S. Liu et al., 2006; Shamoo, Krueger, Rice, Williams, & Steitz, 1997). This motif is conserved in many Family B polymerases, including phage RB69 Pol, eukaryotic Pol δ, and archaebacterial *Desulfurococcus* strain Tok Pol and *Thermococcus* sp.9°N-7 Pol, but no confirmed function has been attributed to this motif (more details below) (S. Liu et al., 2006; Rodriguez, Park, Mao, & Beese, 2000; Swan et al., 2009; J. Wang, Yu, Lin, Konigsberg, & Steitz, 1996; Zhao et al., 1999). The third motif (motif III) within the NTD forms extensive interactions with the fingers subdomain of the polymerase active site, and substitutions in this domain of HSV Pol has been shown to impart resistance to Pol inhibitors and affect dNTP binding and incorporation (Gibbs, Chiou, Bastow, Cheng, & Coen, 1988; Huang et al., 1999). Substitutions in a similar location of T4 Pol and between the NTD and palm domain have been shown to rescue replication in low dGTP conditions by increasing the stability of the polymerase complex and sometimes also confer susceptibility to phosphonoacetic acid (Li, Hogg, & Reha-Krantz, 2010), and this motif has been shown to affect nucleotide discrimination and fidelity in yeast Pol δ (Prindle, Schmitt, Parmeggiani, & Loeb, 2013).

Enzymatic Activities of HSV Pol

HSV Pol exhibits a number of associated enzymatic activities, including the 5'-3' DNA-dependent DNA polymerase (K. W. Knopf, 1979; Marcy, Olivo, Challberg, & Coen, 1990; M. E. O'Donnell, Elias, & Lehman, 1987), 3'-5' exonuclease (Hwang, Liu, Coen, & Hwang, 1997; C. W. Knopf & Weisshart, 1988; M. E. O'Donnell et al., 1987), RNase H (Crute & Lehman, 1989;

Marcy, Olivo, et al., 1990; Weisshart, Kuo, Hwang, Kumura, & Coen, 1994), and 5'-deoxyribose phosphate and apurinic/apyrimidinic lyase activities (Bogani & Boehmer, 2008).

5'-3' Polymerase Activity

The 5'-3' polymerase activity of HSV Pol is responsible for dNTP incorporation into nascent viral DNA strands (K. W. Knopf, 1979; Marcy, Olivo, et al., 1990; M. E. O'Donnell et al., 1987), requiring a 3' hydroxyl for dNTP incorporation and displaying activity on dsDNA or DNA:RNA, with a preference for GC-rich DNA (Cavanaugh & Kuchta, 2009; Weissbach, Hong, Aucker, & Muller, 1973). The polymerase activity is stimulated at high concentrations of salt, including ammonium sulfate, which is inhibitory to cellular polymerases at similar concentrations (Gibbs et al., 1991; Powell & Purifoy, 1977; Weissbach et al., 1973). HSV Pol 5'-3' DNA polymerase activity requires multiple conserved regions, mostly within the C-terminal portion of the protein (Boehmer & Lehman, 1997; Dorsky & Crumpacker, 1988; Haffey et al., 1990; C. W. Knopf & Weisshart, 1988; Weisshart et al., 1994), which includes the palm, finger, and thumb subdomains that form the canonical catalytic center for 5'-3' polymerization activity (Hubscher et al., 2002; S. Liu et al., 2006; T. S. Wang et al., 1989). However, studies looking at HSV Pol substitutions in the third motif of the NTD adjacent to the fingers have shown that this motif may also play an important role in dNTP binding and incorporation (Gibbs et al., 1988; Huang et al., 1999).

3'-5' Exonuclease Activity

Similar to many other Family B polymerases, HSV Pol contains an intrinsic 3'-5' exonuclease activity important for proofreading activity during DNA replication (Gibbs et al., 1991; Hwang et al., 1997; C. W. Knopf & Weisshart, 1988; Weisshart et al., 1994). Residues required for this 3'-5' exonuclease activity have been mapped within three conserved regions

(Exo I, Exo II, and Exo III) (Bernad, Blanco, Lazaro, Martin, & Salas, 1989; C. W. Knopf & Weisshart, 1988; S. Liu et al., 2006; Weisshart et al., 1994). RB69 Pol, which has many structural similarities to HSV Pol, has been shown to coordinate two metal ions required for 3'-5' exonuclease activity through a mechanism conserved among polymerases exhibiting exonuclease activity (reviewed in Steitz, 1999). The residues required for metal ion coordination in structural homologue RB69 Pol map to D114 and E116 of Exo I, D222 of Exo II, and D327 of Exo III (Xia & Konigsberg, 2014), which correspond to HSV Pol residues D368, E370, D471, and D581.

Mutations affecting the exonuclease domain of HSV Pol have been extensively studied for mapping the active site (Gibbs et al., 1991; Hall, Orth, Sander, Swihart, & Senese, 1995; Hwang et al., 1997; Kuhn & Knopf, 1996), their effect on fidelity (reviewed in Y. Zhu, Stroud, Song, & Parris, 2010), antiviral resistance (reviewed in Piret & Boivin, 2011), and stimulation of strand displacement synthesis (Y. Zhu et al., 2003; Y. Zhu, Wu, et al., 2010). Specific mutations within each of these regions of HSV Pol (Exo I mutant D368A; Exo II mutant E460D and G464V; Exo III mutants Y577H and YD12) severely inhibit 3'-5' exonuclease activity *in vitro*, and have been recombined into the virus for characterization in cell culture (Gibbs et al., 1991; Hall et al., 1995; Hwang et al., 1997).

The Exo I mutant D368A exhibits severely impaired exonuclease activity, likely by disrupting metal ion coordination within the 3'-5' exonuclease active site (Hall et al., 1995; Kuhn & Knopf, 1996; Lawler, Mukherjee, & Coen, 2018), despite less than a 2-fold defect in polymerase activity when expressed using recombinant baculovirus expression in insect cells and purified (Hall et al., 1995; Kuhn & Knopf, 1996; Lawler et al., 2018; Y. Zhu, Wu, et al., 2010). Multiple attempts to recombine this mutation into HSV-1 using marker rescue of a temperature-

sensitive (ts) *pol* mutant were unsuccessful, despite successful rescue of the ts mutation and successful introduction of a different mutation using the same marker rescue protocol, suggesting that the D368A mutation is lethal and the exonuclease essential for viral replication (Hall et al., 1995). However, the D368A mutation only showed a 30-fold defect on fidelity *in vitro* (Song, Chaudhuri, Knopf, & Parris, 2004) and some Exo III mutant viruses (described below) were able to form plaques, suggesting that another mechanism may be inhibiting viral replication in cell culture.

The Exo II mutants studied so far (E460D and G464V) have been reported to severely affect polymerase activity *in vitro* and had major effects on viral replication in cell culture (Gibbs et al., 1991; Kuhn & Knopf, 1996). The Y577H and YD12 Exo III mutants, on the other hand, only exhibited a ~3-fold defect on virus replication, while also maintaining at least 80% of polymerase activity and reducing exo activity to 2% or less. Exo III mutants Y577H and YD12 also show that drastic defects in the 3'-5' exonuclease activity decrease fidelity of the enzyme 300-800-fold in cell culture, providing evidence that the mutator phenotype associated with loss of the exonuclease activity is not lethal to viral replication (Hwang et al., 1997).

So, questions remained regarding the mechanism of the defect associated with the D368A mutant in cell culture and whether the 3'-5' exonuclease activity was required for viral replication, as Hall et al. had hypothesized, or whether some other aspect of the D368A virus was inhibiting virus production. It was also unknown whether any potential defect was associated with the RNase H activity of HSV Pol since it was unknown whether this activity was or was not associated with the 3'-5' exonuclease domain, as this activity could be required for removal of RNA primers from the lagging strand during DNA replication.

Lyase Activity

More recently, a 5'-deoxyribose phosphate and apurinic/apyrimidinic lyase activity possibly related to base excision repair (BER)-mediated repair of viral DNA has been attributed to HSV Pol (Bogani & Boehmer, 2008). This activity resembles those associated with the repair polymerase in eukaryotes, Pol β. The lyase activity has been mapped to the C-terminal portion of the protein containing the polymerase domain (Bogani & Boehmer, 2008), but the specific domains/residues required for this activity and its role in viral replication in cell culture has yet to be deciphered.

RNase H Activity

HSV Pol preparations have also been found to contain an RNase H activity (Crute & Lehman, 1989; C. W. Knopf & Weisshart, 1988; K. W. Knopf, 1979; Marcy, Olivo, et al., 1990; Weisshart et al., 1994). Originally, an RNase H activity said to have 5'-3' directionality co-purified with HSV Pol (Crute & Lehman, 1989), but a contaminant, predicted to be the viral alkaline nuclease UL12, was present following a similar protein purification protocol (Hall, Orth, & Claus-Walker, 1996; C. W. Knopf & Weisshart, 1990). Subsequently, RNase H activity intrinsic to HSV Pol was confirmed and mapped to the N-terminal portion of the enzyme containing the 3'-5' exonuclease, NH_2-terminal, and pre-NH_2 terminal domains (Marcy, Olivo, et al., 1990; Weisshart et al., 1994). However, it is unclear whether this RNase H acts on 5' RNA termini, is instead attributable to the 3'-5' exonuclease, or is a different function altogether. Hall *et al.* showed that the D368A mutation ablated cleavage of both ssDNA and dsDNA substrates, and they were unable to detect 5'-3' DNase activity, but they did not test DNA:RNA hybrid templates (Hall et al., 1996).

The RNase H activity has been mapped to the N-terminal portion of the enzyme containing the pre-NH_2-terminal, NH_2-terminal, and 3'-5' exonuclease domains (Weisshart et al., 1994), but the specific domains and residues necessary for these activities have not been determined. Human flap endonuclease-1 (Fen-1) incubated with HSV Pol has been shown to cleave flapped substrates *in vitro* that are ligatable by DNA ligase I (Y. Zhu, Wu, et al., 2010), but the importance of this protein and the mechanism for Okazaki fragment maturation during HSV-1 infection had also not been tested.

The specificity of this HSV Pol RNase H activity for RNA:DNA containing either 5' or 3' termini and whether this activity was dependent on the 3'-5' exonuclease active site remained in question prior to the results contained in this dissertation. It was also unclear whether another domain, such as the RNP motif within the NH_2-terminal domain, could be responsible for a separate 5'-3' RNase H activity.

RNP Motif

The pre-NH_2-terminal and NH_2-terminal domains contain residues that are highly conserved among human herpesviruses, suggesting that they may play a role during infection and DNA synthesis separate from the previously identified activities associated with this enzyme. The second motif of the HSV Pol NH_2-terminal domain resembles a common RNA-binding motif (RNP motif), the βαββαβ motif, and this motif superimposes well with the RNA-binding motif of human ribonucleoprotein A1 (S. Liu et al., 2006; Shamoo et al., 1997). So, it has been hypothesized that this domain can interact with RNA (Ceska & Sayers, 1998; Matsui, Abe, Yokoyama, & Matsui, 2004). A number of highly conserved basic and aromatic residues cluster within the putative RNP motif and could form ionic interactions with the RNA backbone and stacking interactions with the sugars, respectively (Bandziulis, Swanson, & Dreyfuss, 1989;

Birney, Kumar, & Krainer, 1993; Ceska & Sayers, 1998; S. Liu et al., 2006). Additionally, the putative nucleic acid binding site lies adjacent to what is predicted to be the 5' ssDNA-binding groove, an optimal location to interact with RNA primers during strand displacement synthesis (S. Liu et al., 2006). In fact, the structures of RB69 Pol all have a guanine bound within the RNP motif (Franklin et al., 2001; Shamoo & Steitz, 1999; J. Wang et al., 1997).

There is also evidence suggesting that other Family B polymerases may interact with RNA through the NTD. Certain Family B polymerases, such as the T4 Pol and RB69 Pol, have been shown to autoregulate their mRNA translation (Pavlov & Karam, 1994; Tuerk, Eddy, Parma, & Gold, 1990; C. C. Wang, Pavlov, & Karam, 1997), but no one has tested whether the RNP motif interacts with RNA or whether substitutions within this motif affect DNA synthesis or autogenous translational control.

More recently, the crystal structure of *S. cerevisiae* Pol δ has also been shown to contain a motif resembling that of an RNA-binding domain within the NTD similar to HSV Pol (Swan et al., 2009). It is interesting to note that, though the yeast Pol α and Pol ε structures overlap very closely with that of Pol δ, an RNP motif was not noted in relation to those enzymes (Doublie & Zahn, 2014; Jain et al., 2014; Perera et al., 2013). A different group found that providing ssDNA longer than 14 nucleotides after pre-binding labeled template DNA was inhibitory to strand displacement synthesis with Pol δ *in vitro*, and the authors suggested that this inhibition may proceed through an uncharacterized nucleic acid binding domain (Koc et al., 2015).

The presence of the RNP motif within the NTD of HSV Pol and other Family B polymerases has raised questions about whether this motif plays a role during DNA synthesis, and, if so, how important this role is for viral replication and/or DNA synthesis overall. Three different hypotheses have been raised for potential activities associated with this putative RNA-

binding motif: 1) The RNP motif aids in autoregulation of HSV Pol translation and controls its expression during infection (S. Liu et al., 2006). 2) This motif is a catalytic site for a 5'-3' RNase H activity that removes RNA primers for Okazaki fragment maturation (S. Liu et al., 2006). 3) The RNP motif enhances strand displacement synthesis by interacting with the RNA primer and/or recruiting a separate nuclease for 5' flap removal (S. Liu et al., 2006; Swan et al., 2009).

Questions Addressed in This Dissertation

In this dissertation, we plan to address several unresolved questions regarding HSV Pol and its functions. First, we set out to characterize the RNase H activity associated with HSV Pol, specifically whether this activity is due to the 3'-5' exonuclease of Pol or whether it is a separate activity, possibly acting on 5' RNA termini. Next, we further analyzed a 3'-5' exonuclease-deficient mutant, D368A, that had been previously studied *in vitro* but not characterized in cell culture to determine whether the 3'-5' exonuclease activity is required for viral replication or if there was a separate phenotype inhibiting viral replication associated with this mutant. Finally, we investigated the importance of the HSV Pol RNP motif during infection and for viral DNA synthesis.

Chapter 2

HSV-1 DNA Polymerase RNase H Activity Acts in a 3'-5' Direction and is Dependent on the 3'-5' Exonuclease Active Site

This chapter is based on the peer-reviewed publication:

Lawler JL, Mukherjee P, Coen DM. 2017. HSV-1 DNA Polymerase RNase H Activity Acts in a 3' -5' Direction and is Dependent on the 3' -5' Exonuclease Active Site. J Virol. doi:10.1128/JVI.01813-17.

Abstract

The catalytic subunit (Pol) of herpes simplex virus-1 (HSV-1) DNA polymerase has been extensively studied both as a model for other family B DNA polymerases and for its differences from these enzymes as an antiviral target. Among the activities of HSV-1 Pol is an intrinsic RNase H activity that cleaves RNA from RNA:DNA hybrids. There has long been a controversy regarding whether this activity is due to the 3'-5' exonuclease of Pol or whether it is a separate activity, possibly acting on 5' RNA termini. To investigate this issue, we compared wild-type HSV-1 Pol and a widely studied 3'-5' exonuclease-deficient mutant, D368A, for DNA polymerase activity, 3'-5' exonuclease activity, and RNase H activity *in vitro*. Additionally, we assessed the RNase H activity using differentially end-labeled templates with 5' or 3' RNA termini. The mutant enzyme was at most modestly impaired for DNA polymerase activity but was drastically impaired for 3'-5' exonuclease activity, with no activity detected even at high enzyme to DNA substrate ratios. Importantly, the mutant showed no detectable ability to excise RNA with either a 3' or 5' terminus, while the wild-type HSV Pol was able to cleave RNA from the annealed RNA:DNA hairpin template, but only detectably with a 3' RNA terminus in a 3'-5' direction, and at a rate slower than that of the exonuclease activity. These results strongly suggest that HSV-1 Pol does not have an RNase H separable from the 3'-5' exonuclease domain and this domain shows a strong preference for DNA degradation over RNA:DNA.

Introduction

Herpesviruses, including herpes simplex virus 1 (HSV-1), encode their own DNA replication machinery, which is indispensable for copying their dsDNA genomes and for lytic replication within the host. Specifically, HSV-1 requires seven virally-encoded proteins to effect DNA replication: the origin-binding protein (UL9), the single-stranded DNA binding protein (ICP8), the helicase-primase complex (UL5, UL8, and UL52), and the DNA polymerase holoenzyme (UL30 and UL42) (McGeoch et al., 1988; Wu et al., 1988).

HSV-1 DNA replication has been shown to utilize both leading and lagging strand DNA replication *in vitro* (Falkenberg et al., 2000; Stengel & Kuchta, 2011). Leading strand synthesis proceeds continuously following separation of the DNA strands at the replication fork. Lagging strand synthesis, in contrast, requires the synthesis by the helicase-primase complex of RNA primers annealed to template DNA, forming Okazaki fragments. In order to complete lagging strand synthesis, removal of the RNA primers, replacement of these gaps with DNA, and a ligation reaction are required (Balakrishnan & Bambara, 2013). So far, it is unclear how HSV-1 removes RNA primers for completion of lagging strand DNA replication. Two methods for removing RNA primers during HSV-1 DNA replication have been proposed (Figure 2.1) (Crute & Lehman, 1989; Y. Zhu et al., 2003; Y. Zhu, Wu, et al., 2010): 1) The HSV-1 DNA polymerase (HSV Pol) displaces the RNA primer strand during synthesis and a viral or cellular nuclease is recruited for "flap" removal (as for eukaryotic Okazaki fragment maturation) (Figure 2.1A) (Y. Zhu et al., 2003; Y. Zhu, Wu, et al., 2010). 2) HSV-1 Pol has a 5'-3' RNase H activity that removes the RNA prior to the gap-filling reaction (as for *E. coli* Pol I) (Figure 2.1B) (Crute & Lehman, 1989). As HSV-1 Pol has an associated RNase H activity

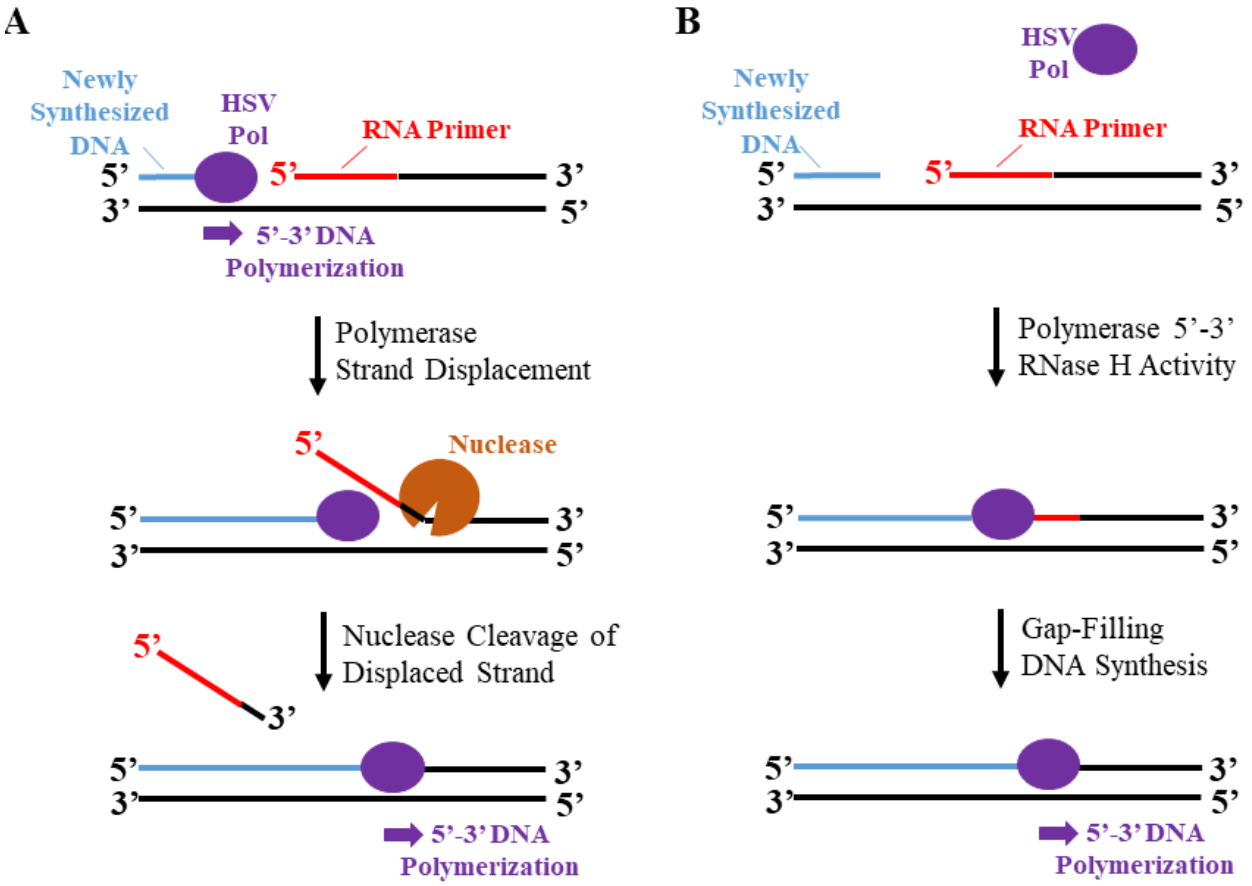

Figure 2.1. Proposed methods of HSV-1 RNA primer removal during lagging strand synthesis. A) Method like that used by eukaryotic cells, where HSV Pol would displace the RNA primer using strand displacement synthesis and recruit a separate endonuclease for 5' removal of the RNA during HSV Pol synthesis from the template strand. B) Method like *E. coli* Pol I, where the 5'-3' RNase H activity associated with the polymerase removes the RNA primer during synthesis of the lagging strand.

[(Crute & Lehman, 1989; C. W. Knopf & Weisshart, 1988; K. W. Knopf, 1979; Marcy, Olivo, et al., 1990; Weisshart et al., 1994); see below], the second proposal has been attractive.

HSV-1 Pol contains four domains: the pre-NH_2-terminal domain, NH_2-terminal domain, 3'-5' exonuclease (Exo) domain, and the polymerase domain, composed of the palm, finger, and thumb subdomains (S. Liu et al., 2006). Like many other family B (pol α family) DNA polymerases (C. W. Knopf & Weisshart, 1988; S. Liu et al., 2006; T. S. Wang et al., 1989), HSV Pol contains an intrinsic 3'-5' exonuclease activity important for proofreading during DNA replication (Hwang et al., 1997; C. W. Knopf & Weisshart, 1988; Weisshart et al., 1994). The Exo domain contains three highly conserved motifs (named Exo I, Exo II, and Exo III) that are required for this 3'-5' exonuclease function (Bernad et al., 1989; C. W. Knopf & Weisshart, 1988; S. Liu et al., 2006; Weisshart et al., 1994). For example, the Exo I mutant D368A exhibits severely impaired exonuclease activity while maintaining high levels of polymerase activity (Hall et al., 1995; Kuhn & Knopf, 1996). Additionally, HSV-1 Pol exhibits intrinsic apurinic/apyrimidinic and 5′deoxyribose phosphate lyase activity specific to the C-terminal portion of the enzyme (Bogani & Boehmer, 2008).

HSV Pol preparations have also been found to contain an RNase H activity (Crute & Lehman, 1989; C. W. Knopf & Weisshart, 1988; K. W. Knopf, 1979; Marcy, Olivo, et al., 1990; Weisshart et al., 1994). Originally, an RNase H activity said to have 5'-3' directionality co-purified with HSV Pol (Crute & Lehman, 1989), but a contaminant, predicted to be the viral alkaline nuclease UL12, was present following a similar protein purification protocol (Hall et al., 1996; C. W. Knopf & Weisshart, 1990). Subsequently, RNase H activity intrinsic to HSV Pol was confirmed and mapped to the N-terminal portion of the enzyme containing the 3'-5' exonuclease, NH_2-terminal, and pre-NH_2 terminal domains (Marcy, Olivo, et al., 1990;

Weisshart et al., 1994). However, it is unclear whether this RNase H acts on 5' RNA termini, is instead attributable to the 3'-5' exonuclease, or is a different function altogether. Hall *et al.* showed that the D368A mutation ablated cleavage of both ssDNA and dsDNA substrates, and they were unable to detect 5'-3' DNase activity, but they did not test DNA:RNA hybrid templates (Hall et al., 1996).

More recently, Liu *et al*. (S. Liu et al., 2006) identified a structural motif in the NH_2-terminal domain that strongly resembles motifs found in certain other RNA-binding proteins, with nearby negatively charged residues that might coordinate divalent cations, reviving the hypothesis (Crute & Lehman, 1989) that HSV-1 Pol has a 5'-3' RNase H activity to remove RNA primers. However, the specificity of this HSV Pol RNase H activity for either 5' or 3' termini and whether it depends on the 3'-5' exonuclease active site remained in question.

To address these questions, we carried out *in vitro* assays utilizing purified WT Pol and the D368A exonuclease-deficient mutant, testing the ability of these enzymes to extend a fluorescently labeled DNA hairpin primer template and degrade dsDNA and RNA:DNA hybrid hairpin substrates over time.

Materials and Methods

Protein Expression and Purification

6xHis-tagged full length WT HSV Pol and a previously-characterized 3'-5' exonuclease-deficient mutant, D368A (Hall et al., 1995; Kuhn & Knopf, 1996), were cloned into the pFastBac HTC vector and expressed in a baculovirus system as previously described (Terrell & Coen, 2012), and purified as follows: Cells were harvested at 65 hours post infection, and centrifuged at 2800xg for 30 minutes. The resulting pellets were washed in Dulbecco's phosphate-buffered saline (*DPBS*) with 10% glycerol, centrifuged at 2800xg for 10 minutes, and frozen at -80˚C. For enzyme purification, cell pellets were resuspended in lysis buffer (25 mM HEPES pH 7.5, 500 mM NaCl, 10% (w/v) sucrose, 5 mM imidazole, 2 Roche complete protease inhibitor tablets per 100 ml) and the cells were lysed on ice in the presence of 1 mg/ml lysozyme by sonication using a Branson Ultrasonics Sonifier S-450 (5 sec pulses with 9 sec pauses at 20% amplitude for 15 minutes). All subsequent steps were performed at 4° C. The suspension was centrifuged at 30,000xg for an hour, and the supernatant was then passed through a 0.45 μm filter. The clarified supernatant was loaded onto a preequilibrated 10-ml GE HiTrap TALON column, washed with 20 column volumes of lysis buffer, and eluted using lysis buffer containing a gradient from 5 to 150 mM imidazole. Fractions determined to contain Pol by Coomassie staining were diluted 10-fold with column buffer (25 mM HEPES pH 7.5, 1 mM DTT, 10% (w/v) sucrose) and loaded onto a preequilibrated 5-ml GE HiTrap heparin HP column. The column was washed with 20 column volumes of column buffer containing 0.1 M NaCl and eluted with column buffer containing a gradient from 0.1 to 1 M NaCl. Fractions shown to contain Pol by Coomassie stain were concentrated with an Amicon Ultra-15 centrifugal unit (Millipore) and dialyzed in storage buffer (25 mM HEPES pH 7.5, 150 mM NaCl, 20% (v/v)

sucrose, 2 mM tris(2-carboxyethyl)phosphine (TCEP)). Proteins were estimated to be at least 90% pure by Coomassie staining, and the major species present were all detected by western blotting with the 1051c mouse monoclonal antibody against HSV Pol (generously provided by C. Knopf) (Strick, Hansen, Bracht, Komitowski, & Knopf, 1997), suggesting that any visible contaminants were cleavage products of Pol (Appendix A.1-3). Samples were quantified using the A_{280} value detected by NanoDrop (Thermo Scientific) and the extinction coefficient calculated using the amino acid sequence (Wilkins et al., 1999), flash frozen, and stored at -80˚C.

Enzyme Assays

6-Carboxyfluorescein (6-FAM) labeled dsDNA and RNA:DNA hairpin primer-template substrates used in the *in vitro* assays were synthesized by IDT (Figure 2.2). Master mixes designed to give final concentrations of 25 mM HEPES pH 7.5, 1 mM DTT, 10% glycerol, and 25 mM NaCl were combined on ice with 40 nM primer/template and differing concentrations of Pol corresponding to the molar ratios of Pol:DNA indicated (1:10, 1:2, 1:1, 2:1, and 10:1). 20 µl DNA polymerase reactions were initiated with the addition of $MgCl_2$ to 8 mM and all four dNTPs to 1 mM, mixed, and incubated at 37˚C. Aliquots were quenched in loading buffer containing 80% formamide and 100 mM EDTA at the following time points: 0, 10 seconds (s), 30 s, 1 minute (m), 2 m, 4 m, 8 m, 16 m, and 32 m (polymerase assays). 40 nM Klenow fragment and *E. coli* RNase H (NEB) were used as controls under the same conditions and quenched at the 32 m time point. Samples were separated on a 7 M Urea 15% denaturing polyacrylamide gel, and the FAM-labeled substrate was detected at 490 nm using an Amersham Imager 600. Exonuclease and RNase H assays were carried out under the same conditions, but in the absence of dNTPs, and the following time points were taken for HSV-1 Pol: 0, 1 m, 2 m,

Fig. 2.2A: S1

Fig. 2.2B: S2

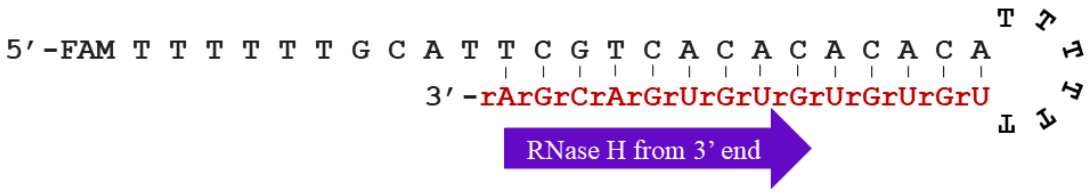

Fig. 2.2C: S3

Figure 2.2. Primer templates and substrates used in the study, their structure, and which activities were assayed using those oligonucleotides. Black letters denote deoxyribonucleotides, and the red letters denote ribonucleotides.

4m, 8 m, 16 m, 32 m, 60 m (exonuclease assays); 0, 8 m, 16 m, 32 m, 60 m, 120 m (RNase H assays), and, for Klenow fragment and *E. coli* RNase H 60 m for both asssays.

Rate Comparisons

ImageQuant TL software was used to quantify the percentage of primer-template extended past the starting primer/template band to longer products for the polymerase assays or the decrease in starting substrate band for the exonuclease and RNase H activities across the different time points. The values were plotted and the slopes of the activities within the initial linear range (initial velocities) were compared across different concentrations of enzyme using GraphPad Prism software. These rates were subsequently plotted against protein concentration using Prism and the slopes of the subsequent fitting were used to quantify activity rates for comparison.

Results

Purified His-WT Pol and His-D368A exonuclease-deficient Pol retain similar polymerase activities.

To test whether the RNase H activity of HSV-1 Pol requires an active 3'-5' exonuclease catalytic site, we analyzed the in vitro activities of purified WT Pol and the previously characterized exonuclease-deficient single mutant, D368A (Hall et al., 1995; Kuhn & Knopf, 1996). We expressed 6xHis-tagged full-length WT Pol and 6xHis-tagged D368A Pol separately using baculovirus expression (Terrell & Coen, 2012) and purified these enzymes for in vitro characterization. Next, we assessed the 5'-3' polymerization function of both enzymes by testing the ability of these Pols and control enzymes to extend a hairpin template (S1) with a 5' overhang and a 5' fluorescent label (Figure 2.2A, Figure 2.3). (Black specks that appear on the gel images are due to background fluorescence from the tray on which the images were taken, and multiple images have been compared to reduce errors in quantitation.) Under the conditions tested, the positive control enzyme, Klenow fragment of E. coli DNA Pol I (which exhibits a specific activity ~25-fold higher than our HSV Pol protein stocks), could extend the primer to the end of the dsDNA hairpin primer template, producing a larger product that co-migrates with a synthesized hairpin template of the correct size, while the negative control enzyme, E. coli RNase H, did not detectably extend the primer (Figure 2.3B). Both WT and D368A Pol exhibited 5'-3' polymerase activity, as evidenced by accumulation of products that co-migrate with the fully extended product produced by Klenow fragment. D368A also produced a slightly slower migrating species (doublet), which is likely due to the addition of a non-templated nucleotide to the 3' terminus of the extended primer, which cannot be removed in the absence of an exonuclease activity (Clark, Joyce, & Beardsley, 1987). The production of a doublet in a

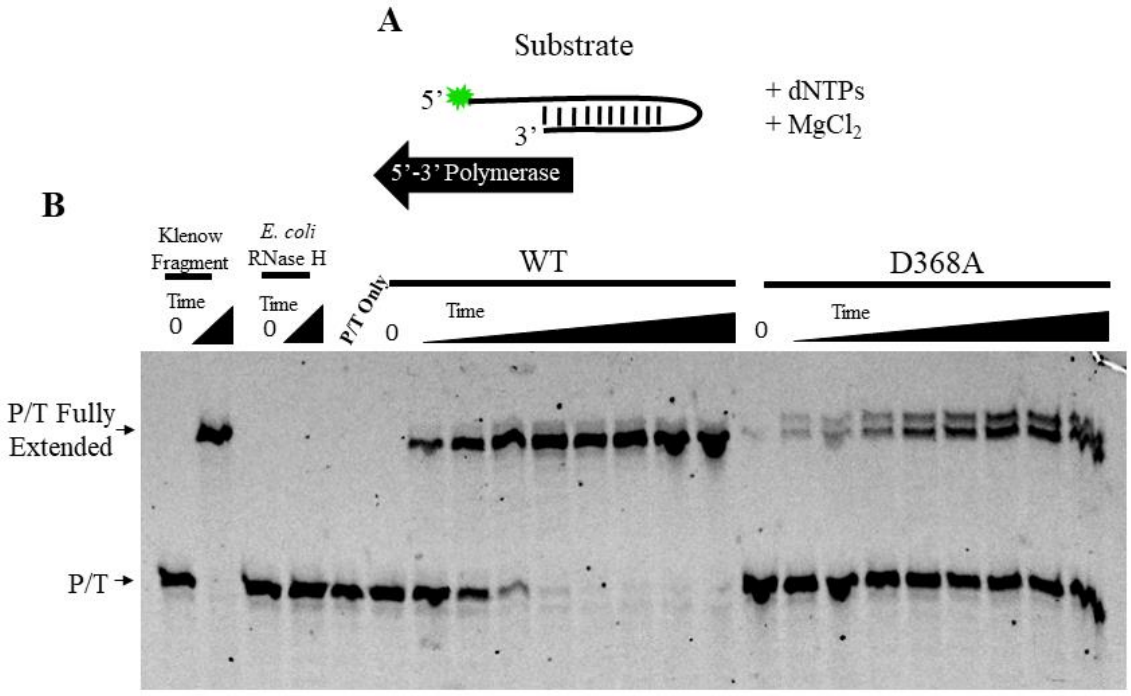

Figure 2.3. His-WT and D368A Pol exhibit similar polymerase activity. A) Cartoon of the 6-FAM labeled DNA hairpin primer template (S1; Figure 2.2) used for the polymerase assays showing the direction of extension of the primer and the addition of dNTPs and $MgCl_2$ to start the reaction. B) Fluorescent image of a denaturing polyacrylamide gel loaded with equal amounts of each polymerase reaction over increasing time points (0, 10s, 30s, 1m, 2m, 4m, 8m, 16m, 32m). The assays shown here contained a two-fold molar excess of primer template to Pol (different ratios shown in Appendix B.1-2). The 0 and 32m control reactions (Klenow fragment and RNase H) are shown. Arrows on the left side of the gel denote the starting and fully extended primer template (P/T).

similar assay has also been reported for another 3'-5'exonuclease deficient herpesvirus polymerase (H. Chen, Beardsley, & Coen, 2014).

Previous comparisons of the polymerase activities of D368A and WT Pols utilized a high ratio of polymerase to primer-template and did not discern any defect in the D368A Pol compared to WT (Hall et al., 1996; Hall et al., 1995; Kuhn & Knopf, 1996). However, it was unclear whether the authors were unable to detect a difference in polymerase function due to the high enzyme concentrations and long time points tested, or whether the activities were truly the same. We therefore performed the assays at a range of concentrations so that the ratios of Pol to primer-template varied from 1:10 to 10:1 (Appendix B.1-2). When we compared the slopes of the initial rates obtained over this wide range of polymerase concentrations, using multiple protein preparations, we observed a minor and not statistically significant decrease in polymerase activity of the D368A Pol relative to WT Pol (Table 2.1 and Figure 2.4), suggesting that this mutation within the exonuclease domain at most slightly impairs the 5'-3' polymerase activity of the enzyme. Furthermore, the polymerase rates of these two enzymes were not statistically different when compared using linear regression analysis (Figure 2.4).

D368A Pol does not exhibit detectable 3'-5' exonuclease activity.

We next wanted to test whether the D368A mutant enzyme retained any detectable 3'-5' exonuclease activity on our hairpin substrate. To that end, we performed assays like the polymerase assays, but in the absence of dNTPs (Figure 2.4), again using hairpin DNA S1, which minimizes background degradation of any unannealed ssDNA (Figure 2.2A, Figure 2.5). The positive control, Klenow fragment, could degrade the starting substrate, producing smaller products (Figure 2.5B). Despite the lack of complete degradation of the substrate on this gel, all

Table 2.1. Comparison of the slopes of the initial velocities of WT and D368A HSV Pol activities plotted against the concentration of enzyme. These values were used to calculate the fold difference in polymerase activity between the WT and D368A Pol and to compare the degradation rate of the exonuclease or RNase H substrate band to that of the polymerization rate of products extended from the starting P/T band with the error denoting the standard deviation. Activities containing the ND designation were not detected, but the limit of detection in each of these assays was used to calculate the maximum rate of these activities.

	Polymerase (min^{-1})	**3'-5' Exonuclease (min^{-1})**	**3'-5' RNase H (min^{-1})**
His-WT Pol	1.54 ± 0.02	0.12 ± 0.05	0.013 ± 0.008
His-D368A Pol	1.1 ± 0.3	< 0.0012 ± 0.0006 (ND)	< 0.001 ± 0.003 (ND)
% D368A Activity Relative to WT Pol	**74%**	**< 0.96% (ND)**	**< 8% (ND)**
Fold Difference (WT Polymerase Activity / WT Other Activity)	**1.0**	**8.1**	**120**

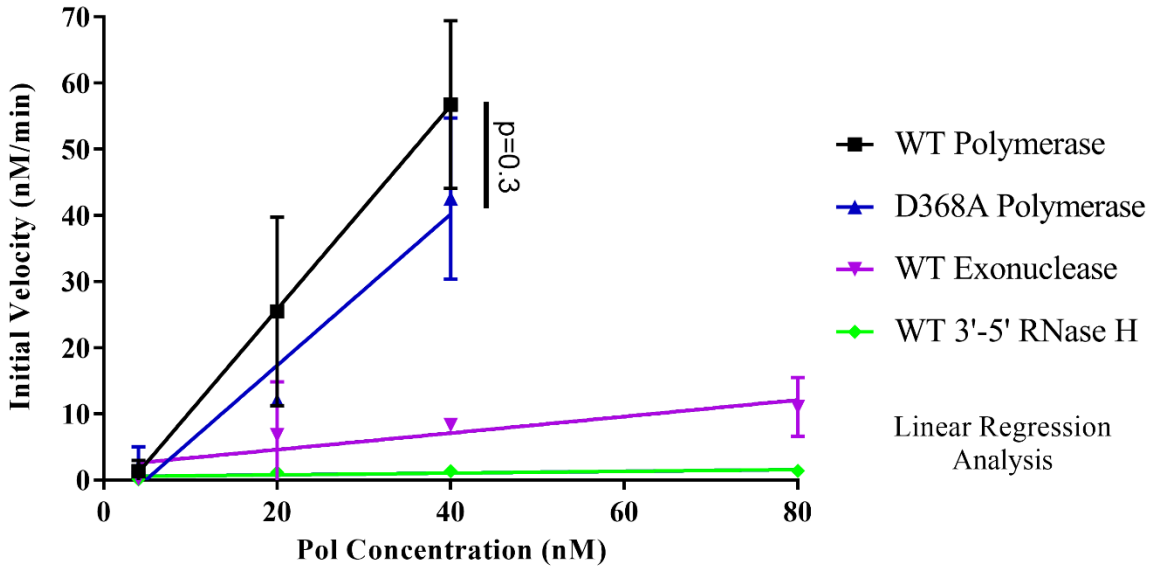

Figure 2.4. Comparison of 5'-3' polymerase, 3'-5' exonuclease, and degradation of RNA:DNA with 3' termini rates over a range of enzyme concentrations. The initial rate of the WT 5'-3' polymerase, D368A 5'-3' polymerase, WT 3'-5' exonuclease, and WT degradation of RNA:DNA with 3' termini was determined by comparing the initial rate of the exonuclease or RNase H activity (quantified by the decrease in amount of the substrate band over time) to the polymerase activity (measured as the amount of primer extended by at least one nucleotide compared to the input primer in each lane) over a range of polymerase concentrations in three indepenedent experiments, and these data were compiled and graphed using GraphPad Prism software. The slopes were calculated to generate some of the data contained in Table 2.1, and the slopes of the polymerase assays were compared using linear regression analysis.

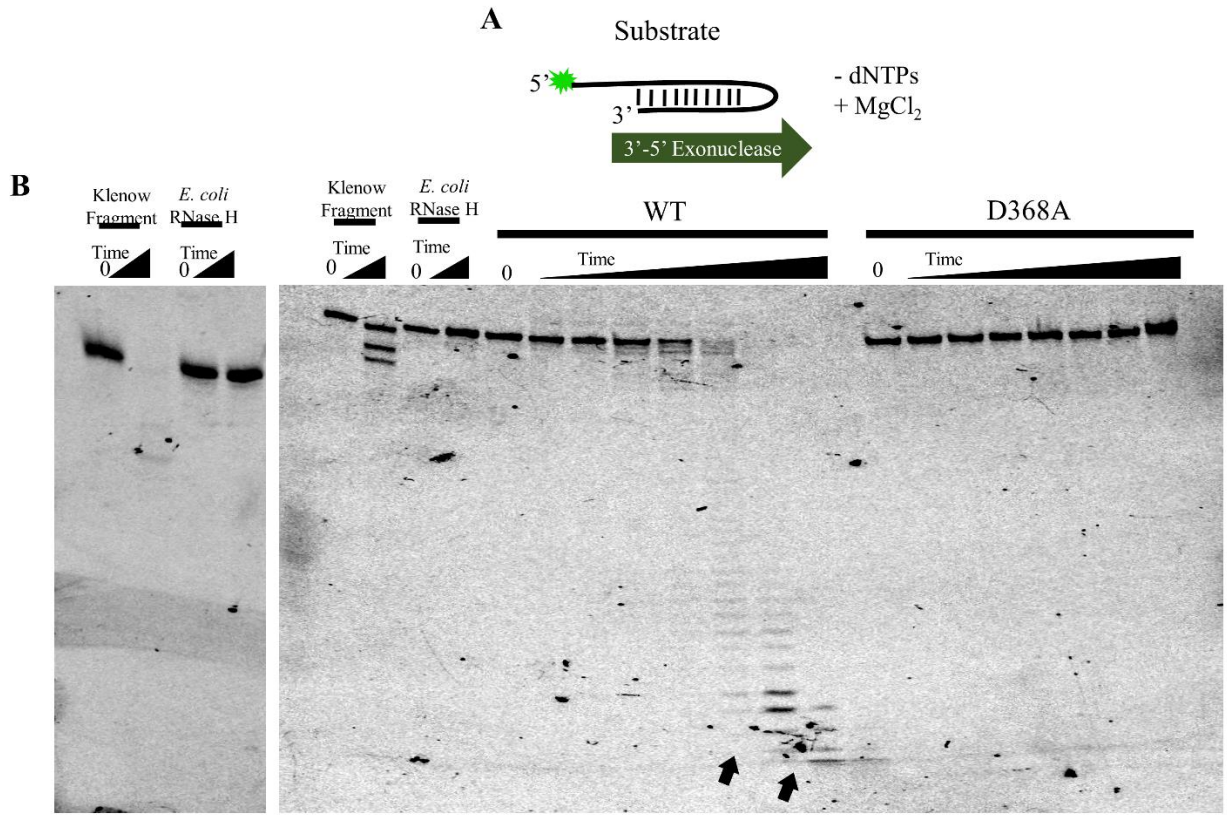

Figure 2.5. D368A Pol shows no detectable 3'-5' exonuclease activity. A) Cartoon of the 6-FAM labeled DNA hairpin substrate used for the exonuclease assays showing the direction of degradation of the substrate (S1; Figure 2.2) and the addition of $MgCl_2$ without dNTPs to start the reaction. B) Fluorescent image of a denaturing polyacrylamide gel loaded with equal amounts of each exonuclease reaction over increasing time points (0, 1m, 2m, 4m, 8m, 16m, 32m, 60m). The assays shown here contained a two-fold molar excess of Pol to substrate (different ratios shown in Appendix B.3). The 0 and 60m control reactions (Klenow fragment and RNase H) are shown and a more representative version is shown on the left. Arrows (bottom of gel) denote smaller products formed upon longer incubation of WT Pol with the substrate.

other control assays worked as expected, showing a "ladder" of smaller products (Figure 2.5B, on left). In contrast, the negative control, E. coli RNase H, was unable to degrade the substrate (Figure 2.5B). We detected 3'-5' exonuclease activity associated with the WT Pol, as expected, producing a "ladder" of smaller products (Figure 2.5B, black arrows indicate very short products). Upon comparing the initial rate of the exonuclease activity (quantified by the decrease in amount of the substrate band over time) to the polymerase activity (measured as the amount of primer extended by at least one nucleotide compared to the input primer in each lane) across varying concentrations of WT polymerase, we determined that the 3'-5' exonuclease activity of HSV Pol is 8.1-fold slower than its 5'-3' polymerase (Table 2.1 and Figure 2.4). This difference in exonuclease activity compared to the polymerase is comparable to what's been previously reported, suggesting between a 12- and 30-fold difference in catalytic rate (Chaudhuri, Song, & Parris, 2003). We were unable, however, to detect any degradation associated with the D368A mutant at all concentrations tested up to a ten-fold molar excess of Pol to substrate (2 Pol:1 substrate in Figure 2.5B, other concentrations in Appendix B.3). These data confirm previous reports on the D368A mutant (Hall et al., 1995; Kuhn & Knopf, 1996), which exhibits at least a 50-fold defect in 3'-5' exonuclease activity, based on the limit of detection, relative to WT (Table 2.1 and Figure 2.4).

WT Pol, but not D368A, has substantial 3'-5' RNase H activity.

To investigate the RNase H activity of HSV Pol and its dependence on the 3'-5' exonuclease domain, we used fluorescently-labeled synthetic RNA:DNA hairpins as substrates with sequences comparable to those of the dsDNA oligos (Figure 2.2B-C), and assayed the degradation of the substrates in the absence of dNTPs, as in the 3'-5' exonuclease assays. First,

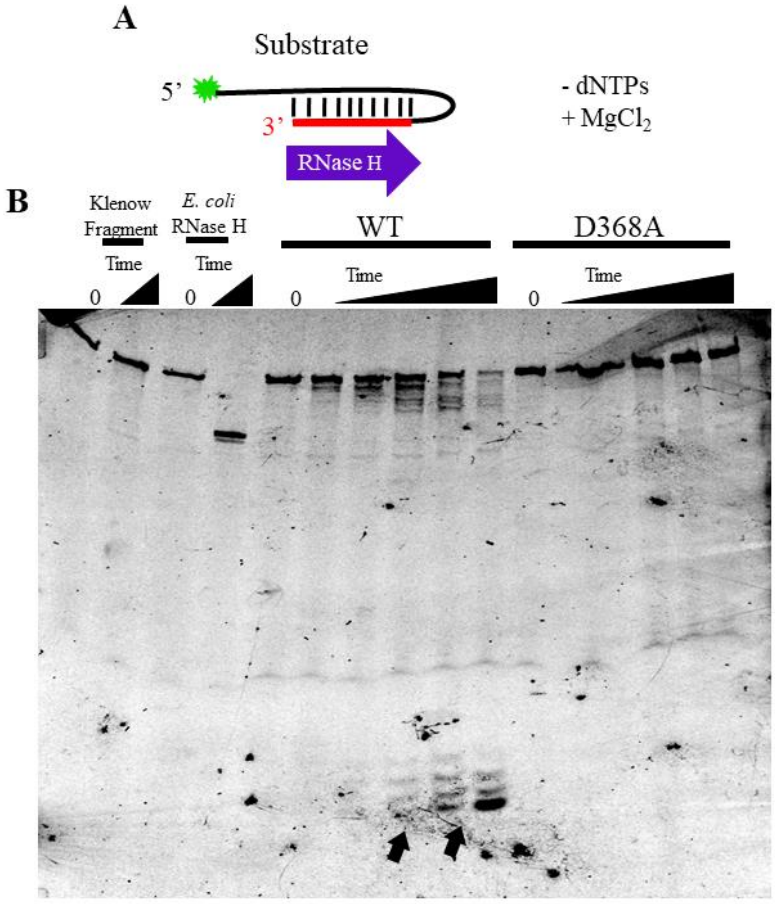

Figure 2.6. WT Pol, but not D368A, shows detectable 3'-5' RNase H activity. A) Cartoon of the 6-FAM labeled hairpin RNA:DNA substrate with a 3' RNA terminus (S2; Figure 2.2) used for RNase H assays showing degradation of the substrate expected for a 3'-5' RNase H activity and the addition of $MgCl_2$ without dNTPs to start the reaction. B) Fluorescent image of a denaturing polyacrylamide gel loaded with equal amounts of each RNase H reaction over increasing time points (0, 8m, 16m, 32m, 60m, 120m). Assays shown contained a ten-fold molar excess of Pol to substrate. The 0 and 60m control reactions (Klenow fragment and RNase H) are displayed. Arrows (bottom of gel) denote the smaller products accumulating upon longer incubation of WT Pol and the substrate

we analyzed the degradation of a 5'-fluorescently labeled substrate, S2, from which we could detect RNase H activity on RNA:DNA with 3' RNA termini (Figure 2.2B, Figure 2.7). HSV Pol was reported to not have an associated 5'-3' DNase activity (Hall et al., 1996), so we did not expect to observe any removal of the fluorescent label on the 5' end of the substrate. Klenow fragment served as a negative control and was unable to degrade the RNA:DNA substrate (Figure 2.6B). As a positive control for RNase H activity, E. coli RNase H, specifically removed the RNA portion of the hybrid hairpin substrate, leaving intact the single stranded DNA portion of the oligonucleotide (Figure 2.6B). WT HSV Pol exhibited readily detectable RNase H activity on this substrate in the 3'-5' direction, as evidenced by the decrease in full-length substrate band, the production of a "ladder" of smaller products, and, at longer times of incubation, the accumulation of much smaller products (Figure 2.6B, see black arrows). These smaller products were shorter than 5 nucleotides based on a comparison to a FAM-labeled oligonucleotide of that size (Appendix B.6). While we see accumulation of the "ladder" at both larger (> 35 nucleotides) and much smaller sizes over the time course, we believe the relative lack of visible products between these sizes is caused by the slow 3'-5' RNase H activity followed by more rapid ssDNA degradation by the 3'-5' exonuclease (see below).

By calculating the slope of the initial velocities of the HSV Pol RNase H cleavage over differing polymerase concentrations (calculated using the same methods as the 3'-5' exonuclease), we compared the polymerase, 3'-5' exonuclease, and RNase H activities. WT HSV Pol-mediated degradation of the RNA:DNA hairpin substrate containing 3' RNA termini was slower than both the cleavage of the 3' DNA terminus-containing substrate and 5'-3' polymerase activity by 30- and 100-fold, respectively (Table 2.1). These data suggest that HSV Pol more rapidly degrades dsDNA than DNA:RNA hybrids in the 3'-5' direction.

D368A Pol, however, showed no reduction of the starting substrate or accumulation of smaller products over time, even at up to ten-fold molar excess polymerase concentrations (Figure 2.6B). Therefore, we conclude that any detectable HSV Pol RNase H activity on RNA:DNA hybrids with 3' RNA termini is dependent upon the 3'-5' exonuclease active site.

Neither WT nor D368A Pol exhibit detectable RNase H activity on substrates with 5' RNA termini.

Next, we analyzed the degradation of a 3'-fluorescently labeled substrate, S3, from which we could analyze RNase H activity upon a hairpin RNA:DNA substrate with a 5' RNA terminus and 3' DNA overhang, as occurs during Okazaki fragment maturation. Since HSV Pol contains a 3'-5'exonuclease, we utilized a bulky, fluorescent FAM label to both detect the changes in the size of our substrate and inhibit 3'-5' exonuclease cleavage of this label from the substrate (Figure 2.2C, Figure 2.7A). The negative control, Klenow fragment, was again unable to degrade the RNA:DNA substrate, and the 3'-5' exonuclease activity was likely inhibited by the FAM label (Figure 2.7B). The positive control, E. coli RNase H, again cleaved only the RNA from the RNA:DNA hairpin template, leaving intact the ssDNA (Figure 2.7B). In contrast to its activity on substrate S2 (Figure 2.6), at concentrations up to and including two-fold excess polymerase, WT HSV Pol exhibited no detectable RNase H cleavage of this substrate, as evidenced by the absence of the production of smaller products, a lack of decrease over time in the intensity of the band corresponding to the starting substrate, and a lack of any smaller species (Figure 2.7B). D368A Pol similarly showed no activity on this substrate at this concentration (Figure 2.7B). At a ten-fold molar excess of WT Pol over oligonucleotide, which was the highest concentration of Pol tested, we could see a small amount of activity at longer time points

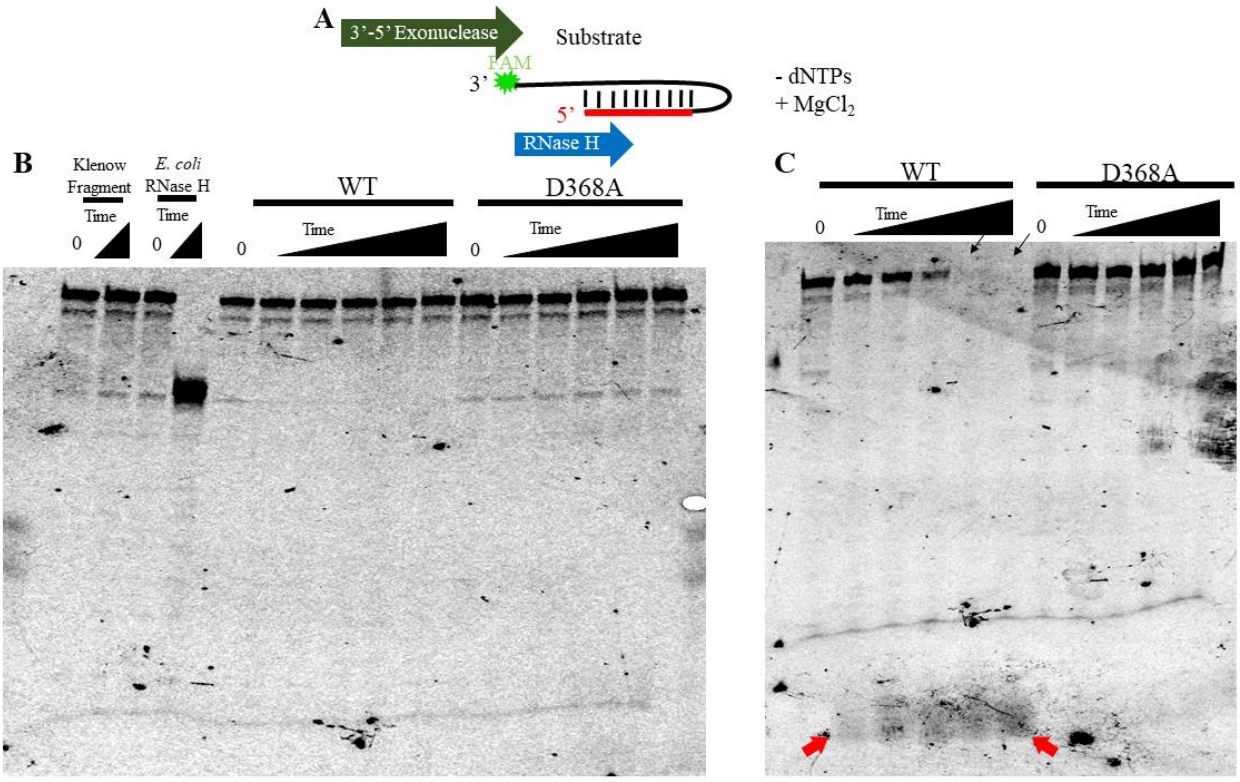

Figure 2.7. Neither WT nor D368A exhibits detectable 5'-3' RNase H activity. A) Cartoon of the 6-FAM labeled hairpin RNA:DNA substrate with a 5' RNA terminus (S3; Figure 2.2) used for RNase H assays showing the degradation of the substrate expected for a 5'-3' RNase H activity and the addition of $MgCl_2$ without dNTPs to start the reaction. Additionally, the direction of 3'-5' exonuclease removal of the fluorescent tag from the 3' end of the substrate is indicated. B) Fluorescent image of a denaturing polyacrylamide gel loaded with equal amounts of each RNase H reaction over increasing time points (0, 8m, 16m, 32m, 60m, 120m). These assays contained a two-fold molar excess of Pol to substrate. The 0 and 60m control reactions (Klenow fragment and RNase H) are shown. C) Fluorescent image of the same reaction as in B but containing a ten-fold molar excess of Pol to substrate. Black arrows (top of gel) denote the disappearance of the substrate over longer incubations with WT Pol. Red arrows (bottom of gel) denote the appearance of a band over longer incubations with WT Pol.

signified by a decrease in the signal of the starting substrate and the accumulation of very short products (Figure 2.7C, see arrows) with no “laddering” of different sized products visible. Neither a decrease in the starting substrate nor the accumulation of smaller species was detected in the presence of the D368A mutant, indicating that this activity is due to 3’-5’ exonuclease removal of the 3’ fluorescent label and not a product of an RNase H activity on an RNA:DNA substrate with a 5’ RNA terminus.

Discussion

By comparing the *in vitro* activities of WT HSV Pol and a 3'-5' exonuclease-deficient mutant, D368A, we find that any detectable RNase H activity proceeds exclusively in the 3'-5' direction and is dependent on an active 3'-5' Exo active site. Thus, the RNase H activity intrinsic to HSV-1 Pol (Crute & Lehman, 1989; C. W. Knopf & Weisshart, 1988; K. W. Knopf, 1979; Marcy, Olivo, et al., 1990; Weisshart et al., 1994) appears to be due to the 3'-5' exonuclease. Though no RNase H activity was detectable by our methods on the substrate with a 5' RNA terminus by the Exo mutant Pol, the possibility that there is some small amount of activity below the sensitivity of our assay does exist. However, concentrations up to a ten-fold molar excess of polymerase over substrate were tested, and either no activity was visible or, for WT Pol, this activity was overshadowed by the 3'-5' exonuclease, even in the presence of a bulky 6-FAM label on the 3' end of the substrate. Additionally, due to the ability to quantify the loss of the starting substrate over a large time course with a high concentration of protein, the sensitivity of these assays was substantial, so our inability to identify any activity over the course of two hours suggests that this activity does not exist under these conditions. These results suggest that, if a 5'-3' exonuclease or endonuclease RNase H activity of HSV-1 Pol does exist, it is miniscule. Additionally, the polymerase activity was not significantly affected in the purified mutant polymerase, ruling out the possibility that it was misfolded or otherwise inhibited by the purification process. These results are consistent with the reported absence of an HSV Pol 5'-3' DNase activity (Hall et al., 1996; C. W. Knopf & Weisshart, 1990). Another possibility is that a 5'-3' RNase H activity is not detectable in the absence of concurrent polymerization towards the RNA:DNA portion and/or displacement of the RNA, as occurs during Okazaki fragment maturation *in vivo.* Since we do not visualize any activity on RNA:DNA containing 5' RNA

ends with a vast molar excess of HSV Pol, however, we view this as an unlikely scenario. Other studies have seen enhanced lagging strand synthesis in the presence of MgOAc instead of $MgCl_2$ (Stengel & Kuchta, 2011) or enhanced translesion synthesis in the presence of $MnCl_2$ (Villani et al., 2002), so it is possible that specific conditions are required to detect any degradation of RNA:DNA with 5' RNA ends, but because we were unable to detect even a small loss of the starting substrate, we strongly suggest that this activity would be unlikely to play any role during infection.

These data show that an active 3'-5' exonuclease is required for not only HSV Pol degradation of ssDNA and dsDNA, as previously shown (Hall et al., 1996), but for RNA:DNA degradation as well. However, the rate of RNA:DNA degradation is much slower than the 3'-5' exonuclease activity on either ssDNA or dsDNA. So, this activity on RNA:DNA with 3' RNA termini may be a nonspecific activity of the 3'-5' exonuclease rather than something that serves a biological purpose during infection. It would also be interesting to test whether other substitutions in and near the 3'-5' exonuclease domain affect the exonuclease degradation of RNA:DNA with 3' RNA ends, as the discovery of a mutant that has increased or decreased specificity for RNA:DNA and dsDNA would help us to understand the function of this domain during infection and whether this RNA:DNA degradation aids viral replication.

The absence of any detectable RNase H degradation in either direction by the 3'-5' exonuclease deficient D368A Pol argues against the hypothesis of a separate activity and/or domain from the 3'-5' exonuclease responsible for this activity (Crute & Lehman, 1989; Haffey et al., 1990; S. Liu et al., 2006; Marcy, Olivo, et al., 1990; Weisshart et al., 1994), such as the hypothesized RNA-binding motif in the NH_2-terminal domain (S. Liu et al., 2006). While these data alone do not rule out the possibility that the NH_2-terminal domain is contributing to the

RNase H activity due to the 3'-5' exonuclease, the large distance (42 Å) between the 3'-5' exonuclease active site and the putative RNA-binding motif makes any connection between these domains for this activity highly unlikely. Rather, we favor the possibility that the putative RNA-binding motif within the NH_2-terminal domain is responsible for a different, still undetermined activity associated with HSV-1 replication. One hypothesis for such an activity is autoregulation of Pol translation via mRNA binding, as suggested by Liu et al. (S. Liu et al., 2006). Another hypothesis, which was raised by Swan et al. upon discovering a similar motif in yeast Pol δ, is interaction with RNA primers to abet strand displacement synthesis or to recruit a 5' flap endonuclease for removal of the RNA primer (Swan et al., 2009). We are currently investigating the role of this motif in HSV-1 replication (see Chapter 4).

Due to the absence of a detectable RNase H activity on RNA:DNA substrates with a 5' RNA terminus, it is unlikely that HSV Pol can remove RNA primers during lagging strand synthesis on its own. Perhaps, HSV-1 uses a mechanism similar to that of eukaryotes for the removal of RNA primers wherein the polymerase displaces the RNA primer and a separate nuclease is recruited for removal of the displaced RNA strand (Balakrishnan & Bambara, 2013). Studies have found that *in vitro*, HSV Pol has a limited strand displacement activity that is improved using the D368A Exo mutant enzyme (likely because the mutation eliminates idling) and that HSV Pol can coordinate with nuclease Fen-1 for the removal of both annealed DNA and RNA and to produce ligatable nicks (Y. Zhu et al., 2003; Y. Zhu, Wu, et al., 2010). However, the applicability of these *in vitro* activities *in vivo* is unknown. Alternatively, a viral protein, such as the viral alkaline nuclease (UL12), could be recruited to cleave the primers. While our study contains evidence against an RNase H activity inherent to HSV Pol that acts on RNA:DNA

hybrids with 5' termini, more work is needed to determine the exact mechanism of RNA primer removal during HSV-1 lagging strand DNA replication.

To our knowledge, this is the first report of a polymerase containing a 3'-5' exonuclease activity that also degrades RNA:DNA. However, multiple RNase H enzymes have been shown to also degrade dsDNA (Auer, Landre, & Myers, 1995; Bhagwat & Nossal, 2001), so it is not unheard of for an enzyme to have decreased specificity in substrate. Furthermore, other viral enzymes, including the HSV-1 thymidine kinase, have been shown to have a very wide substrate specificity (Gentry, 1992). So, it is highly possible that the lack of substrate specificity associated with the 3'-5' exonuclease domain does not play a role during infection and is instead a product of the abundance of enzyme to substrate ratios used here. However, if these two activities can be separated, it would be interesting to determine whether Pol plays some role in mRNA or miRNA processing.

Chapter 3

HSV-1 DNA Polymerase 3'-5' Exonuclease-Deficient Mutant D368A Exhibits Severely Reduced Viral DNA Synthesis and Polymerase Expression

Abstract

Herpesviruses, including herpes simplex virus-1, encode and express a DNA polymerase that is required for replication of their dsDNA genomes. This enzyme contains a 3'-5' exonuclease involved in proofreading during replication. Although certain mutations that severely impair exonuclease activity are not lethal to the virus, one mutation, the substitution of alanine for aspartate 368 (D368A), has been reported to prevent production of infectious virus, raising the possibility that the exonuclease activity is essential for viral replication. To investigate this issue, we produced virus containing this mutation (D368A Pol) using a complementing cell line. D368A Pol virus was unable to form plaques on non-complementing cells, and viral DNA synthesis and polymerase activity were severely inhibited in infected cells, as was expression of the enzyme, suggesting that this mutation prevents viral replication by its effects on polymerase expression rather than on exonuclease activity per se.

Introduction

Herpesviruses encode DNA replication machinery that is crucial for copying their dsDNA genomes and for lytic replication within the host. For herpes simplex virus-1 (HSV-1) this machinery includes the catalytic subunit of the DNA polymerase (Pol), which is a Family B polymerase that contains four domains: the pre-NH_2-terminal domain, NH_2-terminal domain (NTD), 3'-5' exonuclease domain (Exo), and the 5'-3' polymerase domain (C. W. Knopf & Weisshart, 1988; S. Liu et al., 2006; T. S. Wang et al., 1989). Residues important for HSV-1 Pol 5'-3' DNA polymerase activity include multiple conserved regions (Boehmer & Lehman, 1997; Dorsky & Crumpacker, 1988; Haffey et al., 1990; C. W. Knopf & Weisshart, 1988; Weisshart et al., 1994) within the palm, finger, and thumb subdomains that form the canonical catalytic center for 5'-3' polymerization activity (Hubscher et al., 2002; S. Liu et al., 2006; T. S. Wang et al., 1989).

HSV-1 Pol also contains an intrinsic 3'-5' exonuclease activity important for proofreading during DNA replication (Gibbs et al., 1991; Hwang et al., 1997; C. W. Knopf & Weisshart, 1988; Weisshart et al., 1994). Mutations affecting the Exo domain of HSV-1 Pol have been extensively studied for mapping catalytic residues within the active site (Gibbs et al., 1991; Hall et al., 1995; Hwang et al., 1997; Kuhn & Knopf, 1996), their effect on fidelity (reviewed in Y. Zhu, Stroud, et al., 2010), antiviral resistance (reviewed in Piret & Boivin, 2011), and strand displacement synthesis (Y. Zhu et al., 2003; Y. Zhu, Wu, et al., 2010). Residues required for this 3'-5' exonuclease activity have been mapped within three conserved regions (Exo I, II, and III) (Bernad et al., 1989; C. W. Knopf & Weisshart, 1988; S. Liu et al., 2006; Weisshart et al., 1994). Specific mutations within each of these regions of HSV Pol (Exo I mutant apartate 368 subsituted with alanine (D368A); Exo II mutant E460D and G464V; Exo III

mutants Y577H and YD12) severely inhibit 3'-5' exonuclease activity *in vitro*, and have been recombined into the virus for characterization in cell culture (Gibbs et al., 1991; Hall et al., 1995; Hwang et al., 1997). The Exo II mutants studied so far (E460D and G464V) have been reported to severely affect polymerase activity *in vitro* and had major effects on viral replication in cell culture (Gibbs et al., 1991; Kuhn & Knopf, 1996). The Y577H and YD12 Exo III mutants, on the other hand, only exhibited a ~3-fold defect on plaque formation, while also maintaining at least 80% of polymerase activity and reducing exonuclease activity to 2% or less, providing evidence that the mutator phenotype associated with this loss of the exonuclease activity is not lethal to viral replication (Hwang et al., 1997).

The Exo I mutant D368A, which exhibits severely impaired exonuclease activity, likely by disrupting metal ion coordination within the 3'-5' exonuclease active site (Figure 3.1) (Hall et al., 1995; Kuhn & Knopf, 1996; Lawler et al., 2018), retains nearly WT levels of polymerase activity when expressed using recombinant baculovirus expression in insect cells and purified (Hall et al., 1995; Kuhn & Knopf, 1996; Lawler et al., 2018; Y. Zhu, Wu, et al., 2010). Multiple attempts to recombine this mutation into HSV-1 using marker rescue of a temperature-sensitive (ts) *pol* mutant were unsuccessful, despite successful rescue of the ts mutation and successful introduction of a different mutation using the same marker rescue protocol, leading the authors to conclude, potentially prematurely, that the D368A mutation is lethal and that the exonuclease activity in particular is essential for viral replication, overstating the contribution of fidelity to viral replication overall (Hall et al., 1995). These attempts to generate the D368A Pol virus did not utilize a complementing cell line (Hall et al., 1995), however. Thus, the failure to derive the mutant prevented a quantitative assessment of the effects of the mutation on viral replication,

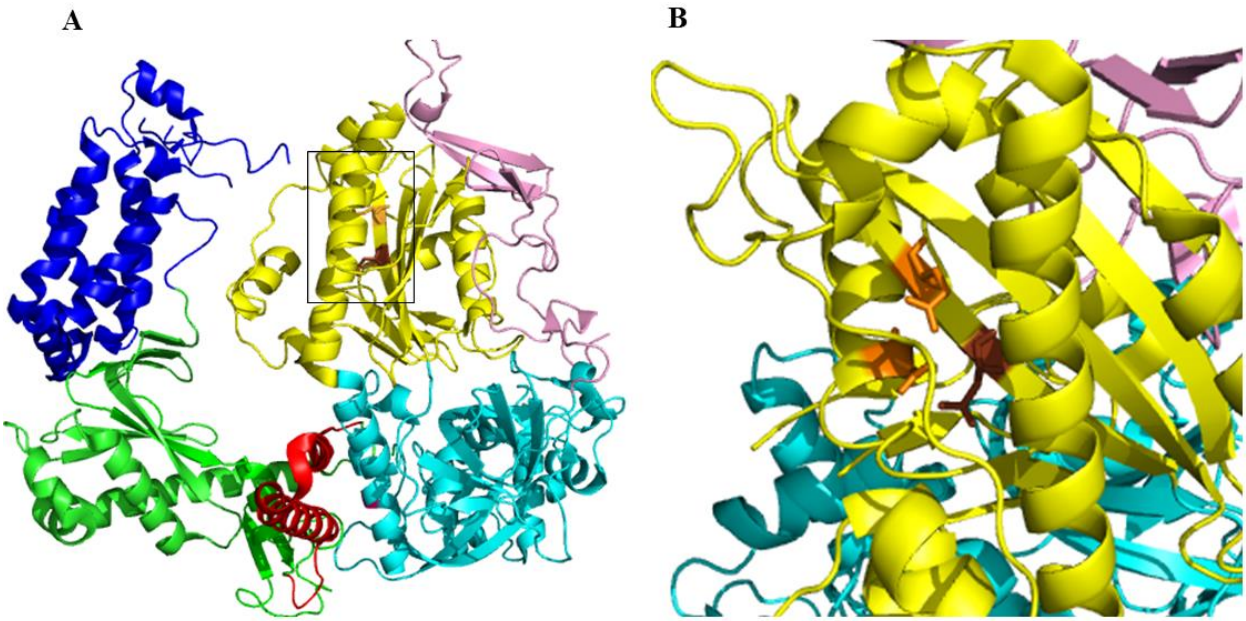

Figure 3.1. Location of the three residues believed to be necessary for metal ion coordination within the 3'-5' exonuclease domain active site. A) Wide view of the enzyme colored by domain as shown in Figure 1.2. The brown (D368) and orange (E370 and D471) residues correspond to residues required for 3'-5' exonuclease activity and are structurally conserved with the corresponding residues from RB69 Pol (S. Liu et al., 2006; Shamoo & Steitz, 1999). B) Close up and turned view of the boxed section from the previous image, giving a better view of the orientation of these residues within the active site.

DNA synthesis, polymerase activity, and expression. Because the aforementioned Exo III mutants with severely impaired exonuclease activity have been conversely reported to have relatively minor defects in virus production (Hwang et al., 1997), we set out to re-investigate the phenotype of the D368A mutation and investigate whether the 3'-5' exonuclease activity of HSV Pol is leading to the lethal phenotype exhibited by the D368A substitution.

Materials and Methods

Cells and Viruses

Vero cells (ATCC; CCL-81) and PolB3 cells (generously provided by Charles Hwang, (Hwang et al., 1997)) which inducibly express WT Pol upon infection, were grown and maintained in Dulbecco's modified Eagle medium (DMEM) supplemented with 5% newborn calf serum (NCS), 1% penicillin and streptomycin. Human embryonic kidney (293T) cells (ATCC; CRL-11268) were propogated in DMEM containing 10% fetal bovine serum (FBS) and 1% penicillin and streptomycin.

The D368A mutation was introduced into an HSV-1 KOS strain expressing FLAG-tagged Pol (Terrell & Coen, 2012) using Red two-step recombination (Tischer, von Einem, Kaufer, & Osterrieder, 2006) and PCR primers GGGGCATGAGCGACCTACCGGCATACAAGCTCATGTGCTTCGCTATCGAATGCAAG GCTAGGGATAACAGGGTAATCGATTT (forward) and GGAAAGGCCAGCTCGTCCTCCCCCCCCGCCTTGCATTCGATAGCGAAGCACATGAGC TTGTATGGCCAGTGTTACAACCAATTACC (reverse) with *Escherichia coli* strain GS1783 (generously provided by Greg Smith, Northwestern University, (Tischer, Smith, & Osterrieder, 2010)) harboring a BAC clone of HSV-1 strain KOS (I. Jurak, C. Cui, A. Pearson, A. Griffiths, P. A. Schaffer, D. M. Coen, unpublished results). The resulting BAC was transfected into PolB3 cells (generously provided by C. Hwang), which inducibly express WT Pol upon infection. Additionally, to test whether any off-target mutations are responsible for the resulting phenotype, a rescued derivative of the D368A Pol virus (D368A Rescue) was produced by recombining the WT sequence into the D368A Pol BAC using primers GGGGCATGAGCGACCTACCGGCATACAAGCTCATGTGCTTCGATATCGAATGCAAG

GCGGGGGTAGGGATAACAGGGTAATCGATTT (forward) and GAAAGGCCAGCTCGTCCTCCCCCCCCGCCTTGCATTCGATATCGAAGCACATGAGCT TGTATGGCCAGTGTTACAACCAATTAACC (reverse). The presence of the D368A mutation and D368A Rescue was confirmed by sequencing the BAC prior to transfection, and the plaque purified viral DNA was purified from infected cells for sequencing of the entire Pol (UL30) coding sequence to ensure that no other mutations were present in the recombinant viruses.

Plating Efficiency and Plaque Diameter Analysis

Plaque purified viruses were titered on PolB3 cells and used to infect $5x10^6$ PolB3 cells at an MOI of 0.1. Five days post infection, the cells were scraped, pelleted at 1000 x g for 10 minutes, and resuspended in 1.5 ml of DMEM containing 5% NCS. Resuspended cells were freeze-thawed and sonicated in a cup horn sonicator (Branson Ultrasonics) for 2x 20 seconds with a minute break between. The resulting lysates were centrifuged for 10 minutes at 3000 xg, and the supernatants were serial diluted in DMEM with 5% NCS for titering in triplicate on Vero and PolB3 cells ($2x10^5$ cells/well). Wells were infected with 0.2 ml of the resulting serial dilutions, incubated at 37˚C for one hour, and the cells were covered with 2 ml of DMEM with 5% NCS and methyl cellulose. 72 hours post infection, the cells were fixed, stained with crystal violet, and plaques were counted to identify the resulting plating efficiency.

The crystal violet-stained plates were imaged under 20x magnification using a digital camera, and the diameter of the plaques was assessed using ImageJ software (NIH). These plaque diameters were compiled using GraphPad Prism software and analyzed for statistical significance by one-way ANOVA with multiple comparisons.

Single-Cycle Growth Curves

Vero or PolB3 cells ($1x10^5$ cells/well) were infected in triplicate at an MOI of 10. After a 1-hour adsorption period at 37°C, wells were washed three times with DPBS and replenished with 0.2 ml of DMEM containing 5% newborn calf serum. The supernatant was collected from the cells at 1, 4, 8, 12, and 24 hours post infection and flash frozen. The supernatants from each time point were thawed and titered on either Vero or PolB3 cells (see above).

Viral Genome Quantification

Vero (and PolB3) cells were infected at an MOI of 10 in triplicate as above, and cell lysates were collected at 1, 8, and 12 hours post infection. Lysates were diluted twenty-fold and DNA was purified alongside mock lysate and spiked viral genome standards. Samples were amplified using primers specific to the viral *thymidine kinase* (*tk*) gene or the cellular *1,3-alpha-galactosyltransferase* gene, TK values were compared to a standard curve of spiked KOS viral genomes, and the amounts of cellular DNA detected in each sample were used to normalize viral DNA values as previously described (Terrell & Coen, 2012). The standard curves used for the calculations and the melting curves associated with the qPCR runs are shown in the Figure 4.A3 and Table 4.A2. The resulting genome copy numbers were compiled using GraphPad Prism software and divided by the copy numbers of the one-hour post infection samples to generate a fold-change in viral copy number over the input at 8 or 12 hours post infection. These data were analyzed using one-way ANOVA with multiple comparisons.

Polymerase Activity Assay

Activated salmon sperm DNA was generated by combining final concentrations of 2.5 mg/ml salmon sperm DNA, 10 mM HEPES (pH 7.5), and 5 mM magnesium chloride. Forty ng/mg of DNA of DNase I (NEB) was added, and the reaction was allowed to proceed at 60˚C for 5 minutes. The DNA was purified using phenol-chloroform extraction and resuspended in distilled water.

The filter-binding polymerization assay was adapted from that of Gibbs et al. (Gibbs et al., 1991). 293T cells ($2x10^6$ cells) infected at an MOI of 5 were incubated at 37˚C for 8 hours, washed 3 times with DPBS, spun down for 10 minutes at 1000 x g, and resuspended in 200 µl cold lysate buffer (20 mM HEPES pH 7.5, 1 mM EDTA, 100 mM NaCl, 10 mM β-mercaptoethanol). The lysates were kept at 4˚C for the following steps: sonication for 2 x 40 seconds in a cup horn sonicator (Branson Ultrasonics) with a minute between sonication steps, centrifugation at 13,000 x g for 10 minutes, and preincubation of 5 µl of supernatant from the cell lysates with designed final concentrations (50 µl total) of 500 µg/ml activated salmon sperm DNA, 60 µM each dNTP minus dTTP, 5 µM ^{32}P-dTTP, 100 mM ammonium sulfate, 20 mM HEPES pH 7.5, 1.0 mM EDTA, 0.5 mM dithiothreitol, 10% glycerol, and either 100 µg/ml phosphonoacetic acid or DMSO, as indicated. The reactions were started with the addition of 8 µM magnesium chloride, and the assays were allowed to proceed for 20 min at 37˚C. The polymerase reaction was stopped by precipitation with 10% TCA (final concentration), allowed to sit on ice for 10 minutes, bound to a GF/C filter (GE), washed twice with 10% TCA, and washed once with 100% ethanol. Five ml of scintillation fluid was added, and the samples were immediately analyzed using scintillation counting to determine the incorporation of radioactive dTTP into the activated salmon sperm DNA. For analysis, the scintillation numbers were

entered using GraphPad Prism software, and the values were compared to the percentage of the WT samples for normalization. Three different experiments are combined for the image, and the error bars indicate the standard deviation.

Protein Expression Determination

Vero and PolB3 cells ($4x10^5$ cells/well) were infected at an MOI of 10. At 8 hours post infection, the cells were washed 3x with DPBS and lysed in 2x Laemmli buffer (Bio-Rad) containing β-mercaptoethanol and complete protease inhibitors (Roche). Samples were boiled at 95˚C for 5 minutes and run on a 4-20% polyacrylamide SDS-PAGE gel (Bio-Rad), transferred onto polyvinylidene difluoride (PVDF) membrane, blocked with 5% milk in DPBS-T (DPBS with % Tween 20), and probed using the following antibodies overnight at 4˚C: α-Pol (mouse 1051c, generously provided by R. Klemm and C. Knopf; 1:1000), α-FLAG (mouse M2, Sigma-Aldrich; 1:500), α-TK (goat polyclonal, generously provided by W. Summers; 1:1000), and α-β-Actin (8226, Abcam; 1:1000). Membranes were washed three times with DPBS-T for 5 minutes at room temperature with rocking and subsequently incubated with secondary antibodies conjugated to horseradish peroxidase (HRP) (Southern Biotech) at 1:1000 for 1 hour at room temperature with rocking, followed by another three 5-minute washes in DPBS-T. Finally, chemiluminescence solution (Pierce) was added to detect signal from the membranes using film.

Results

The D368A Pol virus is incapable of forming plaques on non-complementing cells.

First, we assessed any viral replication defects of the D368A Pol virus (Figure 3.2). Viruses generated from PolB3 cells were collected five days post-transfection, and the supernatants were titrated using serial dilution on either Vero or PolB3 cells alongside wild type (WT) virus and, as a negative control, a virus (HP66) with an insertion of the *E. coli* β-galactosidase gene replacing much of the *pol* gene (Marcy, Yager, & Coen, 1990). The cells were fixed and stained using crystal violet at 72 hours post-infection (hpi). Whereas WT virus could form plaques efficiently upon infection of either Vero or PolB3 cells, the negative control, HP66, was unable to form any plaques on Vero cells but could form plaques on complementing PolB3 cells, suggesting that, while these viruses could infect Vero cells and cause cytopathic effects, they were unable of viral spread to surrounding cells (Figure 3.2A). Like the negative control, the D368A Pol virus was unable to form any plaques on Vero cells even at the lowest dilution tested but could do so on PolB3 cells. As expected, D368A Rescue could form plaques efficiently on Vero cells, indicating that the inability of D368A mutant to form plaques on Vero cells is due to the designed mutation. These data show that the D368A virus is severely inhibited for plaque formation in the absence of complementing Pol protein and is consistent with the previous report that the D368A mutation is lethal (Hall et al., 1995).

HP66 and D368A Pol exhibit a ~10-fold defect on replication in the PolB3 complementing cell line.

Despite the high titers observed, the plaques formed on the PolB3 cells by D368A Pol virus were smaller in size than those of the WT and D368A Rescue viruses. To quantify this

Figure 3.2. D368A Pol virus replication is severely inhibited in non-complementing cells and exhibits a defect in complementing cells. A) Plaque formation of the denoted viruses titrated side-by-side on Vero and PolB3 cells. The lower limit of the vertical axis denotes the limit of detection in this assay. B) Twenty times magnification images of plaque assays from PolB3 cells fixed at 72 hpi and stained with crystal violet. C) Plaque diameters for each denoted virus on PolB3 cells analyzed using one-way analysis of variance (ANOVA) with Šídák correction for multiple comparisons. *: p-value <0.0001, ns: not significant. D) Viral supernatants collected from Vero cells (left column) or PolB3 cells (right column) infected with the indicated viruses at the times post infection (MOI of 10) shown on the x-axis were titrated on either PolB3 cells (top row) or Vero cells (bottom row). The 24 hpi time point was analyzed using one-way analysis of variance (ANOVA) with Šídák correction for multiple comparisons. *: p-value <0.005, ns: not significant.

Figure 3.2 (Continued)

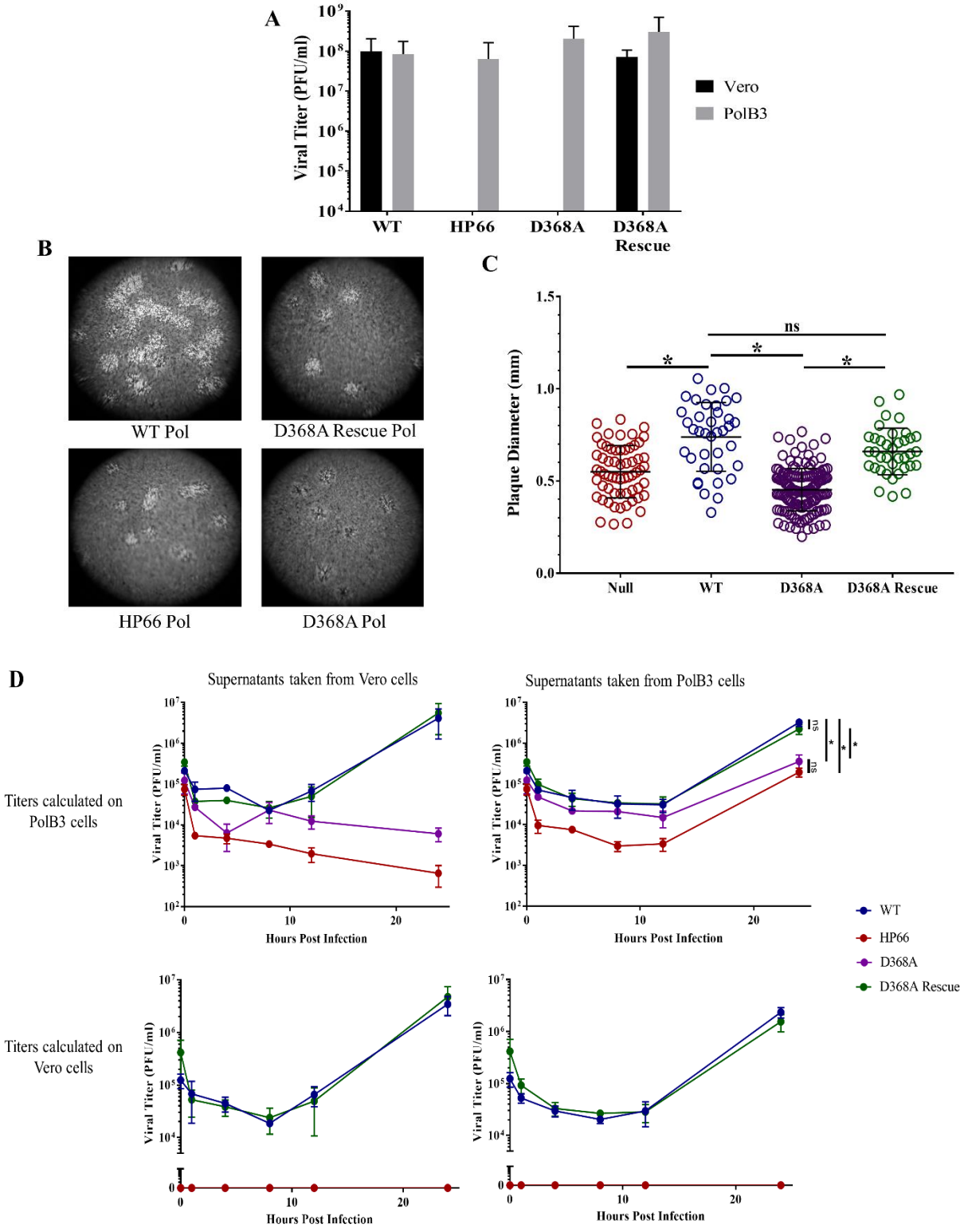

difference, the crystal violet stained plates were imaged at 20x magnification (Figure 3.2B), plaque diameters were measured using ImageJ software, compiled, and analyzed by one way ANOVA using GraphPad Prism software (Figure 3.2C). Both HP66 and D368A plaques were significantly smaller than the WT and D368A Rescue plaques, suggesting that while these viruses form plaques readily on PolB3 cells, they are either producing less infectious virus per cell or are otherwise less efficient at viral spread to surrounding cells, even in the presence of complementing WT Pol expression.

To test whether HP66 and D368A Pol viruses have replication defects in Vero and/or PolB3 cells, single cycle replication kinetics were assessed to identify any defects in viral yield from infected cells and further assess the ability of these mutants to replicate on the complementing cell line. Viruses were plaque purified, and high titer stocks were obtained using PolB3 cells. Vero cells (Figure 3.2D, left column) and PolB3 cells (Figure 3.2D, right column) were infected with WT, HP66, D368A, or D368A Rescue viruses (MOI 10), incubated at 37˚C for an hour, washed 3 times with PBS, media replaced, and the supernatants were collected at 1, 4, 8, 16, and 24 hpi. The resulting supernatants were titrated on both PolB3 cells (Figure 3.2D, top row) and Vero cells (Figure 3.2D, bottom row). Additionally, the titers of the zero-time point were calculated from back titers of the inocula. The positive controls, WT Pol and D368A Rescue, were able to replicate similarly in either Vero or PolB3 cells (Figure 3.2D). The negative control, HP66, did not produce any plaque forming units above what was seen at 1 hpi when infecting Vero cells; indeed, titers dropped after that time point (Figure 3.2D, left column). When HP66 virus was grown on PolB3 cells, a 10- to 20-fold defect in viral yield compared to WT was detected at 24 hpi (Figure 3.2D, right column). Like HP66, following infection of Vero cells, titers of D368A decreased over the time course (Figure 3.2D, top left). In PolB3 cells, we

detected an 9-fold defect in viral replication associated with the D368A mutation compared to WT, and a 6-fold defect compared to the D368A Rescue (Figure 3.2D, top right). The likely cause for this defect in PolB3 cells will be discussed below. We also titrated the supernatants on Vero cells to see whether there was any evidence for reversion to a WT phenotype or a defect not dependent on *pol* gene expression, and none was detected (Figure 3.2D, bottom row). Combined, these results suggest that D368A Pol virus is completely defective for replication unless complemented by the WT *pol* gene.

D368A Pol virus cannot replicate viral DNA and exhibits no detectable polymerase activity. To determine the cause of this defect in viral replication, we next assessed whether the D368A Pol virus was capable of viral DNA synthesis in non-complementing cells. Vero cells were infected at an MOI of 10 and cell lysates were collected at 1, 8, and 12 hpi. Lysates were diluted twenty-fold, and DNA was purified alongside lysates of mock-infected cells containing serial dilutions of spiked viral genome standards. Samples were amplified using primers specific to the viral *thymidine kinase* (*tk*) gene or the cellular *1,3-alpha-galactosyltransferase* gene, *tk* values were compared to the standard curve of spiked KOS viral genomes, and the amounts of cellular DNA detected in each sample were used to normalize viral DNA values as reported previously (Terrell & Coen, 2012). The viral copy numbers are reported as the fold viral genomes replicated over the input viral genomes (1 hpi time point) (Figure 3.3A). The positive controls, WT and D368A Rescue viruses, were able to replicate viral DNA above the input number of genomes by at least 40-fold. The negative control, HP66, on the other hand, did not detectably produce any viral DNA copies over those present at 1 hpi. D368A Pol virus-infected lysates resembled those of HP66; viral DNA copy number never increased over the input levels.

Figure 3.3. D368A Pol virus is deficient in viral DNA synthesis and for polymerase activity. A) qPCR analysis of viral genome copy numbers at 8 and 12 hpi compared to those present following adsorption (1 hour post-infection) analyzed using one-way analysis of variance (ANOVA) with Šídák correction for multiple comparisons. *: p-value <0.002, ns: not significant. B) qPCR analysis of viral genome copy numbers from PolB3 cells collected at 1, 8, and 12 hpi analyzed using one-way analysis of variance (ANOVA) with Šídák correction for multiple comparisons. *: p<0.0006, ns: not statistically significant. C) ^{32}P dTTP incorporated into activated salmon sperm DNA in the presence of high ammonium sulfate concentrations compared to the WT incorporation after 20 minutes in the presence or absence of HSV-1 Pol inhibitor PAA. The data from three assays were combined and plotted as a percentage of incorporated radioactivity compared to WT Pol, with the standard deviations denoted by the error bars and analyzed using one-way analysis of variance (ANOVA) with Šídák correction for multiple comparisons. *: p-value <0.02, ns: not significant.

Figure 3.3 (Continued)

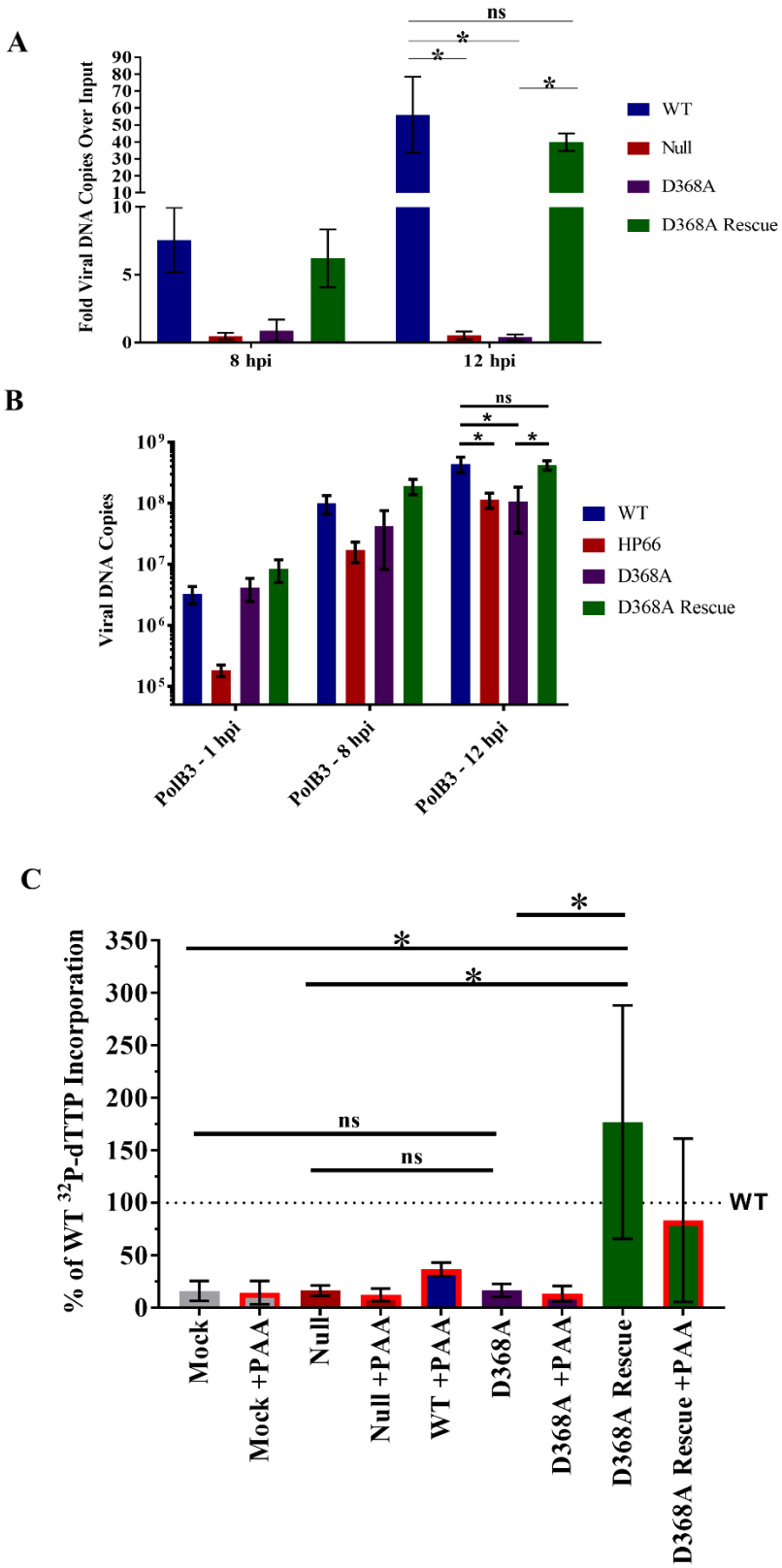

Infection of PolB3 cells with the D368A and HP66 viruses resulted in viral DNA synthesis, though statistically less than that generated by the WT and Rescue viruses (Figure 3.3B). Thus, the D368A Pol virus is highly impaired for viral DNA synthesis during infection.

We and others have purified soluble D368A Pol from recombinant baculovirus-infected Sf9 insect cells and showed that it exhibits near WT levels of 5'-3' polymerase activity (Hall et al., 1995; Kuhn & Knopf, 1996; Lawler et al., 2018), so we wanted to examine whether there was any active HSV Pol in the infected cells. To this end, we utilized an assay (Gibbs et al., 1991) that can discern viral polymerase activity in cell lysates by taking advantage of HSV Pol's resistance to or even activation by high ammonium sulfate concentrations that are inhibitory to cellular polymerases (Weissbach et al., 1973). In this assay, DNA polymerase activity from infected 293T cell lysates was quantified using scintillation counting of filter-bound ^{32}P-dTTP incorporated into activated salmon sperm DNA. Incorporation over that of the mock-infected and HP66-infected lysates was detected from lysates of WT- and D368A Rescue-infected cells in the absence of an HSV Pol inhibitor, phosphonoacetic acid (PAA), but was inhibited upon PAA addition to the reaction (Figure 3.3C). In contrast, there was no ammonium sulfate-resistant polymerase activity above that of the mock-infected samples associated with the D368A Pol virus-infected cell lysates.

D368A Pol virus has drastically decreased Pol expression.

Since we were unable to identify any viral DNA synthesis or viral polymerase activity in D368A Pol virus-infected cells, we next examined Pol expression during infection using Western blotting (Figure 3.4). Vero and PolB3 cells were infected at an MOI of 10, and the cell lysates were collected in Laemmli buffer at 8 hpi. Samples were boiled at 95˚C for 5 minutes and run

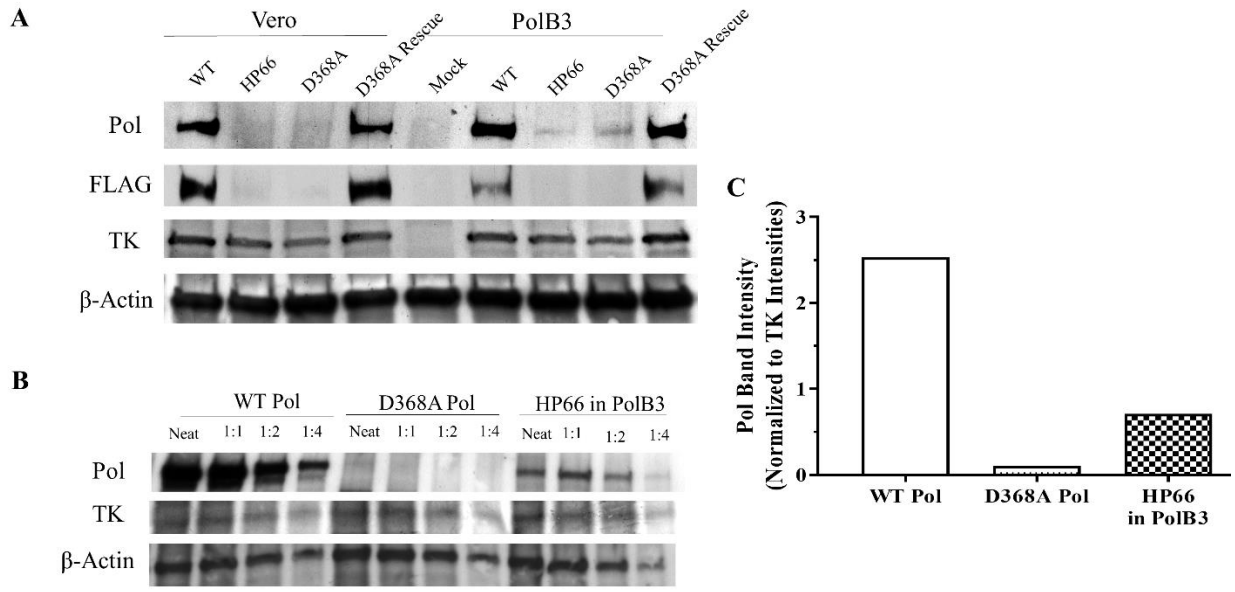

Figure 3.4. D368A Pol expression is substantially decreased in infected cells compared to WT. A) Western blots of cell lysates collected at 8 hpi and detected using antibodies specific for the proteins listed on the left and in the text. Whereas the antibody for Pol detects protein expressed both by the virus and the PolB3 cells, the FLAG antibody only detects Pol expression from the virus and does not detect expression of the WT *pol* gene in PolB3 cells. B) Two-fold dilution series generated to quantify the defect in D368A Pol expression. C) Quantification using QuantityOne software of the 1:2 dilution determined to be within the linear range of signal for the Pol antibody normalized to the TK signal.

on a 4-20% polyacrylamide SDS-PAGE gel (Bio-Rad), transferred onto polyvinylidene difluoride (PVDF) membrane, blocked, and probed using the following antibodies: α-Pol (mouse 1051c, generously provided by C. Knopf), α-FLAG (mouse M2, Sigma-Aldrich; to detect FLAG-tagged Pol expressed from the virus, but not from the *pol* gene resident in PolB3 cells), α-TK (goat polyclonal, generously provided by W. Summers), and α-β-Actin (8226, Abcam). Following washing, the blots were incubated with secondary antibodies conjugated to horseradish peroxidase (HRP) (Southern Biotech) and washed again. Finally, chemiluminescence solution (Pierce) was added to detect signal from the membranes using film.

Vero and PolB3 cells infected with WT and the D368A Rescue viruses produced readily detectable bands indicative of Pol expression at 8 hpi, while Vero cells infected with HP66 or the D36A Pol virus did not exhibit detectable Pol expression (Figure 3.4A). A 2-fold dilution series was run to more accurately quantify the amount of D368A Pol being expressed during infection (Figure 3.4B). The 1:2 dilution was determined to be in the linear signal range for both the TK and Pol antibodies, so this dilution was quantified for determination of the expression level of each of these enzymes in relation to the infection control, TK, using BioRad Quantity One 1-D Analysis software with local background subtraction for each lane individually. Lysates of Vero cells infected with D368A Pol virus produced 24-fold less Pol than those from cells infected with WT virus (Figure 3.4C). Interestingly, even in PolB3 cells infected with either HP66 or D368A, Pol expression was only detected with the mouse anti-Pol antibody, and not with the anti-FLAG antibody (Figure 3.4A, right side), suggesting that only the complementing WT Pol encoded by the PolB3 cells was detectably expressed. This expression of Pol in HP66-infected PolB3 cells was 3.6-fold reduced relative to Pol expression in Vero cells following WT infection (Figure 3.4C), suggesting that only a small amount of Pol is required for the efficient formation of

plaques by HP66 and D368A, and explaining the reductions in virus yield of the two mutant viruses relative to WT in PolB3 cells (Fig. 3.2B-D). Nevertheless, expression of Pol from PolB3 cells infected with HP66 was 6.6-times greater than the expression of D368A Pol in Vero cells when assessed using serial dilution (Figure 3.4B-C), emphasizing how little Pol was expressed from the D368A virus in Vero cells.

Discussion

Combined, these data suggest that the D368A HSV-1 Pol mutant is unable to express enough functional enzyme to facilitate DNA synthesis or virus production within non-complementing cells. These results corroborate previous failed attempts to produce the D368A Pol virus in the absence of a complementing cell line (Hall et al., 1995) and suggest that the D368A mutation within the Exo domain of HSV-1 Pol inhibits transcription, protein synthesis or, more likely, leads to premature degradation within infected cells. So far, it is unclear how this mutant protein can express stably in insect cells but not upon viral infection of Vero cells. We speculate that proteases within Vero cells may be responsible for rapid degradation of the enzyme, but further work is required to specifically characterize this phenotype and determine the step at which expression is inhibited. In order to further test characterize the lack of expression associated with the D368A mutant, we suggest testing expression in other human cell lines, quantifying Pol mRNA using Northern blot, and determining the rate of degradation using a pulse chase experiment in the presence or absence of a proteasome inhibitor, such as MG-132.

From the experiments detailed here, it is difficult to confirm whether there is any small amount of D368A Pol expressed during viral infection. So, it is possible that there is some D368A Pol expressed, and that this lack of replication is due to a combination of both decreased expression compounded by the defect in exonuclease activity, which was shown to have about a ~3-fold effect on replication in the Exo III mutants (Hwang et al., 1997). Due to the minor effects on replication, these mutants must be reasonably well expressed since a 3.6-fold defect in Pol expression resulted in a ~10-fold defect on viral replication during HP66 infection of PolB3 cells, although the expression levels of these Exo III mutant enzymes have not been tested to our knowledge.

The only available HSV-1 Pol structure does not reveal metal ion occupancy within the exonuclease active site (S. Liu et al., 2006), but in the structure of the similar Family B polymerase, RB69 Pol, residues within the Exo III domain play a less critical role in metal ion coordination compared to conserved residues in the Exo I and II domains, which are held together by the metal ion (Shamoo & Steitz, 1999). We speculate, then, that substitution of D368 results in loss of metal ion coordination and thus local unfolding of the Exo domain, making Pol more susceptible to protease digestion, though further work with more conservative charged mutations of the D368 residue would be necessary to test this hypothesis.

Chapter 4

Substitutions of Conserved Residues in the RNP Motif of the HSV-1 DNA Polymerase NH_2-Terminal Domain Strongly Impair Viral DNA Synthesis

Abstract

The NH_2-terminal domain (NTD) of the herpes simplex virus-1 (HSV-1) DNA polymerase (Pol) contains a βαββαβ structural motif found in certain RNA-binding proteins. This motif is highly conserved among many family B DNA polymerases of viruses, bacteriophage, and eukaryotes. The role of this motif and whether it is important for DNA synthesis is unknown for HSV-1 Pol or any polymerase. It had previously been suggested to be important for a proposed 5'-3' RNase H activity of HSV-1 Pol, but we have found no evidence for this activity (Chapter 2). To investigate the importance of this motif during infection, we constructed a mutant virus with substitutions in two conserved aromatic residues within the putative RNA-binding motif and a rescued derivative in which the wild type sequences were reintroduced. The mutant could form plaques and replicate on a complementing cell line but was unable to form plaques or to release virus in a single-cycle experiment in non-complementing Vero cells. This mutant virus also did not detectibly synthesize viral DNA in Vero cells. The rescued derivative, however, formed plaques, produced infectious virus, and synthesized viral DNA similar to the wild type virus. Expression of the NTD mutant Pol was similar to that of WT Pol at peak times of DNA replication during infection, and at least eight-fold higher than that sufficient for complementation of a *pol* null mutant. Additionally, the NTD mutant protein localized to nuclei and colocalized with the single-stranded DNA binding protein, ICP8, at punctate sites like those formed upon treatment with inhibitors of HSV-1 DNA synthesis. Finally, viral polymerase activity was readily detected in the NTD mutant-infected cell lysates at similar though variable levels as in lysates of the WT and rescued derivative-infected cells. Taken together, our results indicate that the NTD βαββαβ motif is essential for HSV-1 DNA synthesis through a mechanism separate from effects in polymerase activity.

Introduction

Herpes simplex virus-1 (HSV-1) encodes its own DNA replication machinery, including a DNA polymerase included among the Family B polymerases (McGeoch et al., 1988; Wu et al., 1988). The catalytic subunit of the HSV-1 DNA polymerase (Pol) contains four domains: the pre-NH_2-terminal domain, NH_2-terminal domain (NTD), 3'-5' exonuclease domain, and the polymerase domain (Figure 1.2) (S. Liu et al., 2006). The NTD of HSV Pol contains three motifs conserved in many Family B polymerases, including phage RB69 Pol, eukaryotic Pol δ, and archaebacterial *Desulfurococcus* strain Tok Pol and *Thermococcus* sp. 9°N-7 Pol (S. Liu et al., 2006; Rodriguez et al., 2000; Swan et al., 2009; J. Wang et al., 1996; Zhao et al., 1999).

The first motif makes up part of the postulated ssDNA-binding groove lined with basic residues; this motif corresponds to the homologous bacteriophage RB69 Pol region, which binds the 5' extension of the ssDNA template (S. Liu et al., 2006; J. Wang et al., 1997). The second motif resembles the ribonucleoprotein (RNP) motif present within many RNA-binding proteins (S. Liu et al., 2006) and has been shown to bind guanine in all of the homologous RB69 Pol structures to date (Figure 4.1, in orange) (Petrov, Ng, & Karam, 2002; J. Wang et al., 1997; M. Wang et al., 2011). The third NTD motif forms extensive interactions with the fingers subdomain of the polymerase active site, and substitutions in this domain of HSV Pol has been shown to impart resistance to Pol inhibitors and affect dNTP binding and incorporation (Gibbs et al., 1988; Huang et al., 1999). Substitutions in the corresponding motif of T4 Pol show a similar phenotype (Li et al., 2010), and this motif has been shown to affect nucleotide discrimination and fidelity in yeast Pol δ (Prindle et al., 2013).

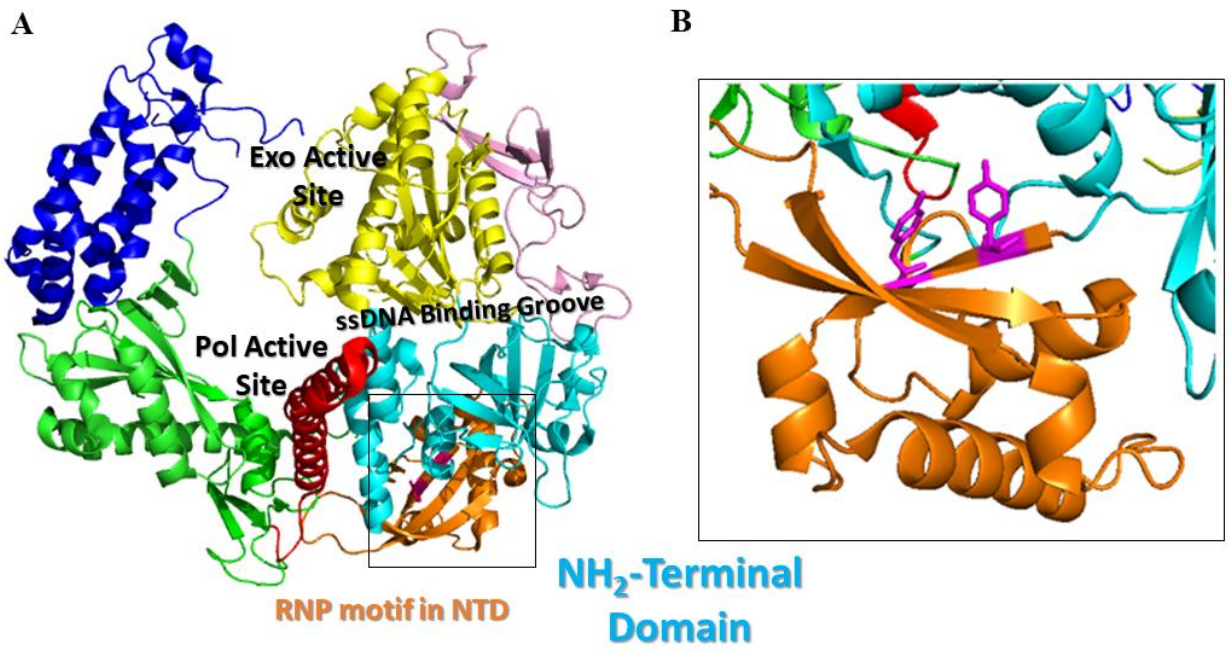

Figure 4.1. Location of the ribonucleoprotein (RNP) motif within the NTD of HSV Pol and the location of the two tyrosine residues conserved among most Family B polymerases that have been mutated to alanines in this study. A) The structure of HSV Pol as colored in Figure 1.2. The Y204 and Y206 residues that have been mutated to alanines are colored in bright pink within the orange RNP motif. B) Closer view of the RNP motif and the tyrosine 204 and 206 residues predicted to bind RNA based on the RNP A1 structure.

There is evidence to suggest that the RNP motif within the HSV Pol NTD may bind RNA and that this activity may be conserved across herpesviruses and other organisms. First, several basic and aromatic residues that are highly conserved among human herpesviruses cluster in and around the motif. These residues could form ionic interactions with the RNA backbone and stacking interactions with the sugars, respectively (Bandziulis et al., 1989; Birney et al., 1993; Ceska & Sayers, 1998; S. Liu et al., 2006). Of these conserved residues within the RNP motif, there are three aromatic residues (Y204, F205, and Y206 in HSV-1 Pol) that are highly conserved among many Family B polymerases (Figure 4.2) with the tyrosines structurally corresponding to highly conserved aromatic residues in the RNP A1 structure that make base-stacking interactions with RNA bound in this pocket (Figure 4.1, in bright pink) (S. Liu et al., 2006; Shamoo et al., 1997).

The presence of this RNP motif raised the hypothesis that the NTD may contain an RNase H catalytic domain with 5'-3' directionality (Crute & Lehman, 1989; S. Liu et al., 2006). We have previously shown that the only detectable HSV Pol RNase H activity acts in a 3'-5' direction (Chapter 2) (5), inconsistent with the hypothesis that a 5'-3' RNase H active site exists in the NTD. However, it is unknown whether this motif plays a different role during infection.

Certain Family B polymerases, such as the T4 Pol and RB69 Pol, have been shown to autoregulate their mRNA translation (Pavlov & Karam, 1994; Tuerk et al., 1990; C. C. Wang et al., 1997), but no one has tested whether the RNP motif interacts with RNA or whether substitutions within this motif affect DNA synthesis or autogenous translational control. While a T4 Pol temperature sensitive mutation that affects autogenous control has been mapped within the NTD (Hughes, Yee, Dawson, & Karam, 1987), this mutant was present on the opposite side of the NTD from the RNP motif within the RB69

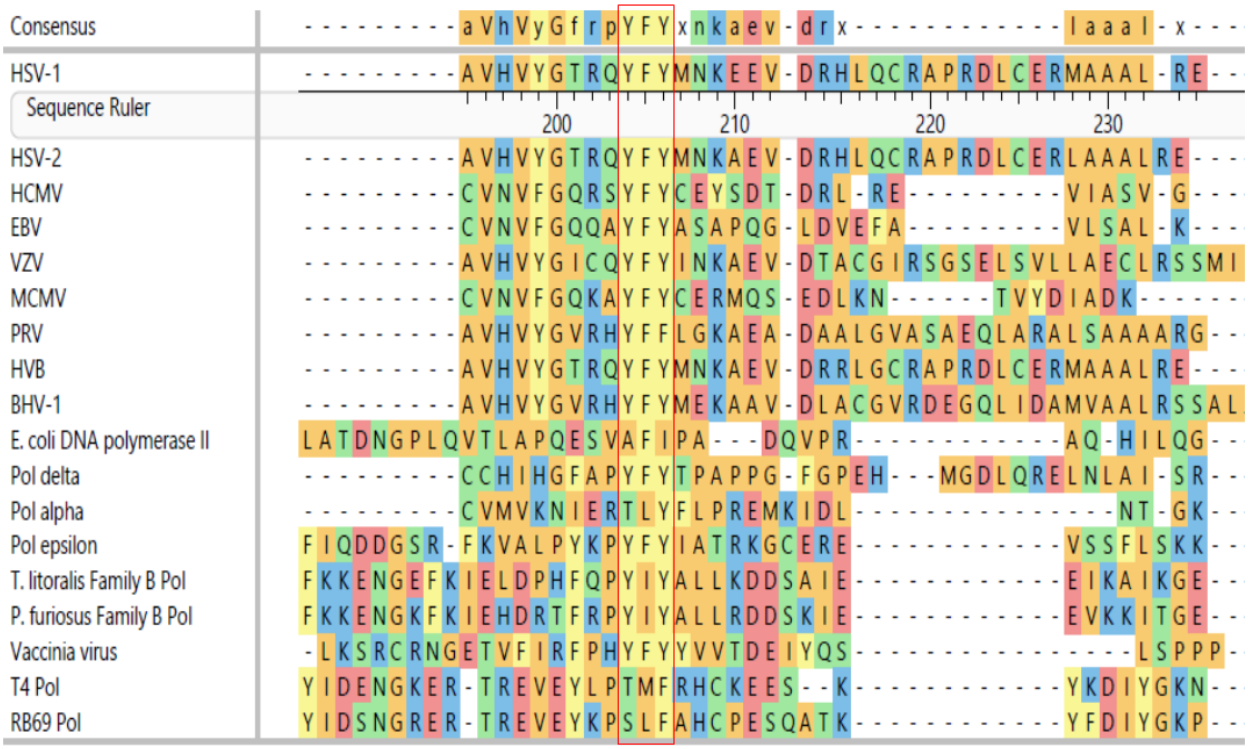

Figure 4.2. The Y204 and Y206 residues are highly conserved among herpesvirus polymerases and among certain Family B polymerases from other organisms. Sequences of Family B polymerases listed on the left (HSV-1: herpes simplex virus-1, HSV-2: herpes simplex virus-1, HCMV: human cytomegalovirus, EBV: Epstein-Barr virus, VZV: varicella-zoster virus, MCMV: mouse cytomegalovirus, PRV: pseudorabies virus, HVB: herpes simian B virus, BHV-1: bovine herpes virus-1, Pol delta: *S. cerevisiae* Pol δ, Pol alpha: *S. cerevisiae* Pol α, Pol epsilon: *S. cerevisiae* Pol ε, T4: bacteriophage Pol, RB69: bacteriophage RB69 Pol) were aligned using MUSCLE alignment in the DNAStar MegAlign Pro software (Edgar, 2004a, 2004b). Sequences similar to aromatic residues 204-206 of HSV-1 Pol are boxed in red for comparison among species.

Pol structure and likely stabilizes this region and interacts with the fingers (Reha-Krantz, 1994). HSV Pol expression is thought to also be regulated at the level of translation and follows an unusual expression pattern compared to other HSV-1 early genes (Bryant & Coen, 2008; Wobbe, Digard, Staknis, & Coen, 1993; Yager & Coen, 1988; Yager, Marcy, & Coen, 1990); however, there is no evidence that HSV Pol controls *pol* mRNA translation.

More recently, the crystal structure of *S. cerevisiae* Pol δ has also been shown to contain a motif resembling that of an RNA-binding domain within the NTD similar to HSV Pol (Swan et al., 2009). The putative RNA-binding site in either of these enzymes is also adjacent to the location of the ssDNA-binging groove in the RB69 Pol homologue (Figure 4.1, labeled in black) (S. Liu et al., 2006; Swan et al., 2009; J. Wang et al., 1997), an optimal location to interact with RNA primers on the lagging strand during strand displacement synthesis (S. Liu et al., 2006). Another group found that providing ssDNA longer than 14 nucleotides after pre- binding labeled template DNA was inhibitory to strand displacement synthesis with Pol δ, and the authors suggested that this inhibition may proceed through an uncharacterized nucleic acid binding domain (Koc et al., 2015).

To our knowledge, the effect of substitutions in the RNP motif of Family B polymerases has not been tested. As the crystal structures of Family B polymerases from yeast, phage, and archaea also have potential RNA-binding sites within their NTD (S. Liu et al., 2006; Rodriguez et al., 2000; Swan et al., 2009; J. Wang et al., 1997; Zhao et al., 1999), this domain may have a function that is highly conserved among a wide range of organisms.

So, we set out to engineer mutations within conserved residues in and around the RNP motif of HSV Pol predicted to affect the RNA-binding ability of this motif, and to identify and characterize any defect in viral replication due to altering this motif. One mutant,

Y204A/Y206A, which expressed Pol abundantly, was further analyzed for its replication, viral DNA synthesis, localization, and polymerase activity.

Materials and Methods

Cells and Viruses

Vero cells (ATCC; CCL-81) and PolB3 cells (generously provided by Charles Bihchen Hwang Upstate Medical University (Hwang et al., 1997)), which inducibly express WT Pol upon infection, were grown and maintained in Dulbecco's modified Eagle medium (DMEM) supplemented with 5% newborn calf serum (NCS), 1% penicillin and streptomycin. Human embryonic kidney (293T) cells (ATCC; CRL-11268) were propagated in DMEM containing 10% fetal bovine serum (FBS) and 1% penicillin and streptomycin.

Escherichia coli strain GS1783 (generously provided by Greg Smith, Northwestern University, (Tischer et al., 2010)) harboring a BAC clone of HSV-1 strain KOS (I. Jurak, C. Cui, A. Pearson, A. Griffiths, P. A. Schaffer, D. M. Coen, unpublished results) was used to generate recombinant RNP mutant viruses through two-step Red recombination techniques (Tischer et al., 2006) and PCR primers listed in Table 4.1. Then, the mutant viruses were generated in PolB3 cells as previously described (Terrell & Coen, 2012). A rescued derivative virus (Y204A/Y206A Rescue) was produced by recombining the WT sequence back into the Y204A/Y206A BAC using primers outlined in Table 4.1
and transfecting this BAC into PolB3 cells. The presence of the designed mutation(s) was confirmed by sequencing the BAC prior to transfection, and viral DNA from plaque purified virus was purified from infected cells for sequencing of the entire *pol* coding sequence to ensure that no other *pol* mutations were present in the recombinant viruses.

Table 4.1. NTD substitutions designed in and around the RNP motif. The rationale and primers used to generate the recombinant HSV-1 viruses containing these mutations are also listed.

Mutant	Rationale	Primer
E294Q	Conserved residues adjacent to putative RNA-binding domain that could be binding metal ions required for catalysis	GTACCTGTGCGACAACTTCTGCCCGGCCATCA AGAAGTACCAGGGTGGGGTCGACGCCACCTA GGGATAACAGGGTAATCGATTT (forward)
		TTGTCCAGGATGAACCGGGTGGTGGCGTCGA CCCCACCCTGGTACTTCTTGATGGCCGGGCGC CAGTGTTACAACCAATTAACC (reverse)
E294N/D306N	Same as above	GTACAACGGTGGGGTCGACGCCACCACCCGG TTCATCCTGAACAACCCCGGGTTCGTCACCTT CTAGGGATAACAGGGTAATCGATTT (forward)
		GTTTGAGACGGTACCAGCCGAAGGTGACGAA CCCGGGGTTGTTCAGGATGAACCGGGTGGTG GCGCCAGTGTTACAACCAATTAACC (reverse)
R255A	Conserved positively-charged residues in putative RNA-binding pocket that could interact with RNA backbone	GCGGCATCTCCGCGGACCACTTCGAGGCGGA GGTGGTGGAGGCCACCGACGTGTACTACTAC GAGTAGGGATAACAGGGTAATCGATTT (forward)
		GTAAAACAGAGCGGGGCGCGTCTCGTAGTAG TACACGTCGGTGGCCTCCACCACCTCCGCCTC GAAGCCAGTGTTACAACCAATTAACC (reverse)
R255A/R270A	Same as above	GACGTGTACTACTACGAGACGCGCCCCGCTCT GTTTTACGCCGTCTACGTCCGAAGCGGGTAGG GATAACAGGGTAATCGATTT (forward)
		GCACAGGTACGACAGCACGCGCCCGCTTCGG ACGTAGACGCGGTAAAACAGAGCGGGGCGCG GCCAGTGTTACAACCAATTAACC (reverse)
Y204A	Conserved aromatic residues in putative RNA-binding pocket that could interact with RNA bases	GGCCACCGGGTGGCCGTTCACGTTTACGGCAC GCGGCAGGCCTTTTACATGAACAAGGAGGTA GGGATAACAGGGTAATCGATTT (forward)
		GTAGGTGCCTGTCAACCTCCTCCTTGTTCATG TAAAAGGCCTGCCGCGTGCCGTAAACGTGCC AGTGTTACAACCAATTAACC (reverse)

Table 4.1 (Continued)

Y206A	Same as above	CCGGGTGGCCGTTCACGTTTACGGCACGCGGC AGTACTTTGCCATGAACAAGGAGGAGGTTGT AGGGATAACAGGGTAATCGATTT (forward)
		GCGGCATTGTAGGTGCCTGTCAACCTCCTCCT TGTTCATGGCAAAGTACTGCCGCGTGCCGTGC CAGTGTTACAACCAATTAACC (reverse)
Y204A/Y206A	Same as above	AGGCCACCGGGTGGCCGTTCACGTTTACGGC ACGCGGCAGGCCTTTGCCATGAACAAGGAGG AGGTTGTAGGGATAACAGGGTAATCGATTT (forward)
		GCGGCATTGTAGGTGCCTGTCAACCTCCTCCT TGTTCATGGCAAAGGCCTGCCGCGTGCCGTAA ACGTGCCAGTGTTACAACCAATTAACC (reverse)
Y204A/Y206A Rescue	Rescued derivative of Y204A/Y206A mutant	GCCACCGGGTGGCCGTTCACGTTTACGGCACG CGGCAGTACTTTTACATGAACAAGGAGGAGG TTAGGGATAACAGGGTAATCGATTT (forward)
		GGCATTGTAGGTGCCTGTCAACCTCCTCCTTG TTCATGTAAAAGTACTGCCGCGTGCCGTAAAC GCCAGTGTTACAACCAATTAACC (reverse)

Plating Efficiency and Plaque Diameter Analysis

Plaque purified viruses were titrated on PolB3 cells and used to infect $5x10^6$ PolB3 cells at an MOI of 0.1. Five days post infection, the cells were scraped, pelleted at 1000 x g for 10 minutes, and resuspended in 1.5 ml of DMEM containing 5% NCS. Resuspended cells were freeze-thawed and sonicated in a cup horn sonicator (Branson Ultrasonics) for 2x 20 seconds with a minute break between. The resulting lysates were centrifuged for 10 minutes at 3000 xg, and the supernatants were serial diluted in DMEM with 5% NCS for titration in triplicate on Vero and PolB3 cells in 12-well plates ($2x10^5$ cells/well). Wells were infected with 0.2 ml of the resulting serial dilutions, incubated at 37˚C for one hour, and the cells were covered with 2 ml of

DMEM with 5% NCS and methyl cellulose. 72 hours post infection (hpi), the cells were fixed, stained with crystal violet, and plaques were counted.

The crystal violet-stained plates were imaged under 20x magnification using a digital camera, and the diameter of the plaques was assessed using ImageJ software (NIH). These plaque diameters were compiled using GraphPad Prism software and analyzed for statistical significance using one-way analysis of variance (ANOVA) with Šídák correction for multiple comparisons.

Replication kinetics

Vero or PolB3 cells in 24-well dishes ($1x10^5$ cells/well) were infected in triplicate at an MOI of 10. After a 1-hour adsorption period at 37°C, wells were washed three times with DPBS and replenished with 0.2 ml of DMEM containing 5% newborn calf serum. The supernatant was collected from the cells at 1, 4, 8, 12, and 24 hpi and flash frozen. The supernatants from each time point were thawed and titrated on either Vero or PolB3 cells (see above).

Viral Genome Quantification

Vero (and PolB3) cells in 24-well dishes were infected at an MOI of 10 in triplicate as above, and cell lysates were collected at 1, 8, and 12 hpi. Lysates were diluted twenty-fold and DNA was purified alongside mock lysate and spiked viral genome standards. Samples were amplified using primers specific to the viral *thymidine kinase* (TK) gene or the cellular *1,3-alpha-galactosyltransferase* gene, *tk* values were compared to a standard curve of spiked KOS viral genomes, and the amounts of cellular DNA detected in each sample were used to normalize viral DNA values as previously described (Terrell & Coen, 2012). The resulting genome copy

numbers were compiled using GraphPad Prism software and divided by the copy numbers of the one-hour post infection samples to generate a fold-change in viral copy number over the input at 8 or 12 hours post infection. These data were analyzed using one-way ANOVA with Šídák correction for multiple comparisons.

Protein Expression Determination

Vero and PolB3 cells ($4x10^5$ cells/well) were infected at an MOI of 10 or mock-infected with media. At 8 hours post infection, the cells were washed 3x with DPBS and lysed in 2x Laemmli buffer (Bio-Rad) containing β-mercaptoethanol and complete protease inhibitors (Roche). Samples were heated at 95˚C for 5 minutes and run on a 4-20% polyacrylamide SDS-PAGE gel (Bio-Rad), transferred onto polyvinylidene difluoride (PVDF) membrane, blocked with 5% milk in DPBS-T (DPBS with % Tween 20), and probed using the following antibodies overnight at 4˚C: α-Pol (mouse 1051c, generously provided by C. Knopf; 1:1000), α-FLAG (mouse M2, Sigma-Aldrich; 1:500), α-TK (goat polyclonal, generously provided by W. Summers; 1:1000), α-ICP8 (383 rabbit polyclonal, generously provided by D. Knipe), and α-β-Actin (8226, Abcam; 1:1000). Membranes were washed three times with DPBS-T for 5 minutes at room temperature with rocking and subsequently incubated with secondary antibodies conjugated to horseradish peroxidase (HRP) (Southern Biotech) at 1:1000 for 1 hour at room temperature with rocking, followed by another three 5-minute washes in DPBS-T. Finally, chemiluminescence solution (Pierce) was added to detect signal from the membranes using film.

Localization of HSV Pol During Infection

Infected (MOI 5) PolB3 cells or Vero cells ($1x10^5$ cells/coverslip) treated with either DMSO or 400 μg/ml PAA were incubated at 37˚C for 8 hours, washed three times with DPBS, fixed at room temperature with 3.7% formaldehyde in DPBS for 15 minutes, and washed another 3 times with DPBS. Cells were then permeabilized at room temperature for 10 minutes using 0.1% Triton-100 in DPBS and blocked overnight in 1% bovine serum albumin (BSA; Sigma) in DPBS. The following dilutions in DPBS with 1% BSA were used for primary staining: rabbit anti-ICP8 1:500 (383, generously provided by D. Knipe), and mouse anti-FLAG antibody 1:500 (M2, Sigma-Aldrich). Primary antibodies were added to the coverslips for one hour at room temperature with rocking. Then, the cells were washed three times with DPBS for 5 minutes each at room temperature and the staining was repeated with the appropriate fluorescently-labeled Alexa Fluor 488 and 568 secondary antibodies (ThermoFisher). The coverslips were stained with 2 μg/ml DAPI during the last 10 minutes of the secondary staining. After another three 5-minute washes with DPBS, the coverslips were mounted on #1.5 glass slides using ProLong antifade reagent (Invitrogen). Imaging was performed using a Yokogawa CSU spinning disk confocal mounted on a Nikon Ti inverted microscope equipped with a Nikon 100x / 1.45 NA Plan Apo λ objective lens and an ORCA-AG cooled charge-coupled device camera (Hamamatsu). Fluorescence was excited with 488 or 561nm laser lines and collected with ET525/50m and ET620/60m emission filters (Chroma) respectively. Post-acquisition image analysis was conducted using MetaMorph and ImageJ software.

Polymerase Activity Assay

Activated salmon sperm DNA was generated by combining 2.5 mg/ml salmon sperm DNA (ThermoFisher), 10 mM HEPES (pH 7.5), and 5 mM magnesium chloride (final concentrations). Forty ng/mg of DNA of DNase I (NEB) was added, and the reaction was allowed to proceed at 60˚C for 5 minutes. The DNA was purified using phenol-chloroform extraction and resuspended in distilled water.

The filter-binding polymerase assay was adapted from that of Gibbs et al. (Gibbs et al., 1991). 293T cells ($2x10^6$ cells) infected at an MOI of 5 or mock-infected were incubated at 37˚C for 8 hours, washed 3 times with DPBS, spun down for 10 minutes at 1000 x g, and resuspended in 200 µl cold lysate buffer (20 mM HEPES pH 7.5, 1 mM EDTA, 100 mM NaCl, 10 mM β-mercaptoethanol). The lysates were kept at 4˚C for the following steps: sonication for 2 x 40 seconds in a cup horn sonicator (Branson Ultrasonics) with a minute between sonication steps, centrifugation at 13,000 x g for 10 minutes, and preincubation of 5 µl of supernatant from the cell lysates, 500 µg/ml activated salmon sperm DNA, 60 µM each dNTP minus dTTP, 5 µM ^{32}P-dTTP, 100 mM ammonium sulfate, 20 mM HEPES pH 7.5, 1.0 mM EDTA, 0.5 mM dithiothreitol, 10% glycerol, and either 100 µg/ml phosphonoacetic acid or DMSO, as indicated (final concentrations, 50 µl total). The reactions were started with the addition of 8 µM magnesium chloride, and the assays proceeded for 20 min at 37˚C. The reactions were stopped by precipitation with 10% TCA (final concentration), allowed to sit on ice for 10 minutes, bound to a GF/C filter (GE), washed twice with 10% TCA, and washed once with 100% ethanol. Five ml of scintillation fluid was added, and the samples were immediately analyzed using scintillation counting to determine the incorporation of radioactive dTTP into the activated salmon sperm DNA. For analysis, the cpm for three different experiments were entered using

GraphPad Prism software, and the values were compared to the percentage of the WT samples from each experiment for normalization prior combining the data for the graph. Error bars indicate the standard deviations.

Results

Substitutions within the RNP motif of the HSV Pol NH_2-terminal domain exhibit severe defects in viral replication.

To investigate the role of the NTD of HSV Pol during infection, we generated several mutations within conserved residues in and around the RNP motif. These mutations were all specifically designed in conserved residues among human herpesviruses in and around the RNP motif that could potentially: interrupt potential metal ion coordination that might be associated with a 5'-3' RNase H activity (E294Q, E294N/D306N) (Ceska & Sayers, 1998; S. Liu et al., 2006), make ionic bonds with the negatively-charged backbone of the RNA (R255A, R255A/R270A) (Bandziulis et al., 1989; Birney et al., 1993), or form base-stacking interactions with RNA (Y204A, Y206A, Y204A/Y206A) (Bandziulis et al., 1989; Birney et al., 1993; Ceska & Sayers, 1998; Matsui et al., 2004). These mutations were recombined into BACs and transfected into a PolB3 cell line (generously provided by C. Hwang) that inducibly expresses WT Pol during infection and can complement HSV *pol*-null mutants (Hwang et al., 1997). Then, the viruses were plaque purified, expanded on PolB3 cells, and titrated to test plaque formation on non-complementing Vero cells and the complementing PolB3 cells.

First, we compared the plating efficiency (PFU/ml determined on Vero cells divided by the PFU/ml determined on PolB3 cells times 100) of these viruses on Vero and PolB3 cells (Figure 4.3A and Table 4.2). Whereas WT could efficiently form plaques in either Vero or PolB3 cells, exhibiting a 48% plating efficiency that may have been due to error introduced into the assay or the low number of replicates, the negative control HP66, which has the *E. coli lacZ* gene replacing much of the *pol* gene (Marcy, Yager, et al., 1990) was unable to replicate on Vero cells but could form plaques on PolB3s. Each of the NTD mutant viruses tested was

Figure 4.3. Mutations made within conserved residues of the HSV Pol RNP motif severely affect viral replication and protein expression. A) Plaque formation analysis of the denoted viruses titrated side-by-side on Vero and PolB3 cells. The lower limit of the vertical axis denotes the limit of detection in this assay and the error bars denote the standard deviation. B) The RNP mutants except for Y204A/Y206A are severely inhibited for Pol expression during infection. Western blots of cell lysates collected at 8 or 16 hours post infection and detected using antibodies specific for the proteins listed on the left and in the text. Whereas the antibody for Pol detects protein expressed both by the virus and the PolB3 cells, the FLAG antibody only detects Pol expression from the virus and does not detect expression of the WT *pol* gene in PolB3 cells.

Figure 4.3 (Continued)

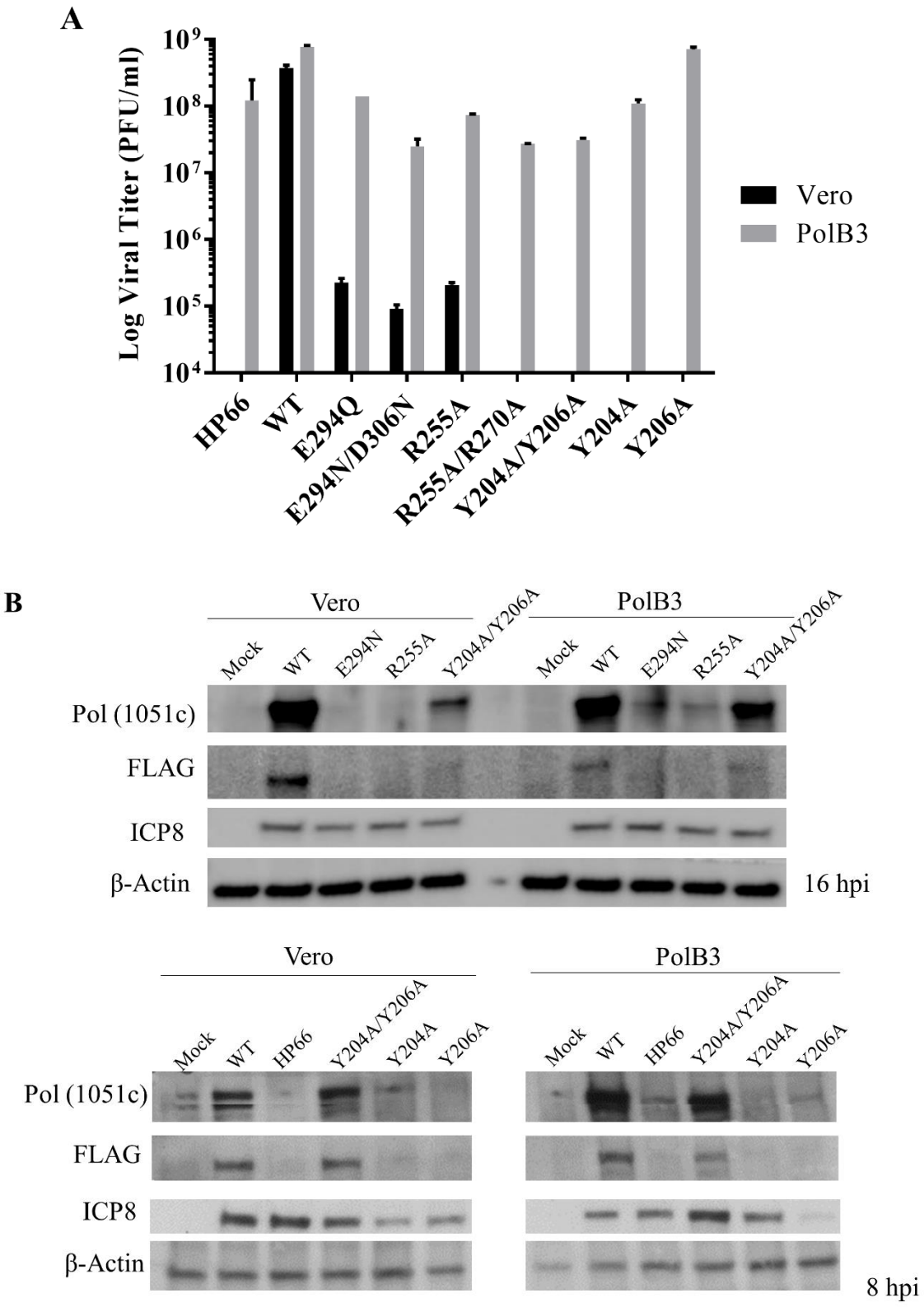

Table 4.2. Plating efficiency of the mutants generated with substitutions in and around the RNP motif of the HSV Pol NTD. Plating efficiency was calculated as the number of plaque forming units calculated on PolB3 cells divided by the plaque forming units calculated on Vero cells and reported as a percentage. ND: not detected, formed no plaques on Vero cells.

Virus	Plating Efficiency (%)
HP66	ND
WT	48
E294Q	0.16
E294N/D306N	0.36
R255A	0.29
R255A/R270A	ND
Y204A/Y206A	ND
Y204A	ND
Y206A	ND

significantly inhibited for plaque formation on Vero cells, varying from about 300-600-fold defects in replication (E294Q, E294N/D306N, and R255A) to viruses that did not form plaques even at a 10-fold dilution, the lowest tested (R255A, R255A/R270A, Y204A, Y206A, and Y204A/Y206A). Upon further analysis, the three viruses that were able to form plaques on Vero cells (E294Q, E294N/D306N, and R255A) were mixed with WT virus sequences. All of the RNP mutant viruses formed plaques efficiently on PolB3 cells, like the HP66 virus, however.

The finding of WT Pol sequences mixed in with the mutant that had been previously plaque purified suggests that these WT viruses are likely due to WT BAC contamination, WT virus contamination, or, most likely, reversion of these viruses to the WT sequence, either through mutagenesis or by recombination with a WT sequence from the PolB3 cells or other virus. Because the PolB3 cells are unable to completely complement the WT Pol expression from the virus, this would also generate an environment where WT virus replication is favored over the mutants, which would have exacerbated the result of any reversion to the WT sequence.

Due to the presence of WT virus in some of the stocks, and because each of the viruses except for the Y204A/Y206A virus showed a phenotype like D368A Pol (Chapter 3), with drastically decreased expression of HSV Pol (examples in Figure 4.3B), only the Y204A/Y206A Pol virus was further characterized in this study. The Y204 and Y206 residues are highlighted in bright pink in Figure 4.1; these two conserved tyrosines are in a similar orientation to aromatic residues within the RNP A1 structure that have been shown to make base-stacking interactions with RNA (S. Liu et al., 2006; Shamoo et al., 1997).

The WT virus was able to form plaques efficiently both on the Vero and PolB3 cells (Figure 4.4A), exhibiting a plating efficiency of 120%. The negative control, HSV-1 HP66 virus, was unable to form plaques on Vero cells but could form plaques efficiently on PolB3

Figure 4.4. NTD mutant Y204A/Y206A Pol virus replication is severely inhibited in non-complementing cells and exhibits a moderate defect in complementing cells. A) Plaque formation analysis of the denoted viruses titrated side-by-side on Vero and PolB3 cells. The lower limit of the vertical axis denotes the limit of detection in this assay. B) Twenty times magnification images of plaque assays showing infection of PolB3 cells fixed at 72 hours post infection (hpi) and stained with crystal violet. C) Plaque diameters for each denoted virus on PolB3 cells analyzed using one-way analysis of variance (ANOVA) with Šídák correction for multiple comparisons. *: p-value <0.0001, ns: not statistically significant. D) Viral supernatants collected from Vero cells (left column) or PolB3 cells (right column) infected with the indicated viruses at the times post infection (MOI of 10) shown on the x-axis were titrated on either PolB3 cells (top row) or Vero cells (bottom row). The 24 hpi time point was analyzed using one-way analysis of variance (ANOVA) with Šídák correction for multiple comparisons, and the p-values are listed.

Figure 4.4 (Continued)

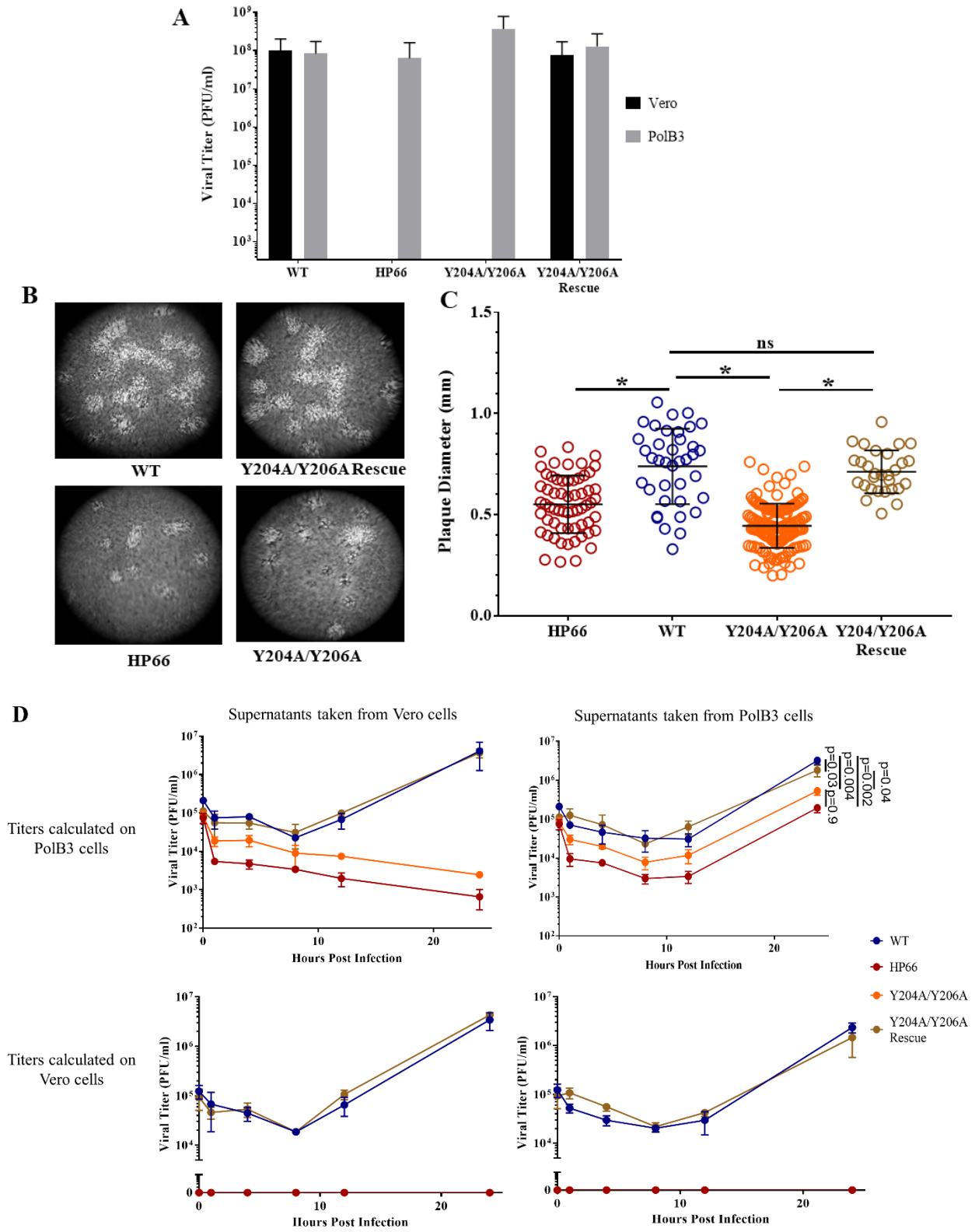

cells. The RNP mutant Y204A/Y206A virus was unable to form any plaques on Vero cells, similar to the HP66 virus, but the plaque formation phenotype was rescued on the PolB3 cell line (Figure 4.4A). A rescued derivative of the Y204A/Y206A Pol virus, Y204A/Y206A Rescue, could also form plaques efficiently on Vero cells (Figure 4.4A), exhibiting a plating efficiency of 60%. Therefore, the Y204A/Y206A mutations severely inhibit viral plaque formation in the absence of complementing Pol protein.

The Y204A/Y206A Pol virus exhibits a moderate effect on replication kinetics in complementing PolB3 cells, like a *pol*-null mutant.

Upon discovering that the Y204A/Y206A mutant virus was unable to form plaques on Vero cells, we next wanted to assess whether there was a small plaque phenotype on PolB3 cells like the D368A and HP66 viruses (see Chapter 3). So, we imaged the crystal violet stained plates (Figure 4.4B) and quantified the plaque diameter using ImageJ software (Figure 4.4C). The plaques formed by the HP66 and Y204A/Y206A Pol virus infection of PolB3 cells were significantly smaller than those of the WT and the Y204A/Y206A Rescue viruses, suggesting that while these viruses can form plaques efficiently, they are less efficient at replication or spread to surrounding cells with the amount of WT Pol expressed from the PolB3 cells. We determined that Pol expression is drastically lower in infected PolB3 cells than WT infection (Chapter 3), suggesting that this Y204A/Y206A virus phenotype is also due to a defect in the polymerase expression and/or activity.

Because we had determined that the D368A and HP66 viruses showed a moderate replication defect in viral replication on PolB3 cells and saw a similar small plaque phenotype, we next wanted to test the single cycle growth curves of the Y204A/Y206A virus. So, Vero cells

(Figure 4.4D, left column) and PolB3 cells (Figure 4.4D, right column) were infected with the corresponding viruses at a high multiplicity of infection, and the lysates were titrated to identify the viral titer on either PolB3 cells (Figure 4.4D, top row) or Vero cells (Figure 4.4D, bottom row). The positive controls, WT Pol and Y204A/Y206A Rescue viruses, were able replicate to high titer on either Vero or PolB3 cells by 24 hours post infection (Figure 4.4D). The negative control, HP66, and the Y204/Y206A mutant were unable to produce any plaque forming units or recover from the initial drop in infectivity on Vero cells (Figure 4.4D, top left). Whereas the HP66 virus displayed a ~15-fold replication defect compared to WT (Figure 4.4D, top right), the Y204A/Y206A virus exhibited about a 5-10-fold defect in replication on PolB3 cells compared to the WT and Y204A/Y206A Rescue virus. When these viruses were titrated on Vero cells, and we were unable to detect any recombinant WT virus being produced, suggesting that we have a homogeneous viral stock (Figure 4.4D, bottom row). These results agree with the smaller plaque size phenotype we identified on PolB3 cells (Figure 4.4B-C), and with other effective Pol-null mutants, suggesting that the Y204A/Y206A virus is severely deficient in viral replication in the absence of complementation.

Y204A/Y206A Pol virus does not detectibly synthesize viral DNA during infection.

Upon discovering that the Y204A/Y206A Pol virus was incapable of replication on non-complementing cells, we wanted to study whether these RNP motif mutations were affecting viral DNA synthesis. So, we used qPCR to identify the fold change in viral genome copy number in infected cells from 1 hpi to 8 and 12 hpi (Figure 4.5A). The WT and Y204A/Y206A Rescue viruses were able to efficiently synthesize viral DNA above the input number of copies by at least 40-fold at 12 hpi. HP66, in contrast, was unable to produce any viral DNA copies

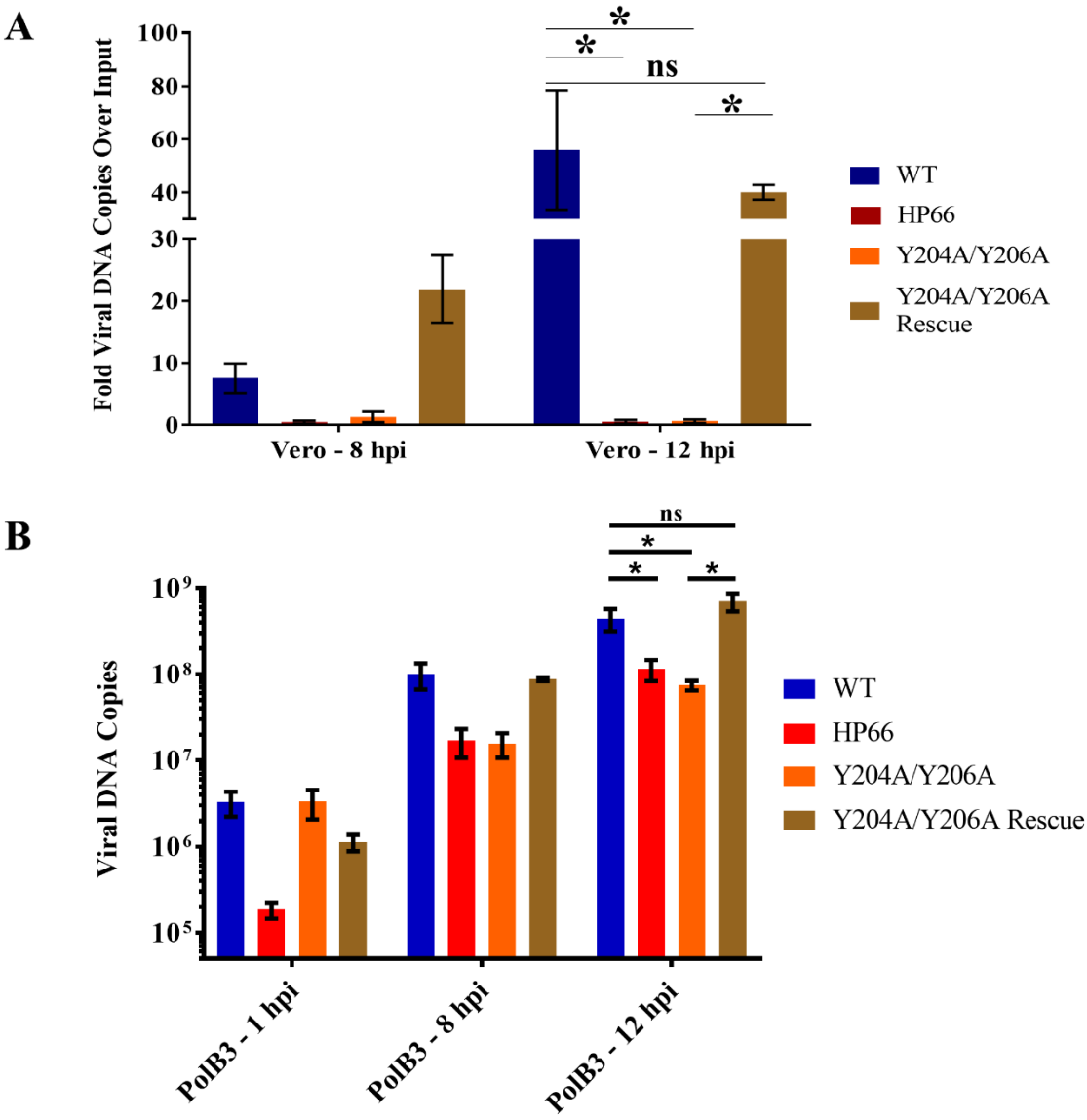

Figure 4.5. Y204A/Y206A Pol virus is severely deficient in viral DNA synthesis. A) qPCR analysis of viral genome copy numbers from Vero cell lysates collected at 8 and 12 hpi compared to those present following adsorption (1 hour post-infection) analyzed using one-way analysis of variance (ANOVA) with Šídák correction for multiple comparisons. *: $p<0.002$, ns: not statistically significant. B) qPCR analysis of viral genome copy numbers from PolB3 cells collected at 1, 8, and 12 hpi analyzed using one-way analysis of variance (ANOVA) with Šídák correction for multiple comparisons. *: $p<0.0006$, ns: not statistically significant.

above those present at 1 hpi. The Y204A/Y206A Pol virus also incapable of viral DNA synthesis, and, like the HP66 virus, was unable to produce any copies of the viral genome above those present during the initial infection. Additionally, infection of PolB3 cells was able to rescue Y204A/Y206A viral DNA synthesis, though with statistically significant defects (Figure 4.5B), suggesting that this defect is specific to these mutations in the *pol* gene. These results show that substitutions in the RNP motif of HSV Pol severely inhibit DNA synthesis.

Expression of Y204A/Y206A Pol during infection is similar to WT Pol.

Since we have previously determined that point mutations in HSV Pol can lead to severe defects in protein expression during infection (Chapter 3), we next tested the expression of this enzyme using Western blot. We detected robust Pol expression during WT infection in both Vero and PolB3 cells using both a Pol-specific antibody and antibody against the FLAG tag on the HSV Pol expressed from the virus by 8 hpi and through 12 hpi (Figure 4.6-7), at which time we were able to see efficient viral DNA synthesis by qPCR (Figure 4.5A). As previously described (Chapter 3), HP66 Pol expression is not detectable in Vero cells, and expression of the Pol gene from the PolB3 cells as identified by the Pol-specific antibody is at least 8-fold lower than WT Pol expression based on a dilution series (Figure 4.6). The Y204A/Y206A virus, unlike the D368A and HP66 mutants, was able to robustly express HSV Pol during infection, exhibiting less than a 2-fold expression defect compared to the WT virus. Additionally, expression of the Y204A/Y206A Pol in Vero cells was at least 8-fold greater than following HP66 infection of PolB3 cells (Figure 4.6). As this level of Pol expression was sufficient to permit viral plaque formation and replication (Figure 4.4), the Y204A/Y206A mutant Pol expression from the virus, as displayed using the FLAG antibody, is more than enough to mediate plaque formation.

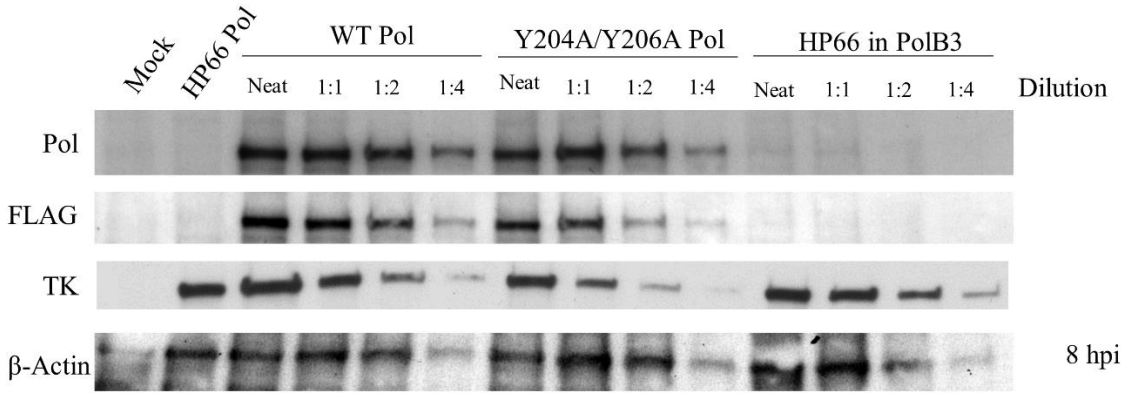

Figure 4.6. Y204A/Y206A Pol expression during infection is similar to the WT virus. Western blots of lysates from Vero cells (except for the HP66 infection of PolB3 cells as indicated) collected at 8 hours post infection and detected using antibodies specific for the proteins listed on the left and in the text. Whereas the antibody for Pol detects protein expressed both by the virus and the PolB3 cells, the FLAG antibody only detects Pol expression from the virus and does not detect expression of the WT *pol* gene in PolB3 cells. Numbers above the images denote a two-fold dilution series of the corresponding samples for more quantitative comparison of protein expression.

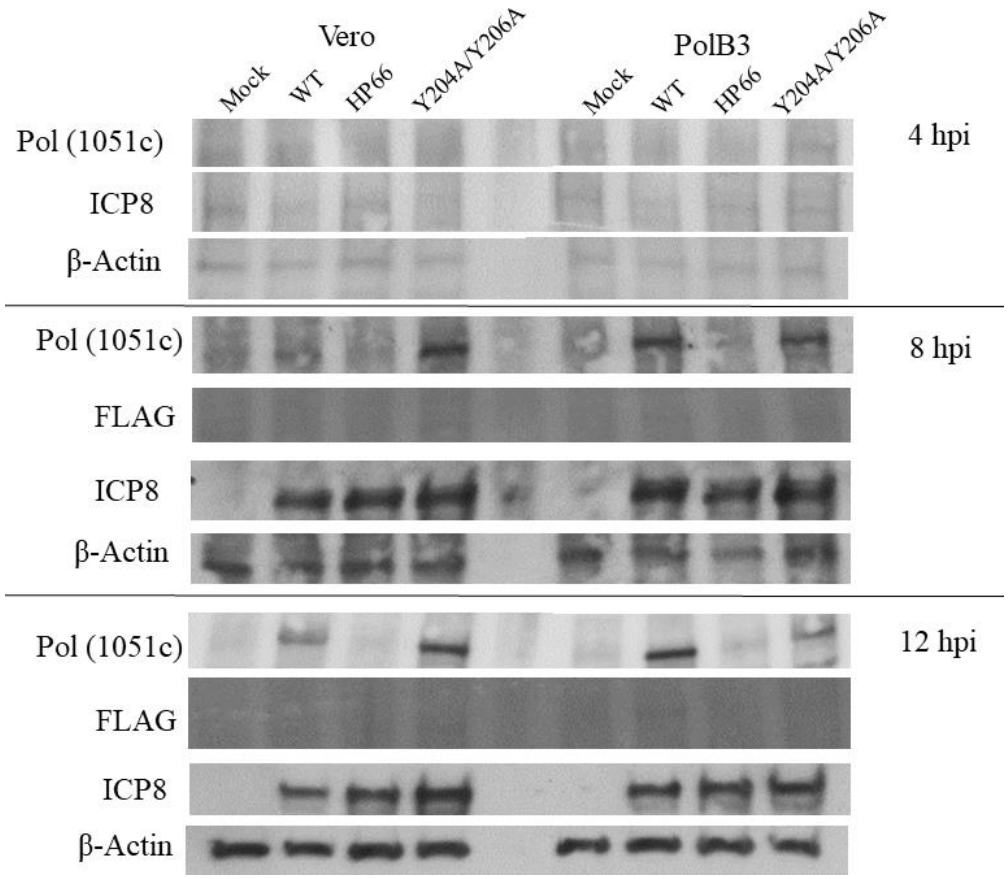

Figure 4.7. Y204A/Y206A Pol expression does not greatly differ from WT at 4, 8, or 12 hours post infection. Western blots of cell lysates collected at 4, 8, and 12 hours post infection and detected using antibodies specific for the proteins listed on the left and in the text. Whereas the antibody for Pol detects protein expressed both by the virus and the PolB3 cells, the FLAG antibody only detects Pol expression from the virus and does not detect expression of the WT *pol* gene in PolB3 cells.

Figure 4.8. Y204A/Y206A Pol localizes in Vero cells to punctate nuclear structures resembling those formed upon treatment of infected cells with HSV Pol inhibitor PAA. Vero or PolB3 cells (denoted on the left of the images) treated with either DMSO or PAA were fixed at 8 hpi, permeabilized, and stained with: DAPI to identify cell nuclei (blue), M2 anti-FLAG antibody to determine the localization of polymerase being expressed by the recombinant viruses (green), and rabbit anti-ICP8 Ab 383 to identify replication compartment structures and prereplicative sites (red).

Figure 4.8 (Continued)

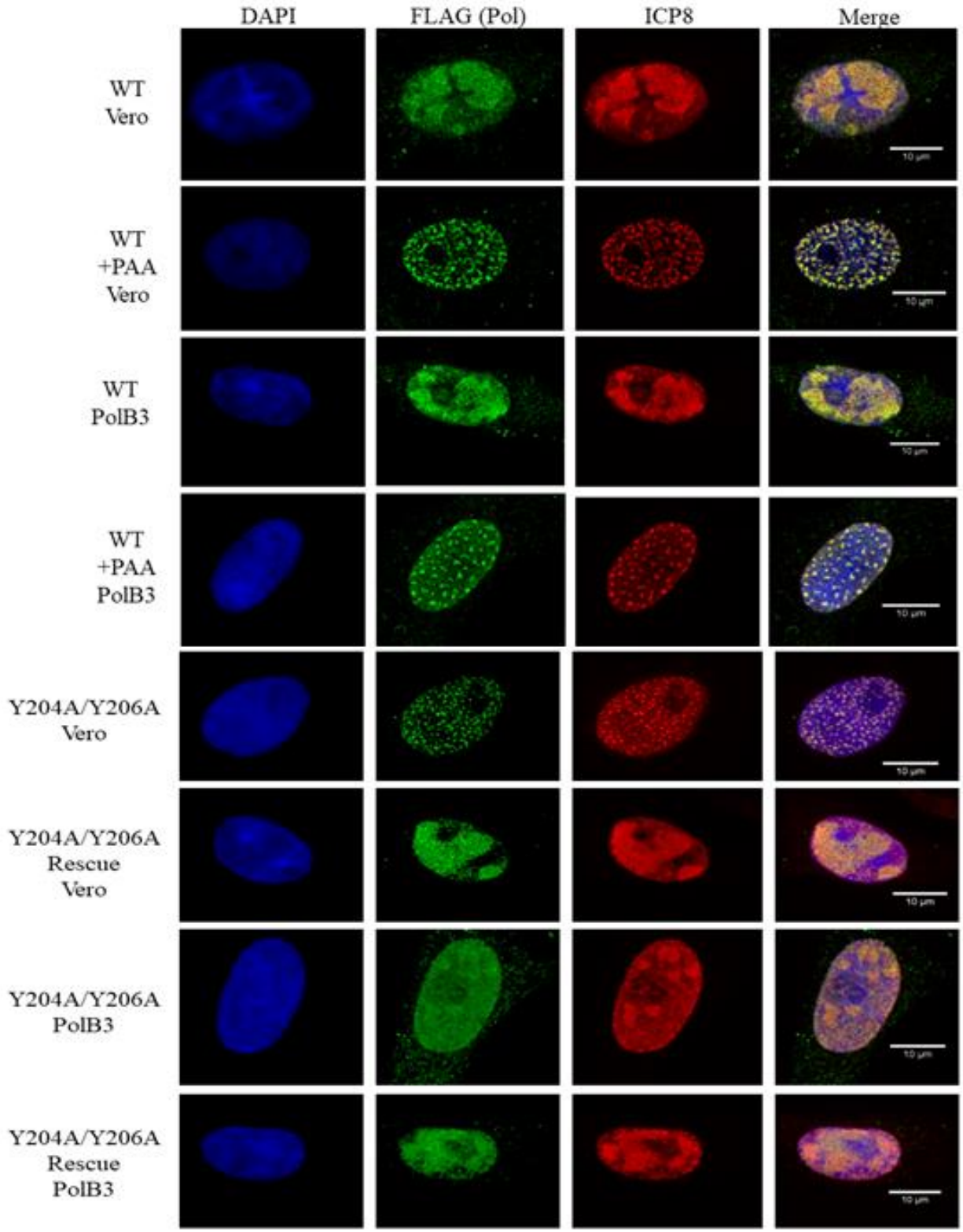

Additionally, when Pol expression is analyzed over a time course at 4, 8, and 12 hpi, we were unable to visualize any detectable differences in expression, suggesting that regulation of HSV Pol expression does not seem to be drastically affected during infection (Figure 4.7).

Y204A/Y206A Pol localizes to the nucleus and colocalizes with ICP8 at punctate structures resembling treatment with a viral DNA synthesis inhibitor.

Because we were able to detect expression of Y204A/Y206A Pol in infected cells, we next wanted to determine whether this mutant protein was able to localize to the nucleus and colocalize with other viral replication machinery, as either of these could affect viral DNA synthesis. To test the localization of Y204A/Y206A during infection, we used immunofluorescence microscopy. Either Vero or PolB3 cells were infected, fixed at 8 hpi, and antibodies were used to detect the following proteins. Antibody against the FLAG tag was used to detect Pol expressed from the viruses (and not Pol expression from the PolB3 cells), and antibody against ICP8, the HSV-1 single-stranded DNA binding protein, demarcated prereplicative sites and replication compartments in the nuclei of infected cells and was used to determine colocalization with a viral DNA replication protein (rabbit 38-3 anti-ICP8 antibody was a generous gift from the Knipe lab). We also visualized WT-infected cells treated with 400 μg/ml phosphonoacetic acid (PAA), an inhibitor of HSV-1 viral DNA replication, as a control for cells which were inhibited for DNA replication (Purifoy, Lewis, & Powell, 1977). Upon infecting either PolB3 cells or Vero cells with the WT and Y204A/Y206A Rescue viruses, large replication compartments containing colocalized ICP8 and Pol were visible in the nuclei (Figure 4.8). PAA-treated WT-infected Vero and PolB3 cells displayed small, punctate structures resembling prereplicative sites dispersed throughout the nucleus where Pol and ICP8 both

localized, similar to previous reports of the localization of these enzymes upon viral DNA replication inhibition (Liptak et al., 1996; Taylor et al., 2003). Infection of Vero cells with the Y204A/Y206A virus showed a phenotype similar to treatment with PAA, displaying punctate structures containing colocalized ICP8 and Pol within the nucleus. These results corroborated our qPCR data showing that the Y204A/Y206A virus was highly defective for viral DNA synthesis. In the presence of complementing WT Pol expression from the PolB3 cells, however, the Y204A/Y206A Pol (marked by anti-FLAG antibody) was able to localize to large replication compartments, showing that this mutant is able to localize to sites of viral DNA synthesis during infection and is not exclusively confined to these punctate structures. Therefore, the defect in viral DNA synthesis associated with the RNP motif mutant Y204A/Y206A is not attributable to a lack of Pol expression, inability to enter the nucleus, or inability to localize to sites of viral DNA synthesis.

Y204A/Y206A virus-infected cell lysates exhibit polymerase activity *in vitro*.

We next tested whether the DNA synthesis defects associated with the Y204A/Y206A mutant virus were attributable to loss of the polymerase activity of the enzyme. We utilized an assay (Gibbs et al., 1991) that takes advantage of HSV Pol stimulation in the presence of high ammonium sulfate concentrations. At these high salt concentrations, cellular polymerases are inhibited and HSV Pol is unaffected and potentially stimulated (Weissbach et al., 1973), allowing quantification of viral polymerase activity *in vitro* with infected cell lysates by assessing radiolabeled dNTP incorporation into activated salmon sperm DNA (Figure 4.9). Treatment with the HSV-1 DNA polymerase inhibitor PAA further confirmed that any activity seen in these lysates was specific to HSV Pol. To account for the variability in radioactivity

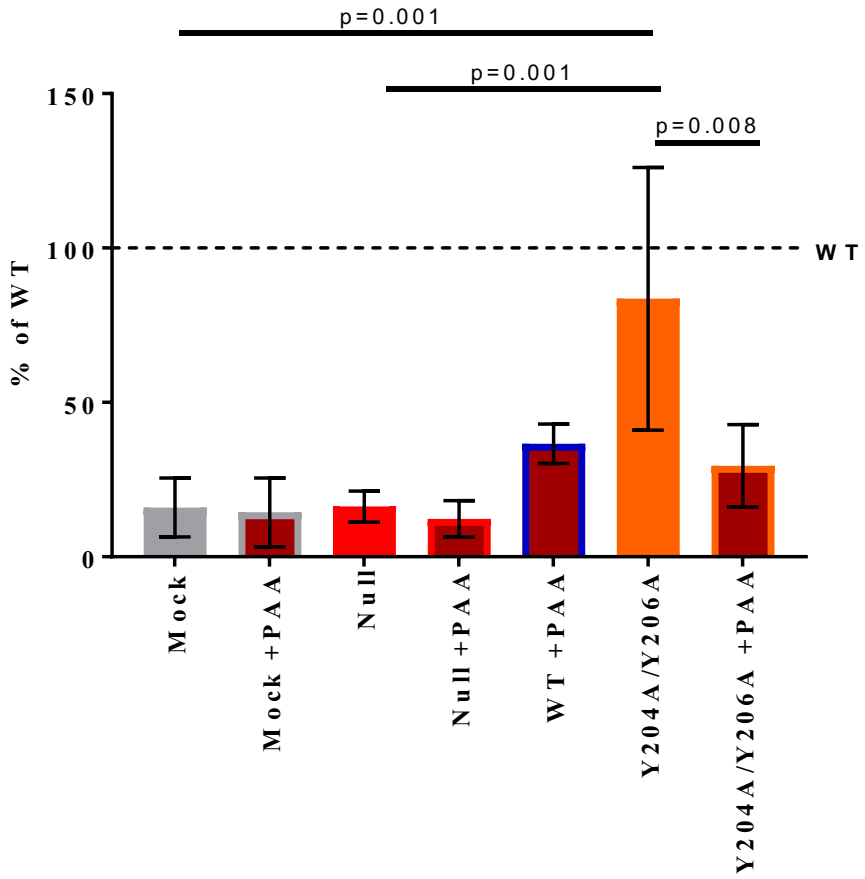

Figure 4.9. Y204A/Y206A Pol virus exhibits detectable ammonium sulfate-resistant polymerase activity in infected cell lysates. Graph displaying ^{32}P-dTTP incorporated into activated salmon sperm DNA in the presence of high ammonium sulfate concentrations from infected 293T cells lysates compared to the WT incorporation after 20 minutes in the presence or absence of HSV-1 Pol inhibitor PAA. The data from three assays were combined and plotted as a percentage of incorporated radioactivity compared to WT Pol (the dotted line), with the standard deviations denoted by the error bars and analyzed using one-way analysis of variance (ANOVA) with Šídák correction for multiple comparisons.

counts between assays, we compared the cpm values to those of the WT-infected lysates to determine the percentage of WT activity.

Incorporation of radiolabeled dNTPs was drastically lower in the HP66 and mock-infected lysates than in those infected with the WT virus (Figure 4.9). Additionally, the activity detected in the mock and HP66 cell lysates was resistant to PAA treatment. Incorporation detected from the WT-infected cell lysates decreased in the presence of PAA, however, suggesting that the detected activity is specific to HSV Pol. The Y204A/Y206A mutant Pol also exhibited polymerase activity significantly greater than the mock- and HP66-infected cell lysates, and this incorporation was significantly inhibited by the addition of PAA. The amount of radioactivity incorporated by the Y204A/Y206A-infected cell lysates was variable relative to WT in each assay (ranging from 40-125% of the WT activity), but in each case was significantly sensitive to PAA treatment by 2-4-fold, suggesting that these lysates contain HSV Pol-specific polymerase activity well above background despite the virus being incapable of replicating viral genomes in cell culture (Figure 4.5A). As the amount of Pol expression induced during HP66 infection of PolB3 cells is at least 8-fold lower than Pol expressed during WT Pol infection (Figure 4.6) but generated plaques (Figure 4.4A), we conclude that the defect in HSV replication and DNA synthesis associated with the Y204A/Y206A is largely attributable to a defect separate from the polymerase activity of this enzyme. We hypothesize that the lack of detectable viral DNA synthesis during infection (Figure 4.5A) is due to the generation of multiple stalled replication forks that are unable to be resolved in the absence of lagging strand synthesis.

Discussion

The Y204A/Y206A Pol substitutions within the RNP motif of the NTD of HSV-1 Pol caused a severe viral replication defect in cell culture and ablated viral DNA synthesis during infection without exhibiting any meaningful effects on Pol expression, localization, or polymerase activity. Based on these results, we conclude that the RNP motif of HSV Pol plays a role in viral DNA synthesis separate from the polymerase activity.

Interestingly, we did not detect any viral DNA synthesis occurring during replication by qPCR (Figure 4.9) despite being able to detect polymerase activity *in vitro* (Figure 4.5A). We hypothesize that the lack of detectable viral DNA synthesis during infection (Figure 4.5A) is due to the generation of multiple stalled replication forks that are unable to be resolved in the absence of lagging strand synthesis. Another possibility is that the activity associated with this mutant is somehow related to resolving the transition from theta replication to a rolling circle mechanism, in which case only small amounts of DNA would be synthesized before stalling as well. Further work should be done to determine the exact defect associated with this mutant.

RNP motifs have been structurally identified in the NTDs of several Family B polymerases from different species including phage RB69 Pol, eukaryotic Pol δ, and archaebacterial *Desulfurococcus* strain Tok Pol and *Thermococcus* sp. 9°N-7 Pol (S. Liu et al., 2006; Rodriguez et al., 2000; Swan et al., 2009; J. Wang et al., 1996; Zhao et al., 1999). However, this is the first characterization of a phenotype associated with mutagenesis of this specific RNP motif in any Family B polymerase. Considering the high degree of conservation of these two tyrosine residues among polymerases in this family (Figure 4.2), further work should be conducted to identify the potential novel function of this motif.

Upon determining the crystal structure of HSV Pol, the authors suggested that this RNP motif in the NTD may catalyze a 5'-3' RNase H activity that was previously suggested to be associated with HSV Pol (S. Liu et al., 2006). In a previous study, we were unable to identify a 5'-3' RNase H activity associated with HSV Pol and instead found that the only activity of this enzyme on RNA:DNA degraded the substrates from the 3' RNA end and that this activity was dependent upon the 3'-5' exonuclease activity (Chapter 2) (Lawler et al., 2018). The 3'-5' exonuclease mutant that we reported to exhibit no activity on RNA:DNA, D368A, was further tested to identify any potential defects in viral replication (Chapter 3). Despite determining that this mutant was unable to form plaques in Vero cells, the defects associated with this virus were associated with the expression of this protein during infection. Other 3'-5' exonuclease-deficient mutants have been shown to exhibit a 2-3-fold decrease in viral plaque formation, suggesting that the 3'-5' exonuclease is likely not crucial for replication in cell culture or for viral DNA synthesis (Hwang et al., 1997).

Another hypothesis raised regarding the function of the RNP motif during infection suggested that this motif may interact with the *pol* mRNA for autogenous translational control of protein expression. Two other Family B polymerases, T4 Pol and RB69 Pol, have been shown to autogenously regulate protein expression using this mechanism. So, if we saw defects in viral replication that corresponded to an overexpression of the Y204A/Y206A Pol during infection, we expected this hypothesis to be a plausible explanation. However, we found that these substitutions in the RNP motif completely ablated viral DNA synthesis during infection. Furthermore, we observed no drastic difference in the expression of this enzyme at 4, 8, or 12 hpi (Figure 4.6-7), and the effect on viral DNA synthesis is more severe than we would expect given the difference in protein expression. Previously, a 2-3-fold increase in HSV Pol expression

associated with a deletion of a portion of the leader sequence exhibited only a 6-fold defect in viral replication (Bryant & Coen, 2008) despite overexpression of the polymerase severely inhibiting replication in other viral systems (Meier, Harmison, & Schubert, 1987). So, while the hypothesis that the HSV Pol RNP motif is regulating translation of its own mRNA is not entirely ruled out by this study, it is unlikely to be the only phenotype associated with this Y204A/Y206A mutant.

Given these data, it is also unlikely that the HSV Pol RNP motif interacts with another replication protein that is necessary for recruiting Pol to sites of DNA synthesis. The Y204A/Y206A mutations did not prevent polymerase from colocalizing with ICP8 at replication compartments in the presence or absence of WT Pol expression (Figure 4.8). It cannot be ruled out, however, that these mutations could be affecting an interaction that orients Pol at the replication fork after recruiting the protein to replication compartments.

The hypothesis that we currently favor based on the characterization of this Y204A/Y206A mutant was raised upon discovering an RNP motif in the NTD of *S. cerevisiae* Pol δ (Swan et al., 2009). As Pol δ plays a role in processive lagging strand synthesis and exhibits strand displacement synthesis activity but its mRNA has not been shown to be regulated at the level of translation, Swan *et al*. postulated that this RNP enhances strand displacement synthesis or binds and orients RNA primers for degradation by a 5' flap endonuclease. They suggested that this motif may stimulate strand displacement synthesis through an interaction with the RNA primer, recruiting a separate nuclease for 5' "flap" degradation, orienting the RNA primer for enhanced nuclease degradation, or a combination of these mechanisms (Figure 4.10). The human endonuclease FenI has been shown to remove "flaps" generated by HSV Pol strand displacement synthesis *in vitro* (Y. Zhu, Wu, et al., 2010). So, further work to express and purify

Y204A/Y206A mutant enzyme for *in vitro* characterization is underway (Appendix Figure A.3). If we are unable to generate recombinant Y204A/Y206A Pol using a baculovirus expression system, we plan to test some of these hypotheses using infected mammalian cell lysates.

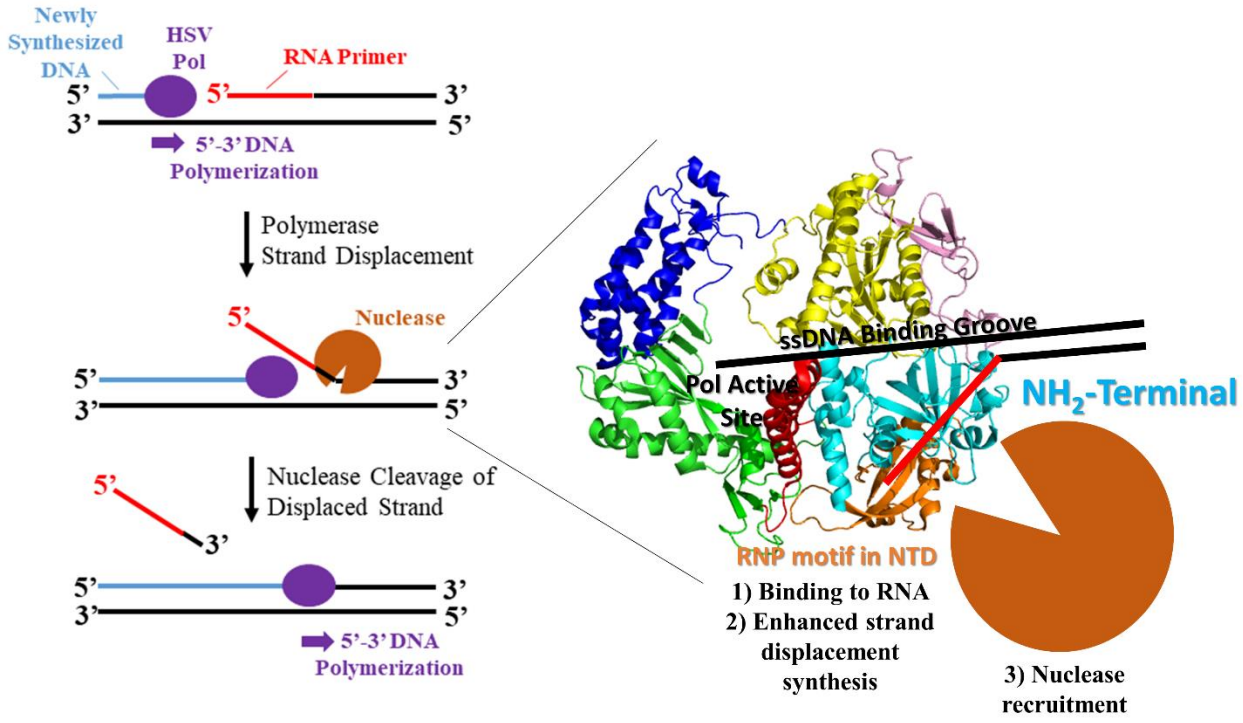

Figure 4.10. Model for the role of the RNA-binding activity of the NTD RNP motif during lagging strand DNA synthesis. The potential activities of the NTD in RNA binding and degradation are numbered.

Chapter 5

Discussion

Summary of Results

The herpes simplex virus-1 (HSV-1) catalytic subunit of the DNA polymerase (Pol) has been extensively studied, both as a model for Family B polymerases and as a successful antiviral target. There were still questions regarding the enzyme and its functions that had not been fully resolved despite decades of work, especially related to the RNase H activity, the 3'-5' exonuclease activity, and a putative RNA-binding motif with no defined activity. We set out to answer some of these questions and further define the activities associated with HSV Pol in order to identify key similarities and differences with other Family B polymerases. In the studies presented in this dissertation, we have resolved some unanswered questions associated with HSV Pol and worked to characterize the putative RNA-binding motif. These findings have implications not only for human herpesviruses but may also frame future studies for Family B polymerases from other organisms.

First, we studied a controversy regarding whether an RNase H activity intrinsic to HSV-1 Pol is due to the 3'-5' exonuclease of Pol or whether it was a separate activity, possibly acting on 5' RNA termini. Using purified WT and a 3'-5' exonuclease-deficient mutant Pol and synthesized fluorescently-labeled hairpin RNA:DNA substrates, we discerned that the RNase H activity associated with HSV Pol only detectably degraded RNA:DNA with 3' RNA ends *in vitro*, and showed that this RNA:DNA degradation was dependent upon the active site of the 3'-5' exonuclease. Furthermore, we determined that the degradation of RNA:DNA with 3' RNA ends was much slower than the degradation of dsDNA, suggesting that the 3'-5' exonuclease has a more relaxed specificity than originally thought. Although there are some caveats (see below), our data do not support the hypothesis that HSV Pol degrades RNA primers using a separate 5'-

3’ RNase H domain and instead suggest that a separate nuclease may be recruited to perform this activity.

Next, we set out to study a 3’-5’ exonuclease-deficient mutant (D368A) that had been previously studied *in vitro* but not characterized in cell culture. The group that designed this substitution was unable to generate a virus containing D368A Pol, suggesting that the 3’-5’ exonuclease domain was essential for viral replication in cell culture. However, another group had looked at two different exo$^-$ mutants with undetectable exonuclease activity that had less severe effects on viral replication. So, we generated this virus using a complementing cell line, and we determined that the D368A virus was incapable of replicating or synthesizing DNA during infection of non-complementing cells. However, we also found that this substitution severely affected expression of the protein during infection. These data suggest that the D368A Pol was not expressed at high enough levels to synthesize DNA and that instability was the cause of this defect, not a requirement for the 3’-5’ exonuclease activity per se; i.e., due to an accumulation of deleterious mutations.

Finally, we generated viruses containing substitutions within a putative RNA-binding motif that had been identified in the NH_2-terminal domain of Pol to test whether disruption of this motif had an effect on viral replication or DNA synthesis. Most of these mutants exhibited severe defects in Pol expression during infection, but one mutant, Y204A/Y206A, was expressed at levels similar to WT. We identified that this Y204A/Y206A mutant was incapable of viral replication and viral DNA synthesis, with no meaningful defects in expression, localization, or polymerase activity, suggesting that this motif plays a role in viral DNA synthesis separate from the polymerase activity. As we had previously found that Pol exhibits no detectable 5’-3’ RNase H activity, these results suggest that motif domain plays a crucial role in DNA synthesis that may

have to do with binding to the RNA primer and stimulating strand displacement synthesis, recruiting a separate nuclease to degrade the RNA primer, or orienting the primer correctly for nuclease degradation.

Together, these data answered several unresolved questions related to the HSV-1 DNA polymerase and identified the RNP motif as crucial for viral DNA synthesis. Our results argue that the RNP motif's function during viral DNA synthesis is not a 5'-3' RNase H. Additionally, we were able to provide evidence that the defects in replication associated with a well-studied 3'-5' exonuclease mutant were due to expression and not the exonuclease per se. Next, we've laid out our current thoughts on these topics and future experiments that could help to illuminate some of the unanswered questions regarding HSV Pol functions.

Hypotheses and Future Directions

Which nuclease removes RNA primers from the lagging strand during HSV-1 DNA replication?

The directionality and dependence of the RNase H activity associated with HSV Pol had been a point of controversy for years, though the crystal structure of HSV Pol brought this issue to the forefront because the discovery of an RNP motif present in the NTD of the enzyme raised the possibility of a separate RNase H domain (S. Liu et al., 2006). Our findings are not consistent with a nuclease activity associated with any domain other than the HSV Pol 3'-5' exonuclease. These results also agree with previous studies that were unable to identify a 5'-3' nuclease activity on dsDNA (Hall et al., 1996). It is possible that we have not identified the conditions that allow us to detect a 5'-3' RNase H activity associated with this enzyme. The possibility exists that a 5'-3' RNase H activity may require concurrent DNA synthesis toward the 5' RNA end, a forked structure like the replication fork, or another factor not present in these *in*

vitro assays. So, further work determining whether another viral or cellular nuclease aids in Okazaki fragment processing may shed more light on this process. 5'-3' RNase H activity has not been identified in any other Family B polymerases to our knowledge, though, so we highly indorse that this activity is specific to Pol I and its homologues. This finding steers the potential hypotheses surrounding HSV-1 Okazaki fragment maturation from one resembling *E. coli* Pol I to one requiring the recruitment of a separate nuclease for RNA primer degradation.

The lack of a detectable 5'-3' RNase H activity associated with HSV Pol opens the possibility for identifying a novel viral or cellular factor required for viral DNA synthesis that may play a role in RNA primer degradation. The viral alkaline nuclease, UL12, is nonessential, but may serve a role in degradation of RNA primers. This enzyme has been suggested to be a resolvase for removing branched structures during DNA replication and is important for packaging viral genomes into capsids, so it would not be surprising to see UL12 play a role in Okazaki fragment maturation (Goldstein & Weller, 1998; Grady et al., 2017; Schumacher et al., 2012). However, because this enzyme does not seem to be crucial for HSV-1 DNA replication (Grady et al., 2017), if UL12 does play a role, it is probably also complemented by other enzymes.

Another possibility is that a cellular nuclease such as Fen1 is recruited for Okazaki fragment maturation. Fen1 has been shown to be present in replication compartments during infection (Y. Zhu, Wu, et al., 2010), and eukaryotes express multiple nucleases that have 5' flap endonuclease activity (Balakrishnan & Bambara, 2013). It is also possible that more than one of these nucleases are utilized for RNA primer degradation during infection; this would decrease the requirement for a specific enzyme to be present at all replication forks and require less stringent regulation by the virus. Since there are multiple complementing activities that can

perform this function in humans, if a single factor is found to mediate this activity in HSV-1, this nuclease could potentially serve as an antiviral target.

Does the 3'-5' activity on RNA:DNA with 3' RNA ends play a role during infection?

Interestingly, the rate of the 3'-5' RNase H degradation seems to be much slower than ssDNA degradation, dsDNA degradation, or the 5'-3' polymerase activity associated with this enzyme. These data suggest that the 3'-5' activity on RNA:DNA with 3' RNA termini may be a reflection of relaxed activity of the 3'-5' exonuclease. Because this activity is not separable from the 3'-5' exonuclease, though, it will be difficult to study any potential viral replication defects associated with this activity specifically. However, as two exonuclease-deficient Exo III mutants have been shown to exhibit only modest defects in viral replication in cell culture (Hwang et al., 1997), we find it likely that, the degradation of RNA:DNA with 3' RNA termini is unimportant for viral replication, or that a similar activity is present during infection that is able to complement this activity. The possibility exists that specific substitutions in the enzyme will limit either DNA or RNA binding to the 3'-5' exonuclease pocket. In that case, it would prove prudent to attempt to determine the contribution of either of these activities to viral replication and DNA synthesis separately.

What is the contribution of 3'-5' exonuclease-mediated proofreading to viral replication?

Despite years of research on the 3'-5' exonuclease associated with HSV Pol in relation to many different activities, the most widely studied of the 3'-5' exonuclease-deficient mutants, D368A, still had not been previously characterized in cell culture with the use of a complementing cell line. The authors who originally studied the effect of the D368A mutation

on viral replication in cell culture performed a number of controls to support their conclusion that the mutation ablated viral replication, but because this group did not utilize a complementing cell line to generate this D368A virus, questions were left unresolved as to whether there really was a replication defect and, if so, the cause of this defect and the phenotype of this mutation compared to other 3'-5' exonuclease mutations that had not affected viral replication as severely (Hall et al., 1995). The authors did further work *in vitro* and tried to attribute this D368A mutant phenotype to increased stalling at mismatches (Baker & Hall, 1998), but without virus generated by a complementing cell line, it was impossible to characterize this defect directly in cell culture.

A different group identified two exonuclease-deficient mutants (YD12 and Y577H) from a different conserved Exo domain of HSV Pol that displayed a ~3-fold defect in viral replication, presumably due to a 300-800-fold decrease in fidelity (Hwang et al., 1997). These results were in opposition to the results showing that the D368A mutation was completely unable to form plaques in cell culture (Hall et al., 1995). The Exo II mutants studied (E460D and G464V) were reported to severely affect polymerase activity *in vitro* and had major effects on viral replication in cell culture (Gibbs et al., 1991; Kuhn & Knopf, 1996). So, with these differences in the phenotype associated with different exonuclease-deficient mutants, it was difficult to determine whether HSV-1 was dependent on the 3'-5' exonuclease for viability and whether the lack of replication observed from the D368A mutation was due to the mutation of the 3'-5' exonuclease or another unidentified phenotype.

Upon discovering the two Exo III mutations that can form plaques on non-complementing cells, the authors also discovered that these Exo III mutants were unable to completely complement growth of the HP66 virus and that these mutants may affect dNTP interactions with the polymerase active site (Hwang et al., 1997; Hwang, Smith, Gao, & Hwang,

1998). Their results brought up the possibility that there were other deleterious effects associated with these mutants separate from the accumulation of mutations in the viral genome. We confirmed the previous results that D368A Pol was incapable of forming plaques on non-complementing cells and determined that this defect was associated with a lack of viral DNA synthesis instead of an accumulation of deleterious mutations in the virus. Furthermore, a lack of protein expression was the cause of the replication defect rather than an activity specific to the 3'-5' exonuclease domain. These results suggest that the phenotypes associated with the loss of 3'-5' exonuclease activity may not be related to fidelity, but other phenotypes related to the enzyme. These results favor the hypothesis that the 3'-5' exonuclease activity contributes to viral replication, but it not strictly required. We cannot rule out that there are differences in other activities associated with the exonuclease, idling, binding specificity, or movement of the template DNA between the polymerase and exonuclease active sites that contribute to the difference in replication. However, it is difficult to tease out these specific differences with this mutant due to the significant defects in either polymerase activity or expression of the enzyme masking other potential phenotypes. It is possible that we would not see the same degradation of these mutants in certain cells other than Vero cells or baculovirus expression in insect cells. Since we already have these viruses made, this is something we plan to test in the future.

How do the 3'-5' exonuclease domain and NTD contribute to the stability of HSV Pol?

Though we were able to detect this drastic drop in expression associated with the D368A mutant, it is unclear why this protein is not stable for expression during HSV infection of Vero cells when the mutation has no effect on expression in a baculovirus system. We speculate that the proteases present in these cells, or another cellular or viral factor is likely causing the

instability seen in these assays. As the expression of other 3'-5' exonuclease mutants during infection has not been reported but is high enough to see only a 2-3-fold decrease in viral plaque formation, it is impossible to tell whether there is a general intolerance to substitutions in this domain or whether the Exo I domain is playing a larger role in the stability of the enzyme.

In addition to the instability associated with the D368A mutant, many of the substitutions in the NTD were also not expressed in infected Vero cells. So, it is likely that this enzyme is not tolerant of many substitutions. Ironically, the opposite phenotype is exhibited by the Y204A/Y206A mutant, which is insoluble upon baculovirus expression but is expressed at levels similar to WT Pol during infection. It is so far unclear what would be causing these differences in expression, but, as stated previously, it would be advantageous to further study whether this expression defect is conserved among other cell types.

What is the function of the NTD RNP motif in HSV-1 DNA synthesis?

The results in this dissertation do not rule out the possibility that the RNP motif may autogenously regulate translation of its own mRNA. However, if this RNP motif performs this translational control, it is not likely crucial for replication and not the only activity performed by this motif, as this phenotype is likely not being utilized in some other Family B polymerases containing RNP motifs (Swan et al., 2009). Furthermore, it is unlikely that the less than 2-fold difference in Pol expression exhibited by the Y204A/Y206A mutant would exhibit such a drastic change in DNA synthesis, especially considering that the more drastic decrease in Pol expression from the HP66 cells compared to WT infection only causes a 15-fold decrease in viral replication (Chapter 3). Further work to determine whether the RNP motif can bind RNA, specifically

interact with *pol* mRNA, and whether this interaction affects Pol expression during infection will have to be carried out to characterize this potential activity further.

Because the RNase H activity associated with HSV Pol was dependent on the 3'-5' exonuclease, several new potential activities associated with the RNP motif within the HSV Pol NTD have become favored. To test whether there was any function associated with the RNP motif of HSV Pol, we used the similar ribonucleoprotein A1 RNA-binding domain structure and conserved residues in and around the RNP motif to design substitutions that we deemed likely to play a role in RNA binding and/or any metal ion coordination that could play a catalytic function. Though most of these substitutions affected the expression of the enzyme during infection, adding more evidence for the sensitivity of the stability of this protein to substitutions, one double mutation (Y204A/Y206A) was expressed at levels similar to the WT Pol during infection. This mutant was studied further and was determined to be required for plaque formation in non-complementing Vero cells. Additionally, the Y204A/Y206A virus was incapable of synthesizing viral DNA during infection, without any meaningful effect on expression, localization, or the polymerase activity.

This Y204A/Y206A mutation had a severe effect on viral replication and DNA synthesis, and this is the first report of a phenotype associated with the RNP motif of a Family B polymerase. As the 3'-5' exonuclease is not required for plaque formation (Hwang et al., 1997), this motif seems to play a more crucial role than even the 3'-5' exonuclease for viral replication. Additionally, substituting all six residues of the FYNPYL motif in the pre-NH_2-terminal mutations with alanine only had about a 10-fold defect in replication in cell culture, suggesting that the activity present in this domain (Terrell & Coen, 2012), suggested to be a protein interaction, is also not as crucial as this RNP motif.

We detected a variable amount of polymerase activity from the cell lysate assays determining incorporated radioactivity into activated salmon sperm DNA, so it is unclear what the actual defect in polymerase activity, if any, associated with this mutant is. Attempts to express and purify the Y204A/Y206A mutant have thus far been unsuccessful, as the protein is insoluble using procedures that have been used to purify WT Pol. We determined that this enzyme was more sensitive to freeze-thaw than the WT lysates, suggesting that it may be more difficult to work with and requires further optimization.

The most promising hypothesis regarding the function of the RNP motif, which may also be applicable in other organisms, is that this motif binds RNA for the enhancement of strand displacement synthesis and/or the recruitment of a 5' flap endonuclease for removal of the RNA primer during Okazaki fragment maturation. Human Fen1 has been shown to degrade RNA that has been displaced by HSV Pol *in vitro* and colocalizes with replication compartments during infection in cell culture (Y. Zhu, Wu, et al., 2010), but it's unclear whether this activity is relevant during infection. Fen1 has been shown to interact with Pol δ, the SSB RPA, and PCNA (the human processivity factor) (Kathera et al., 2017), but it is unclear what viral replication protein may interact with Fen1 during infection. There are also other complementing pathways that are able to remove 5' RNA flaps during eukaryotic DNA replication, so it is possible that there may also be multiple pathways that remove RNA primers during infection.

Pol δ, in addition to containing an RNP motif, has inhibited strand displacement synthesis when an excess of DNA is added (Koc et al., 2015). So, it is possible that the RNP motif can bind both RNA and DNA. It is unclear whether this phenotype is applicable to HSV Pol and whether it plays any role during infection, as this could be a less specific activity of the RNA binding. As DNA binding inhibited strand displacement synthesis with Pol δ, this activity could

serve to inhibit strand displacement past the RNA primer, slow strand displacement synthesis until a nuclease is recruited, or could serve to stall the polymerase long enough to fall off the template strand. If we are able to express and purify this mutant or other RNP mutants for analysis *in vitro*, it will be possible to test binding to RNA and/or DNA, determine whether binding to either one is preferred and if this binding is competitive, and identify any inhibition of strand displacement synthesis associated with the HSV Pol enzyme. Alternatively, we plan to attempt to replace the HSV Pol RNP motif with that of the yeast Pol δ, Pol α, or RB69 Pol to determine whether these domains can complement viral DNA synthesis and hopefully can answer some of these questions regarding the specificity and conservation of any activities associated with this domain. This may also help us to determine whether this DNA binding is specific to Pol δ and plays any role in the HSV-1 system.

Is the function associated with the RNP motif conserved among other Family B polymerases?

Because this motif exists in other enzymes that have been shown to have no associated RNase H activity and the motif is required for viral DNA synthesis, it is more likely that this activity is conserved among several Family B polymerases. And, due to the high level of conservation of this motif, it is possible that we have identified a novel activity basic to DNA replication on a wider scale. As the required interactions and mechanisms for RNA primer removal are not fully elucidated, further work is required to determine the importance of this motif in a number of different systems.

Of the domains that form the structure of Family B polymerases, the least studied is the NTD. This domain is highly variable among Family B polymerases in terms of length, structure, and sequence. As more structures have become available, though, it has become clear that this

RNP motif in the NTD is more ubiquitous than predicted based on sequence comparisons. Structures resembling the RNP motif have been identified in at least the following enzymes: yeast Pol δ (Swan et al., 2009), RB69 Pol (J. Wang et al., 1997), HSV Pol (S. Liu et al., 2006), and two archaeal Pols (Rodriguez et al., 2000; Zhao et al., 1999). Additionally, upon analyzing the structures of yeast Pol α (Perera et al., 2013), yeast Pol ε (Jain et al., 2014), and human Pol α (Coloma, Johnson, Prakash, Prakash, & Aggarwal, 2016), there is high similarity between the yeast Pol δ RNP motif and the structure of the corresponding motif within yeast Pol α, yeast Pol ε, and human Pol α (Figure 5.1). Considering that this RNP motif, and the tyrosines present within the center of the putative RNA binding site, are highly conserved despite the substantial variation in the overall structure of the NTD, it is likely that a similar mechanism is being used by these enzymes that requires this putative RNA binding.

As Pol α is not associated with strand displacement synthesis and has an inactive 3'-5' exonuclease domain, it is possible that the function related to the RNP motif is not related to Pol α but is specific to a different process intrinsic to other Pols in this family. Additionally, the 3' end of the primer extends from the opposite side of the polymerase structure from the RNP motif pocket (Perera et al., 2013; Swan et al., 2009; J. Wang et al., 1997), suggesting that this motif may not be associated with initiation of polymerase activity from the 3' end of the RNA primer and is more likely to play a role in RNA primer degradation. The pocket predicted to bind the 5' ssDNA end is adjacent to the RNP motif, so it would make more sense that the RNA primer would bind to form a conformation separating the RNA and DNA strands rather than for polymerase initiation from the RNA:DNA. However, further work is required to determine the function associated with the RNP motif during DNA synthesis.

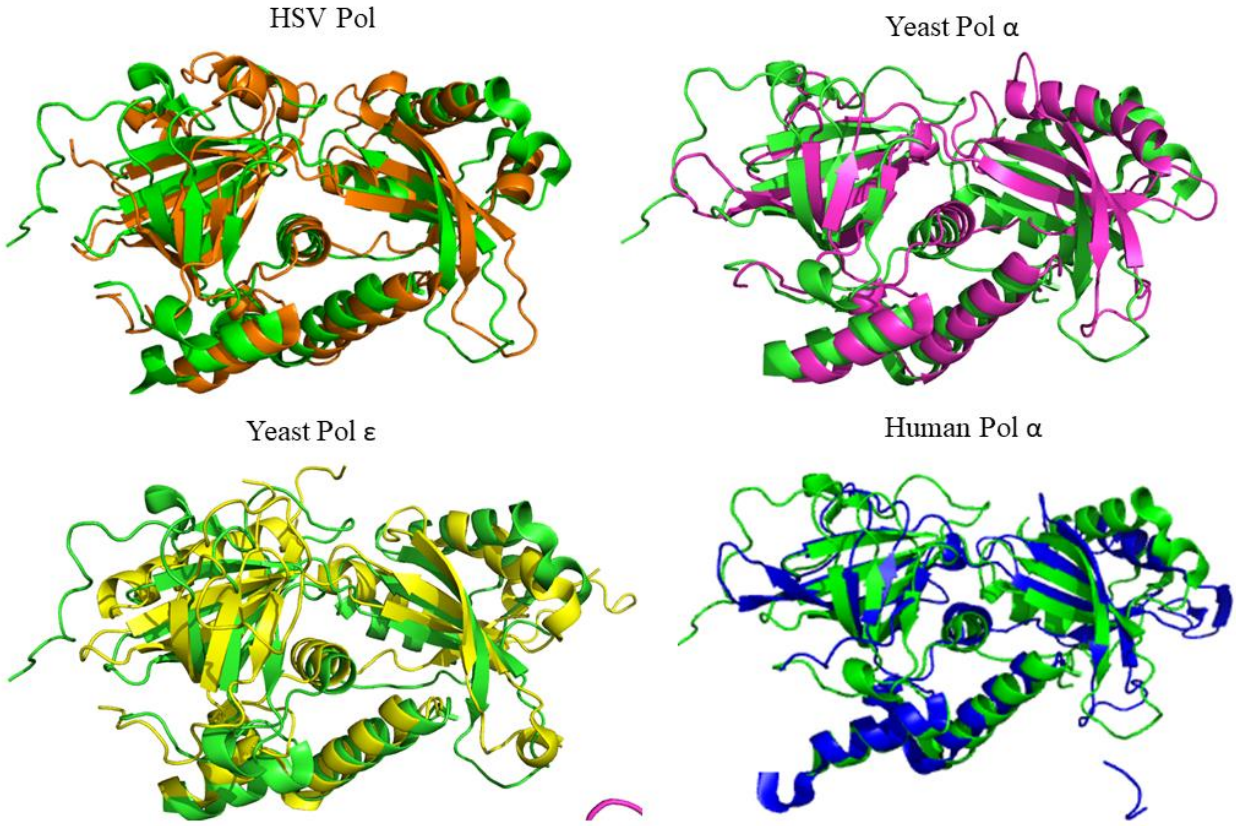

Figure 5.1. Structural similarities between the NTDs of yeast, human, and HSV-1 Family B polymerases. Each of the polymerases listed above the perspective structure is aligned to the structure of *S. cerevisiae* Pol δ in green. The RNP motif is in the upper right of each structure.

Additionally, it will be interesting to know whether substitution of the RNP motif with that of another polymerase maintains the function associated. As many of the substitutions in the RNP motif have affected expression of the enzyme, it is unclear whether this experiment will return solid results but knowing whether this domain is conserved among more polymerases would help in answering whether this is a druggable target or a more conserved activity. Either way, this is an interesting question that we believe should be further investigated.

These results have impacts on the study of not only HSV-1 DNA replication, but also on the larger scale for DNA replication associated with many Family B polymerases. Several different routes to study the contribution of the RNP motif within the NTD and nucleases associated with viral Okazaki fragment maturation have emerged. Furthermore, any findings detailed about either of these two topics has the potential to identify novel druggable targets for antiviral treatment and/or a greater understanding of the underlying mechanisms governing DNA replication across many very diverse organisms.

Appendix A

Protein Expression and Purification

Materials and Methods

Protein Expression and Purification

Expression and purification methods for both 6xHis-tagged WT Pol and D368A Pol are listed in the Materials and Methods Section of Chapter 2. 6xHis-tagged Δ42-Y204A/Y206A HSV Pol was cloned into the pFastBac HTC vector and expressed in a baculovirus system as previously described (Terrell & Coen, 2012), and purified as follows: Cells were harvested at 65 hours post infection, and centrifuged at 2800 x g for 30 minutes. The resulting pellets were washed in Dulbecco's phosphate-buffered saline (DPBS) with 10% glycerol, centrifuged at 2800xg for 10 minutes, and frozen at -80˚C. For enzyme purification, cell pellets were resuspended in lysis buffer (25 mM HEPES pH 7.5, 500 mM NaCl, 10% (w/v) sucrose, 5 mM imidazole, 2 Roche complete protease inhibitor tablets per 100 ml) and the cells were lysed on ices in the presence of 1 mg/ml lysozyme by sonication using a Branson Ultrasonics Sonifier S-450 (5 sec pulses with 9 sec pauses at 20% amplitude for 15 minutes). All subsequent steps were performed at 4° C. The suspension was centrifuged at 30,000xg for an hour, and the supernatant was then passed through a 0.45 μm filter. The clarified supernatant was loaded onto a preequilibrated 10-ml GE HiTrap TALON column, washed with 20 column volumes of lysis buffer, and eluted using lysis buffer containing a gradient from 5 to 150 mM imidazole. The samples were combined with 2x Laemmli buffer (Bio-Rad) containing β-mercaptoethanol and complete protease inhibitors (Roche), boiled at 95˚C for 5 minutes, and run on a 4-20% polyacrylamide SDS-PAGE gel (Bio-Rad). The resulting gels were stained for 30 minutes at room temperature using SimplyBlue Safe Stain (ThermoFisher), destained in water overnight, and imaged using the colorimetric setting of an Amersham Imager 600 (GE).

Results

Expression and purification of full-length WT Pol and D368A Pol for *in vitro* functional analysis in Chapter 2.

The full-length constructs of both His-tagged WT and D368A Pol were expressed and purified using a baculovirus system in Sf9 insect cells as detailed in the Materials and Methods of Chapter 2. The gels within this appendix detail the purification methods and purity of each enzyme during the process using Coomassie-stained polyacrylamide gel. Half of the experiments run were using a very clean WT Pol stock from Shariya Terrell (Figure A.1A, methods for expression and purification can be found in reference (Terrell & Coen, 2012)), and the other half were run using my own stock of WT Pol, which was less clean but yielded similar results (Figure A.1B). The results from these stocks are described in more detail in Appendix B. The D368A Pol results were mostly analyzed using a single stock of enzyme (Figure A.2A) but were confirmed using a second stock (Figure A.2B). Each of these enzymes was at least 90% pure by analysis using GE ImageQuantTL software.

Y204A/Y206A Pol is not soluble for purification in the baculovirus system.

In the hopes of achieving sufficient expression of the Y204A/Y206A Pol mutant for *in vitro* analysis (Chapter 4), we generated a baculovirus expressing Y204A/Y206A Pol with a deletion of the N-terminal 42 residues of HSV Pol (Δ42). This deletion has been shown to increase expression of the WT polymerase in the baculovirus system and has no effect on the polymerase activity of the enzyme or viral replication in cell culture (S. Liu et al., 2006; Terrell & Coen, 2012). Following the optimized protocol we have used multiple times to generate and

purify recombinant Pol from insect cells using baculovirus expression (Lawler et al., 2018), we attempted to express the Y204A/Y206A Pol mutant. However, this protein, while showing similar protein expression to the WT in infected cells and exhibiting polymerase activity in infected cell lysates, is extracted during the ultracentrifugation step of the purification with the pellet, suggesting that this enzyme is not soluble or aggregates upon expression within insect cells (Figure A.3). Optimization of Y204A/Y206A expression and purification is ongoing, but, so far, has not yielded promising results, making *in vitro* characterization of this enzyme difficult.

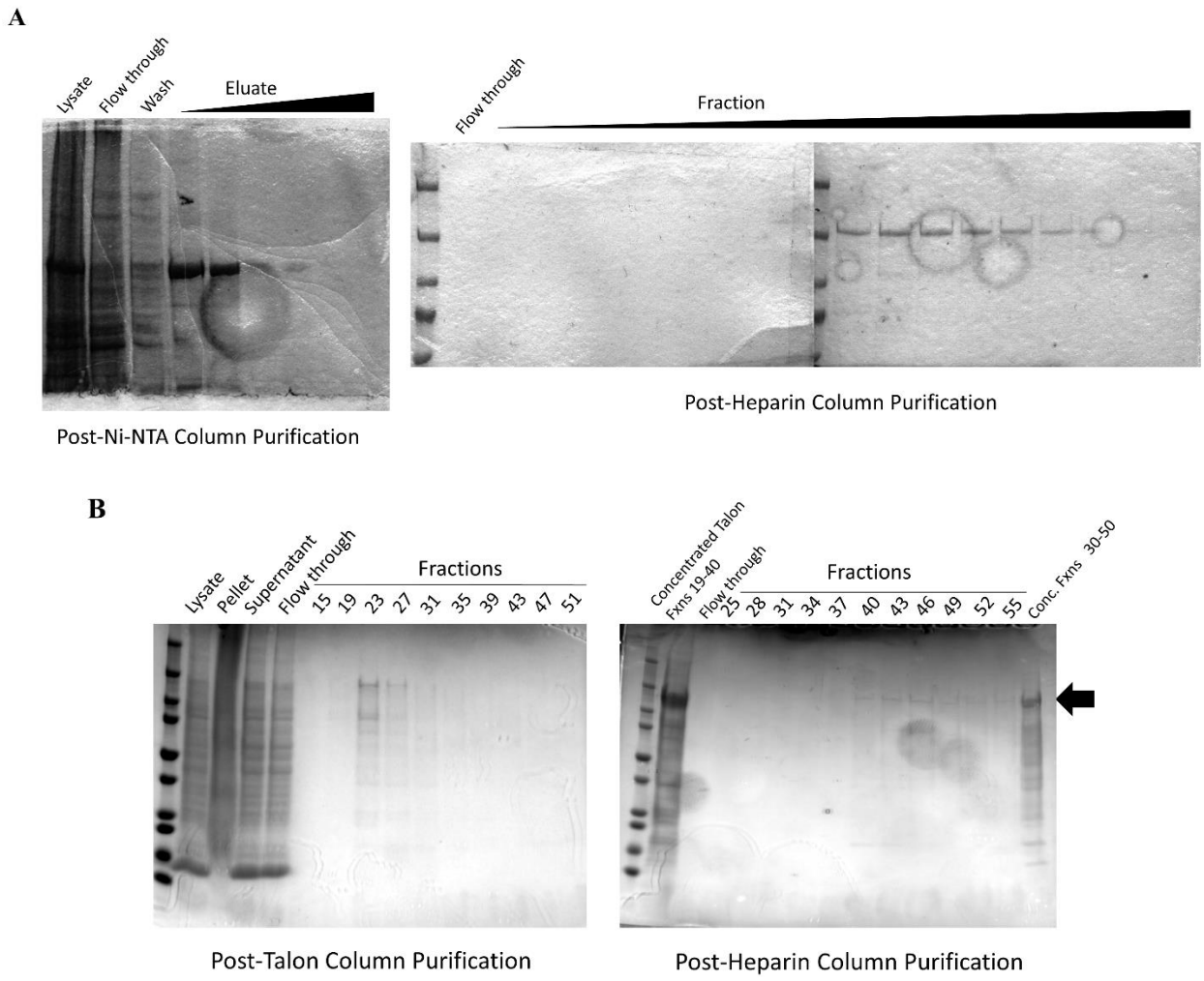

Figure A.1. His-WT Pol enzyme expressed and purified for *in vitro* analysis in Chapter 2. Samples collected following the sonication (Lysate), ultracentrifugation (Supernatant and Pellet), Ni-NTA or TALON column purification (Flow through and Wash), and selected eluted fractions from the Ni-NTA, TALON, or Heparin column (as indicated underneath each gel image) are compared by Coomassie staining of a 4-20% polyacrylamide gel. His-Pol runs at ~140 kD and is marked by the black arrow. Enzymes were expressed and purified by Shariya Terrell (A) or Jessica Lawler (B) at different times with different purity but yielded similar results (Appendix B).

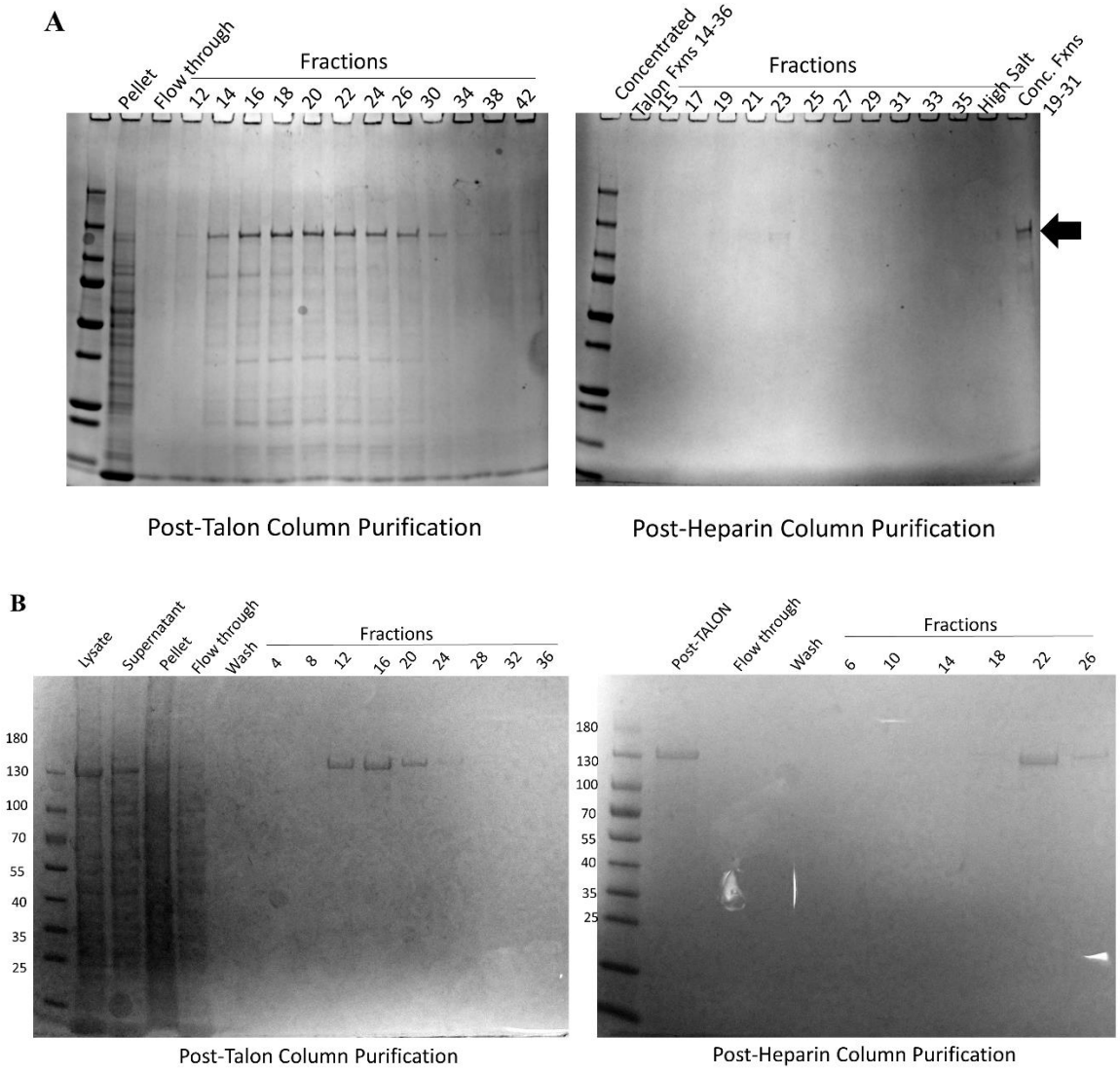

Figure A.2. His-D368A Pol enzyme expressed and purified for *in vitro* analysis in Chapter 2. Samples collected following the sonication (Lysate), ultracentrifugation (Supernatant and Pellet), TALON column purification (Flow through and Wash), and selected eluted fractions from the TALON or Heparin column (as indicated underneath each gel image) are compared by Coomassie staining of a 4-20% polyacrylamide gel. His-Pol runs at ~140 kD and is marked by the black arrow. Enzyme in (A) was used for a majority of the assays in Chapter 2, and (B) was purified at a different time with higher purity but yielded similar results (Appendix B).

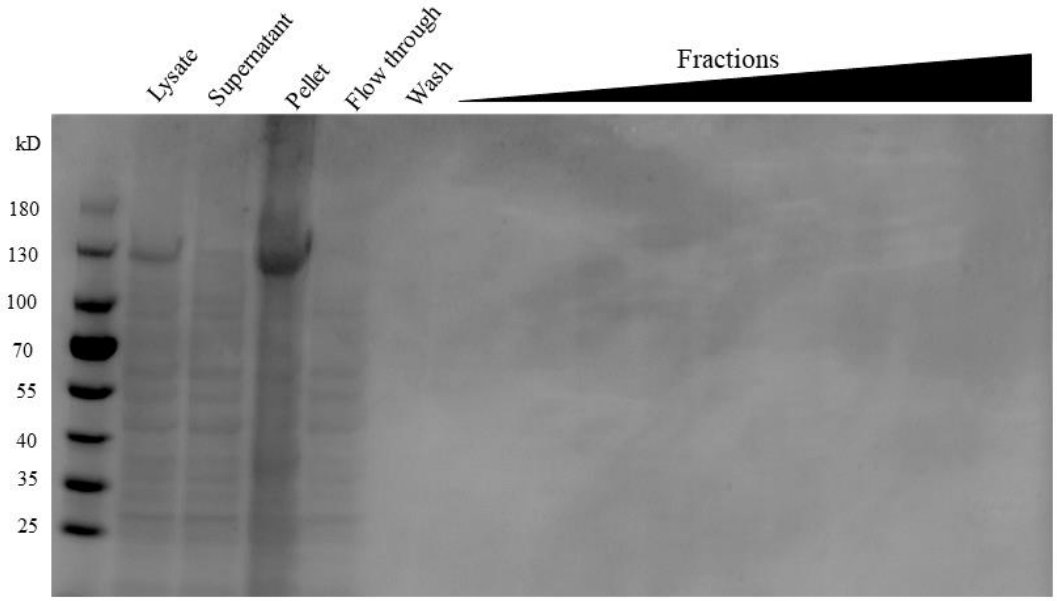

Figure A.3. His-Δ42-Y204A/Y206A Pol is insoluble following the protocols used to express and purify WT Pol. Samples collected following the sonication (Lysate), ultracentrifugation (Supernatant and Pellet), TALON column purification (Flow through and Wash), and selected eluted fractions from the TALON column are compared by Coomassie staining of a 4-20% polyacrylamide gel.

Appendix B

Supplemental Results for Chapter 2

Materials and Methods

In vitro Enzymatic Assays

The polymerase, exonuclease, and RNase H assays used to collect the data in Figures B.1-6 were described in the Chapter 2 Materials and Methods section. 6-Carboxyfluorescein (6-FAM) labeled linear DNA and unlabeled RNA primer-template substrates used in the *in vitro* assays were synthesized by IDT (listed in the respective figures) and were annealed in equal concentration mixtures. WTΔN42 (Δ42) is a construct of WT Pol with the N-terminal 42 residues removed that was expressed and purified following the methods outlined in Chapter 2. Single turn over assay conditions in Figures B.7-9 are as follows: Master mixes designed to give final concentrations of 25 mM HEPES pH 7.5, 1 mM DTT, 10% glycerol, and 25 mM NaCl were combined on ice with 40 nM primer/template, 400 nM Pol, and with 800 nM UL42 or protein storage buffer (see Chapter 2). 20 µl DNA polymerase reactions were initiated with the addition of $MgCl_2$ to 8 mM and all four dNTPs to 1 mM, mixed, and incubated at 37˚C. Aliquots were quenched in loading buffer containing 80% formamide, 100 mM EDTA, and bromophenol blue at the time points listed above the gels. Samples were separated on a 7 M Urea 15% denaturing polyacrylamide gel, and the FAM-labeled substrate was detected at 490 nm using an Amersham Imager 600. RNase H assays in Figure B.9 were carried out under the same conditions, but in the absence of dNTPs. Steady state assay conditions in Figures B.7-8 use the same conditions as the single turn over conditions above with the exception that final concentrations of 1 µM primer/template, 20 nM Pol, and with 40 nM UL42 or protein storage buffer were used.

Results

In addition to the assays published in Chapter 2, we also wanted to clarify the rest of the results from the varied enzyme concentrations that were used to characterize the activity rates and to show some other interesting results that we identified related to this study but that did not fit in for publication. As shown in Appendix A.1, we used two different preparations of WT Pol to characterize the polymerase, exonuclease, and RNase H activities associated with HSV Pol. The first, expressed and purified by Shariya Terrell, was of higher purity but lower concentration (Figure A.1A). The second WT Pol stock that I had generated was less pure (Figure A.1B). When we compared the activities associated with these two stocks of WT Pol, we determined that the specific activity of the WT Pol from Shariya's stock was higher than my own (Figure B.1 and B.2, respectively). However, my stock displayed a closer polymerase activity to my own D368A stocks and did not show any difference in exonuclease or RNase H activity (Figure B.3-5). So, we were able to strongly make the conclusions published in Chapter 2. Each of these figures displays a wider range of concentrations of Pol that were all used to generate Figure 2.4 and Table 2.1 for reference.

We also analyzed the products generated from the RNA:DNA substrates with either 3' or 5' RNA ends to attempt to discern whether the products of S2 were of similar size to those generated by S3 (Figure B.6). Interestingly, the products generated by substrate S2 (on the left) were shorter than 5 nucleotides but were larger than those produced by S3 (on the right). Additionally, the small band generated by the S3 substrate was the only band visible, was generated at the same rate as the loss of the starting substrate band, and did not display "laddering" as seen with S2, suggesting that the FAM label or a single nucleotide was removed from the 3' end of the DNA portion of the S3 substrate by the 3'-5' exonuclease activity of HSV

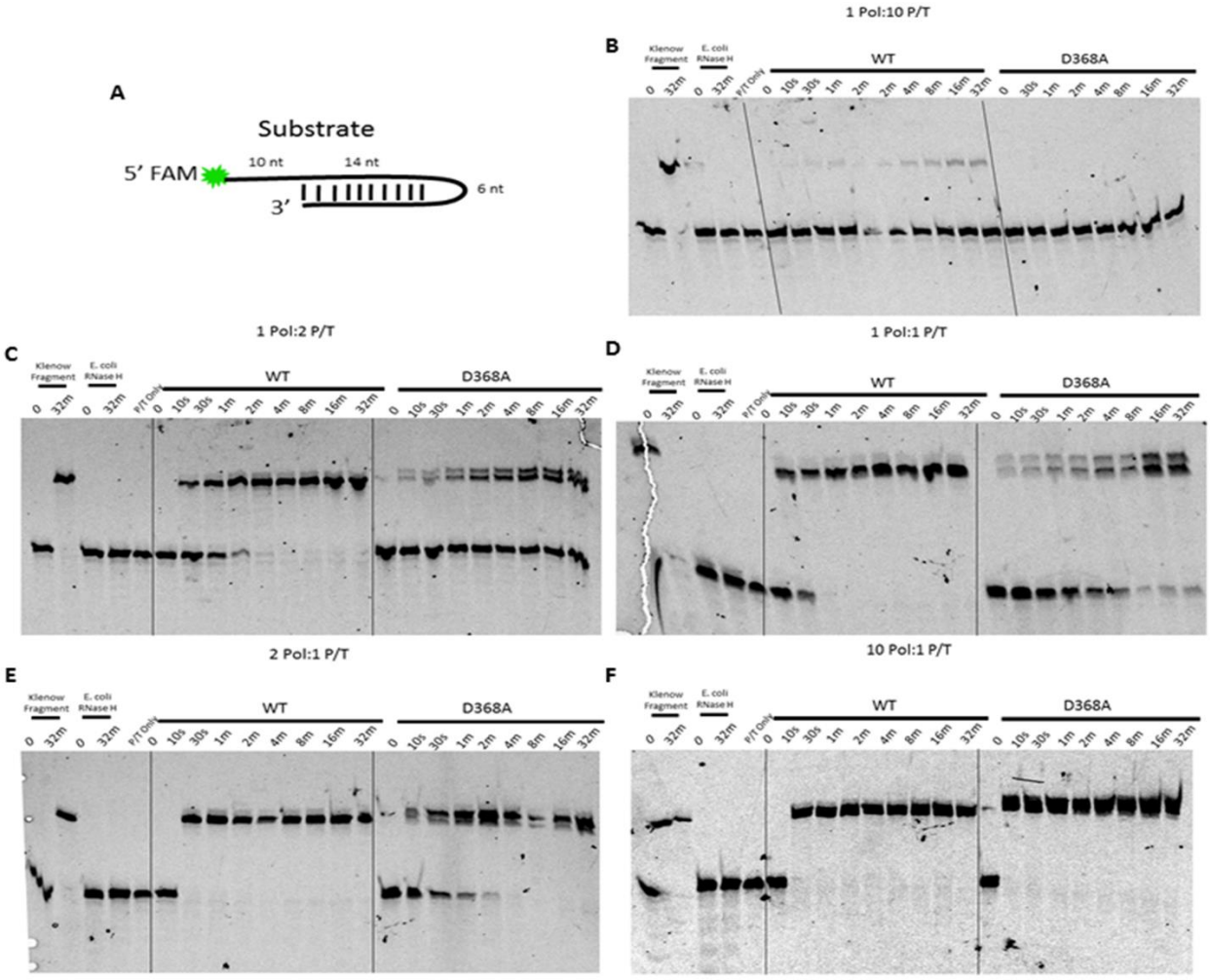

Figure B.1. His-WT and D368A Pol polymerase assays at varying Pol:P/T concentrations using Shariya Terrell's protein WT Pol stock. A) Cartoon of the 6-FAM labeled DNA hairpin primer template (S1; Figure 2.2) used for the polymerase assays. B-F) Fluorescent image of a denaturing polyacrylamide gel loaded with equal amounts of each polymerase reaction over increasing time points at a range of different enzyme concentrations (indicated over the gel). The 0 and 32m control reactions (Klenow fragment and RNase H) are shown.

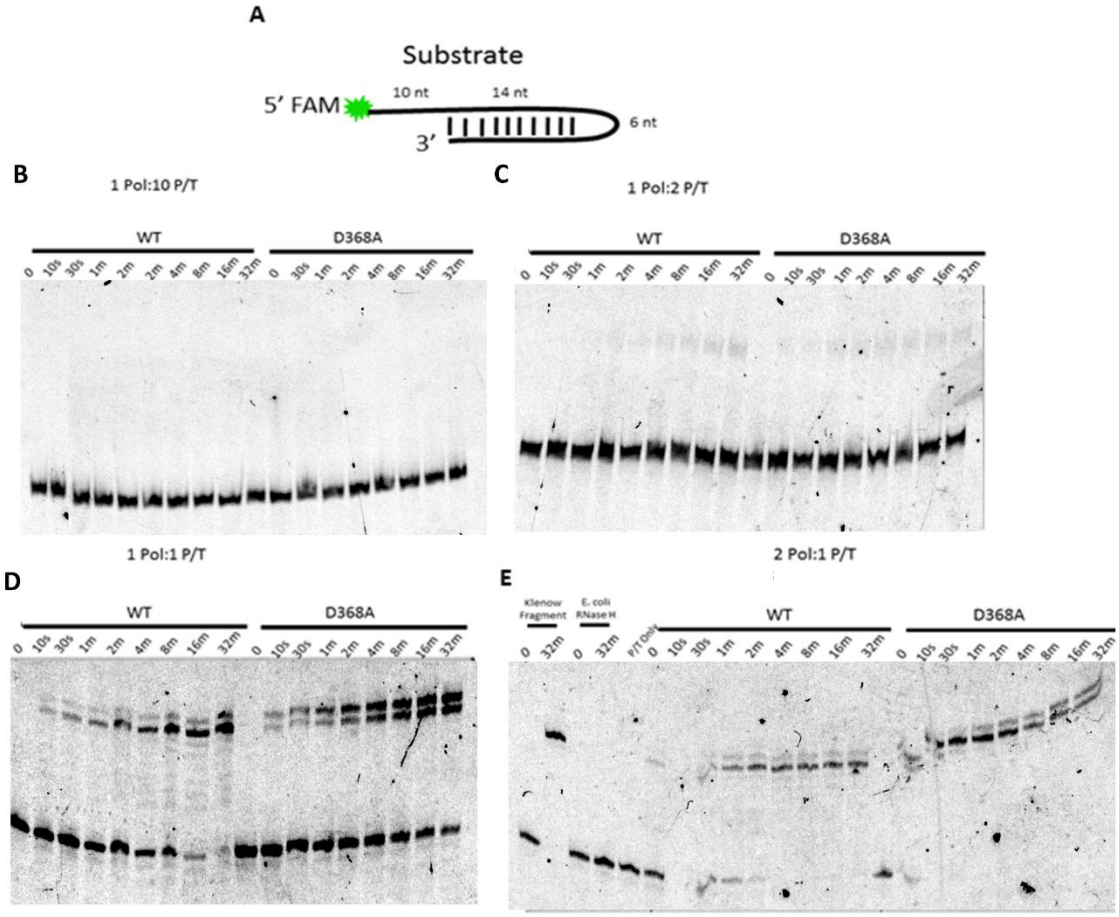

Figure B.2. His-WT and D368A Pol polymerase assays at varying Pol:P/T concentrations using my own protein stocks. A) Cartoon of the 6-FAM labeled DNA hairpin primer template (S1; Figure 2.2) used for the polymerase assays. B-E) Fluorescent image of a denaturing polyacrylamide gel loaded with equal amounts of each polymerase reaction over increasing time points at a range of different enzyme concentrations (indicated over the gel). The 0 and 32m control reactions (Klenow fragment and RNase H) are shown.

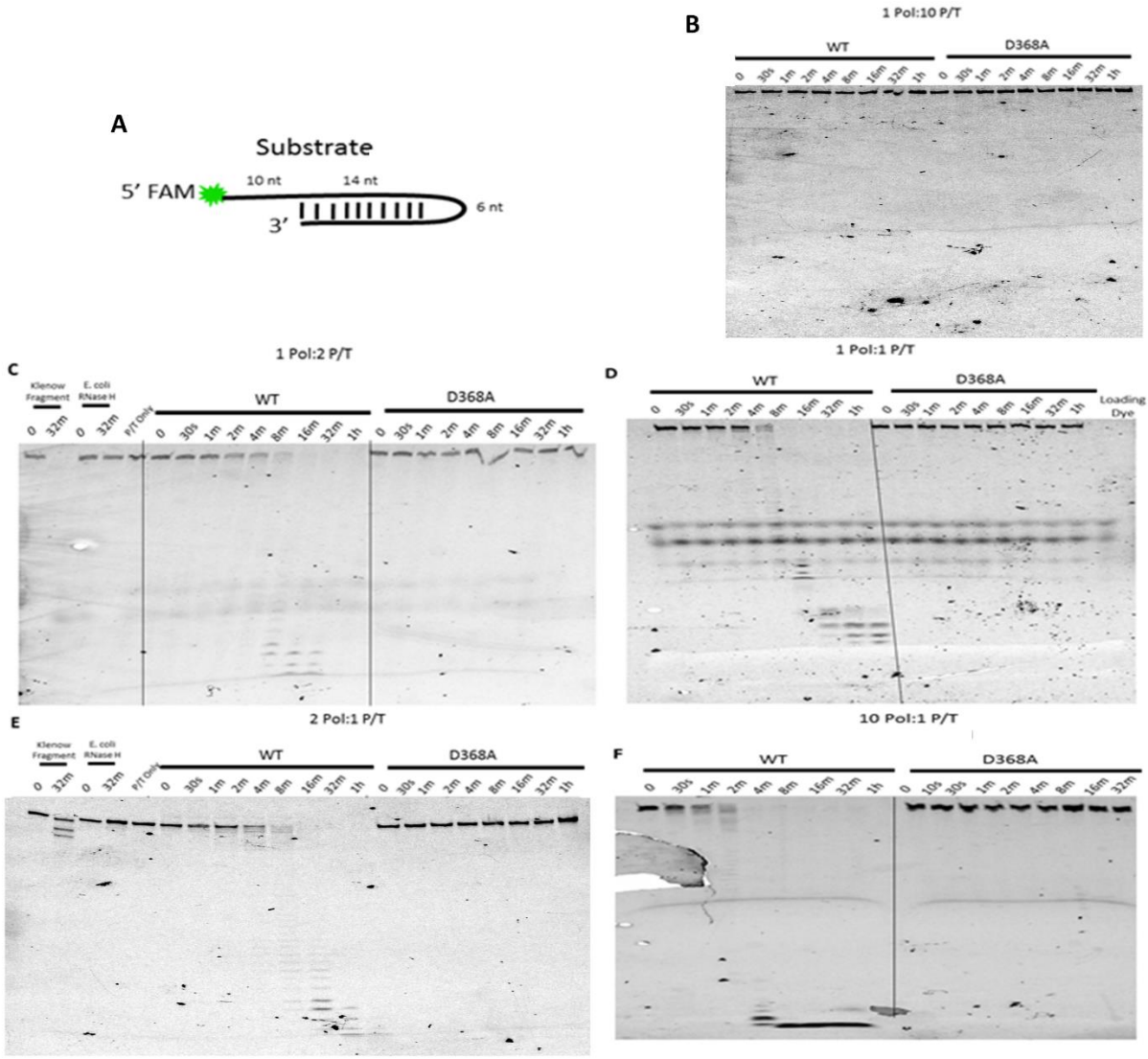

Figure B.3. His-WT and D368A Pol exonuclease assays at varying Pol:P/T concentrations. A) Cartoon of the 6-FAM labeled DNA hairpin primer template (S1; Figure 2.2) used for the exonuclease assays. B-F) Fluorescent image of a denaturing polyacrylamide gel loaded with equal amounts of each reaction over increasing time points at a range of different enzyme concentrations (indicated over the gel). The 0 and 32m control reactions (Klenow fragment and RNase H) are shown. Signal present in all lanes below the starting substrate band corresponds to background fluorescence from bromophenol blue in the loading dye that was later removed.

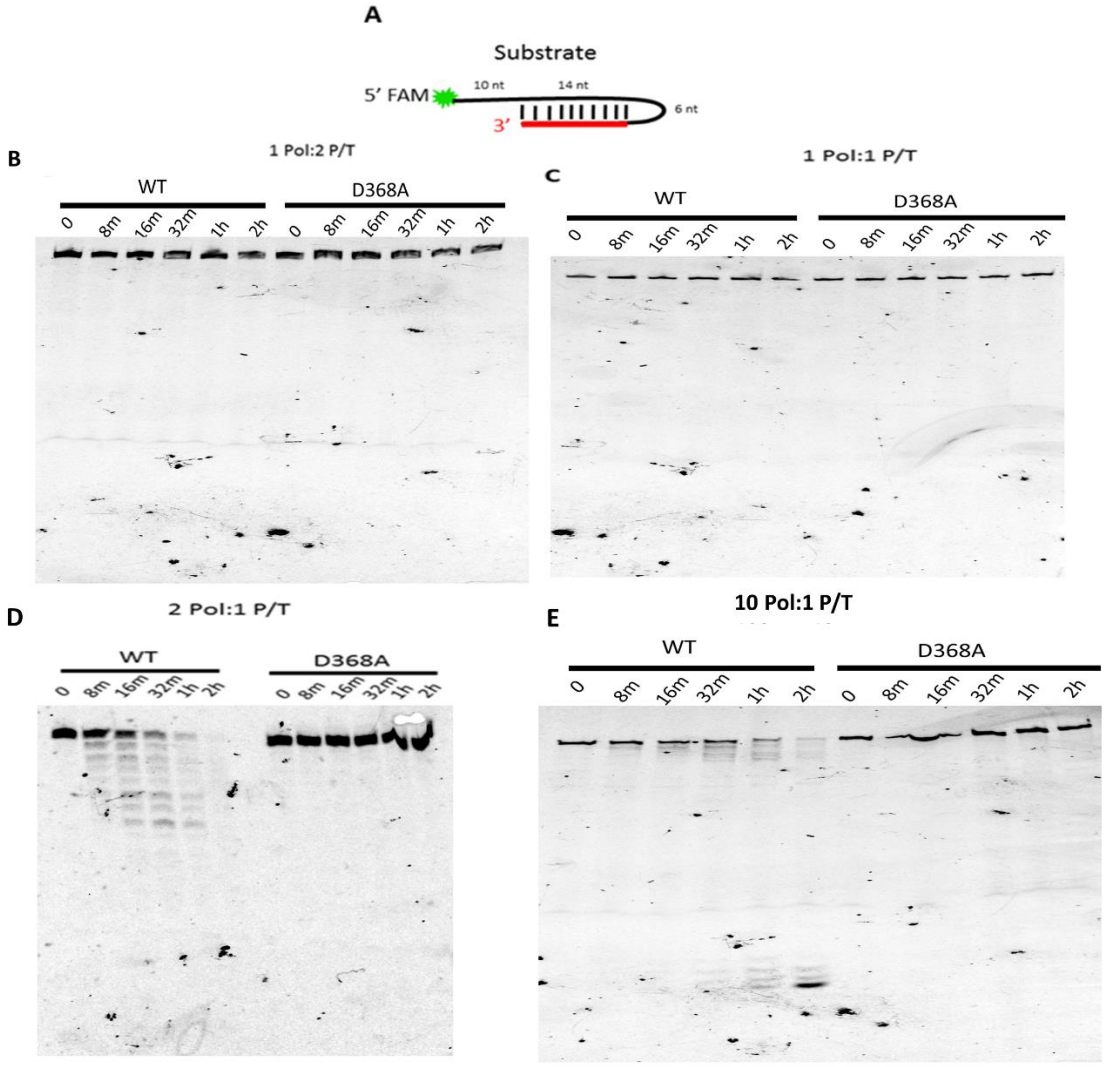

Figure B.4. His-WT and D368A Pol RNase H assays with 3' RNA termini at varying Pol:P/T concentrations. A) Cartoon of the 6-FAM labeled RNA:DNA hairpin primer template (S2; Figure 2.2) used for the RNase H assays. B-E) Fluorescent image of a denaturing polyacrylamide gel loaded with equal amounts of each reaction over increasing time points at a range of different enzyme concentrations (indicated over the gel). The 0 and 32m control reactions (Klenow fragment and RNase H) are shown. Signal present in all lanes below the starting substrate band corresponds to background fluorescence from bromophenol blue in the loading dye that was later removed.

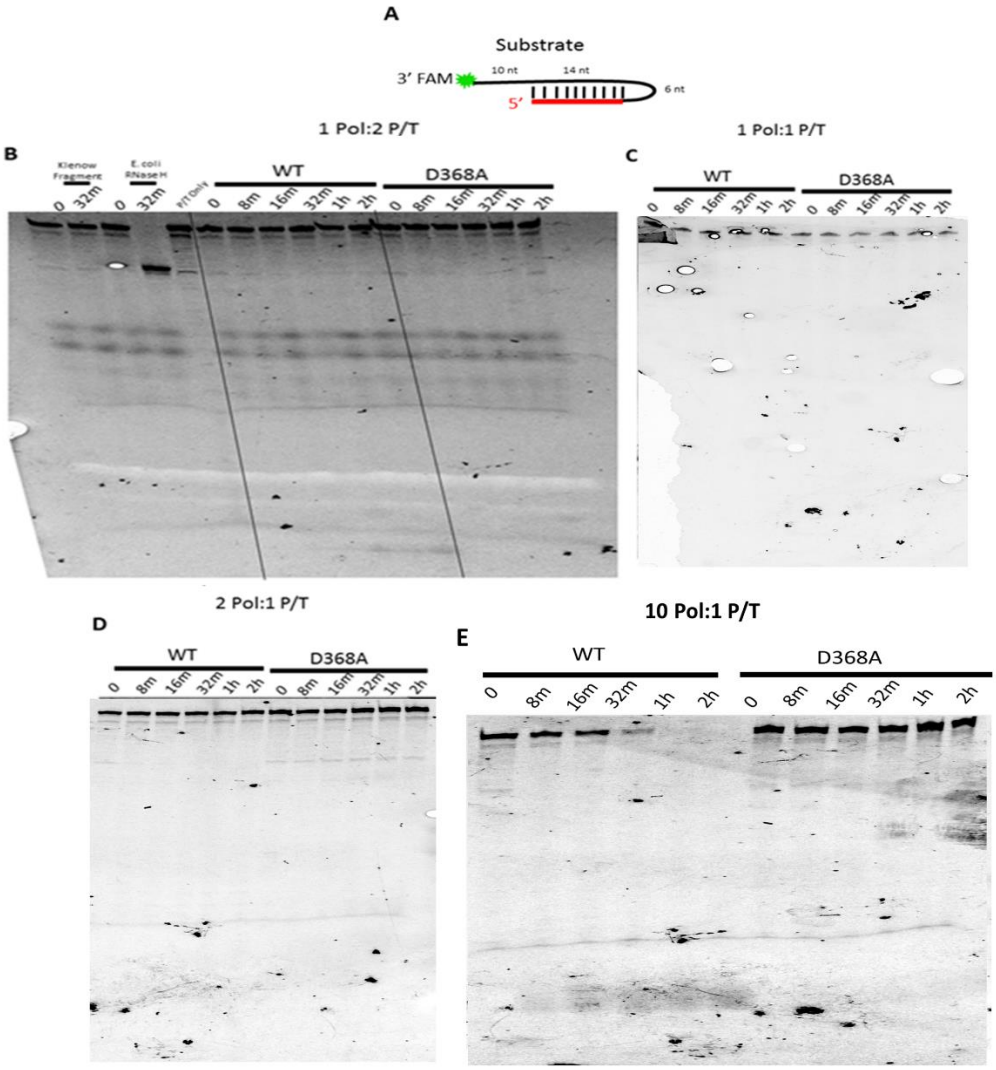

Figure B.5. His-WT and D368A Pol RNase H assays with 5' RNA termini at varying Pol:P/T concentrations. A) Cartoon of the 6-FAM labeled RNA:DNA hairpin primer template (S3; Figure 2.2) used for the RNase H assays. B-E) Fluorescent image of a denaturing polyacrylamide gel loaded with equal amounts of each reaction over increasing time points at a range of different enzyme concentrations (indicated over the gel). The 0 and 32m control reactions (Klenow fragment and RNase H) are shown. Signal present in all lanes below the starting substrate band corresponds to background fluorescence from bromophenol blue in the loading dye that was later removed.

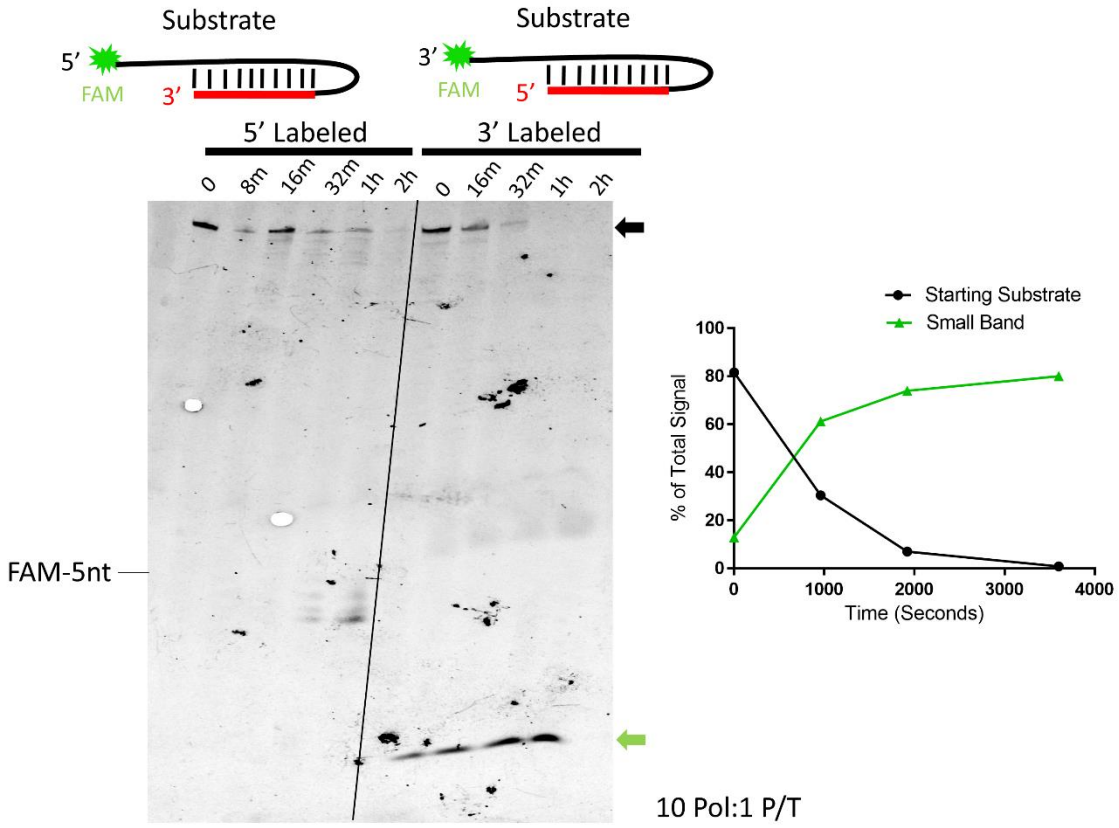

Figure B.6. Size comparison for degradation of RNA:DNA with 3' or 5' RNA ends by WT Pol. Cartoon of the 6-FAM labeled RNA:DNA hairpin primer template (S2 and S3; Figure 2.2) used for the RNase H assays is shown above. Below is the fluorescent image of a denaturing polyacrylamide gel loaded with equal amounts of each reaction over increasing time points at a 10:1 molar excess of enzyme to substrate, with the size of a FAM-TTTTT oligonucleotide shown on the left of the gel. The starting substrate band (black arrow) and the species generated from the reaction on the right (green arrow) were quantified and the disappearance/generation of each species is graphed to the right of the gel.

Pol. These data further argue against a 5'-3' RNase H activity associated with HSV Pol.

Next, we also analyzed the ability of HSV Pol to strand displace past an RNA primer using our protein stocks in a few different assays. These assays made use of a third preparation of WT Pol with a deletion of the N-terminal 42 residues (Δ42) that was generated using the same technique as my own WT Pol stocks. This mutant in our hands has better expression levels but does not affect replication of the virus in cell culture (Terrell & Coen, 2012). Using stocks with both very high and very low concentrations of HSV Pol compared to the concentration of P/T, we first analyzed the ability of WT Pol to complete polymerization past an RNA stretch at the end of the small linear primer/template (Figure B.7). Both WT and D368A Pol were able to displace and polymerize past the RNA primer to the end of the template with a delay at the start of the RNA:DNA portion. Additionally, this activity did not seem to be affected in the presence or absence of the processivity factor, UL42, for the D368A enzyme. However, since this is an annealed template, it's difficult to tell how much of this activity is due to incomplete annealing, melting, or incorrect molar equivalency of the strands. So, for the assays used in Chapter 2, we utilized hairpin templates to more accurately state our results. In a similar assay using an extended template with excess ssDNA past the RNA:DNA stretch, we were also able to detect stand displacement synthesis, though to a lesser degree (Figure B.8). It is unclear why we detected less synthesis to the end of the template, though, and it is possible that this assay had more robust annealing or stalling by polymerase bound to the 3' end of the RNA:DNA.

When we analyzed degradation of labeled RNA annealed to ssDNA, we detected similar results to our assays using the hairpin templates. While the RNA with a free 3' end was degraded and formed a "ladder" on the gel, the RNA with a free 5' end was not degraded by

either WT Pol or the D368A mutant (Figure B.9). So, these results strengthen the results found in Chapter 2.

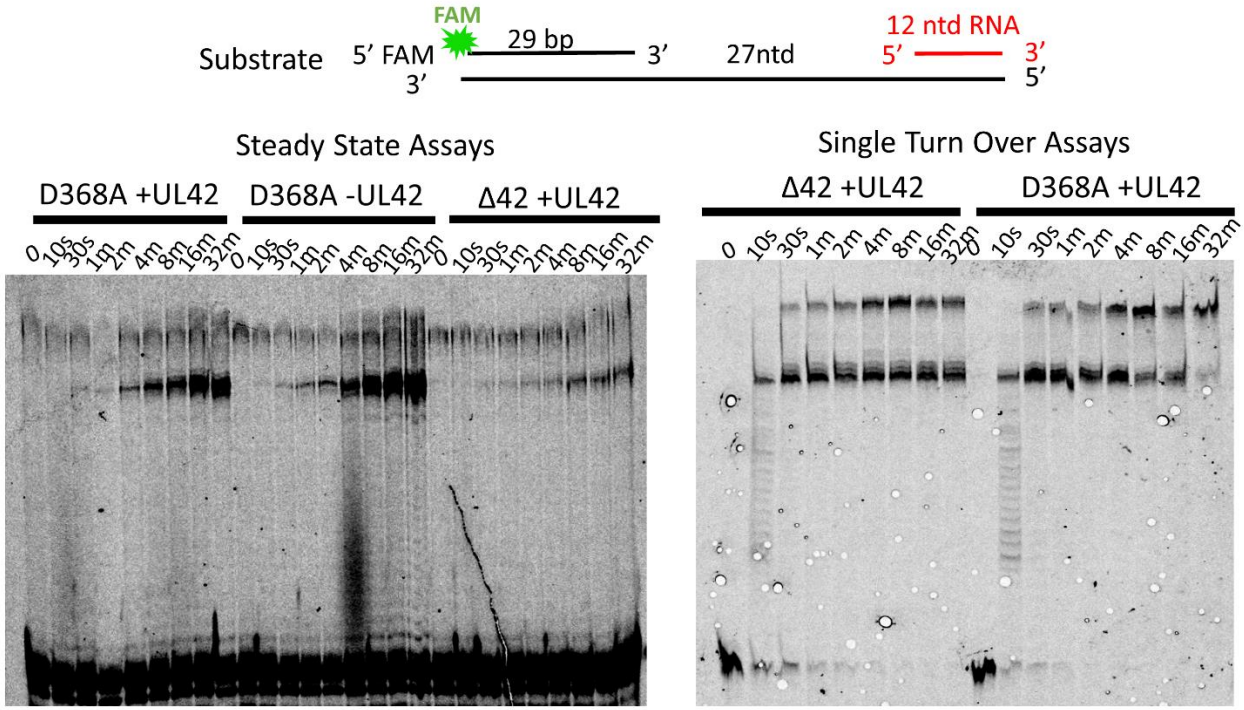

Figure B.7. Analysis of strand displacement synthesis past an RNA primer at the end of a linear template. Above the gel is a cartoon of the primer/template used in this experiment with the lengths of each section of the annealed linear P/T labeled. Below is the fluorescent image of two denaturing polyacrylamide gels loaded with equal amounts of each polymerase reaction over increasing time points at a 1:50 molar deficit of enzyme to P/T (on the left) and a 10:1 molar excess of enzyme to P/T (on the right). The presence or absence of UL42 (the processivity factor) and the enzyme used (WTΔN42 or D368A) are listed above the gel.

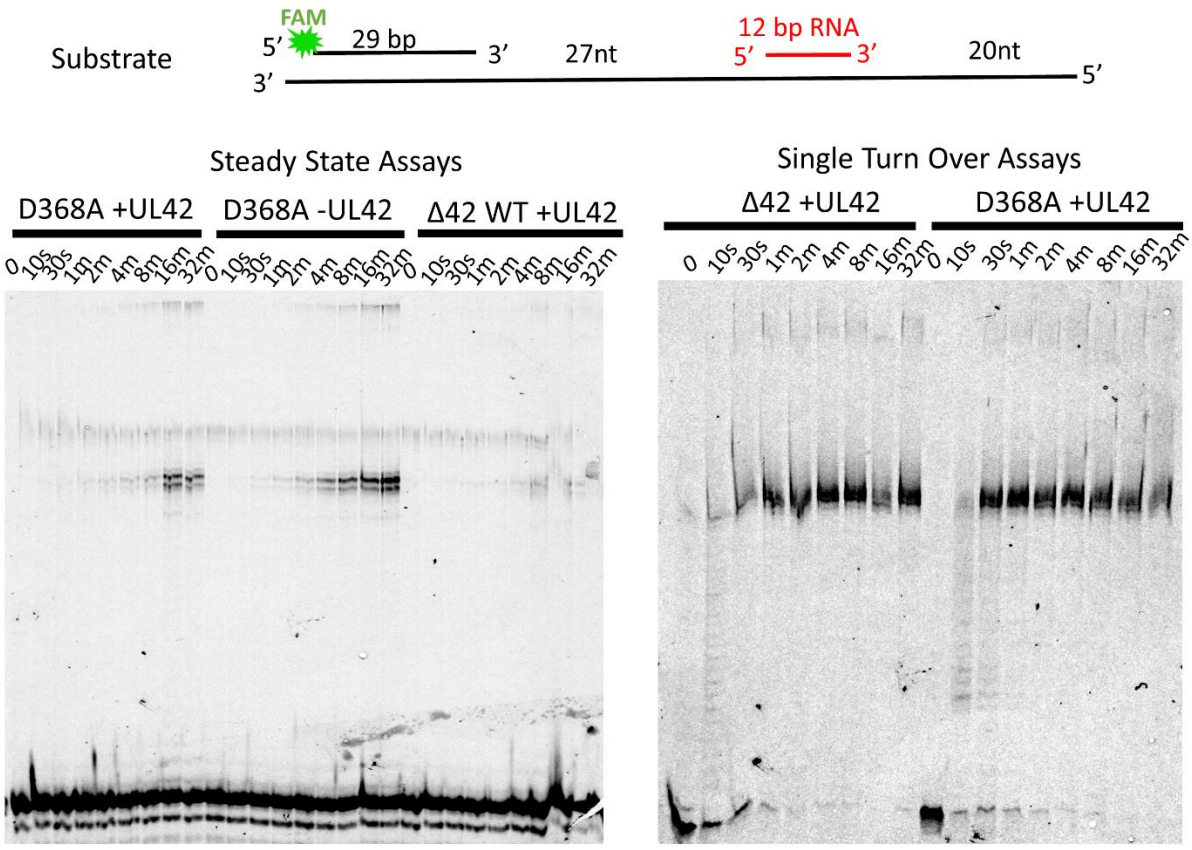

Figure B.8. Analysis of strand displacement synthesis past an RNA primer in the middle of a linear template. Above the gel is a cartoon of the primer/template used in this experiment with the lengths of each section of the annealed linear P/T labeled. Below is the fluorescent image of two denaturing polyacrylamide gels loaded with equal amounts of each polymerase reaction over increasing time points at a 1:50 molar deficit of enzyme to P/T (on the left) and a 10:1 molar excess of enzyme to P/T (on the right). The presence or absence of UL42 (the processivity factor) and the enzyme used (WTΔN42 or D368A) are listed above the gel.

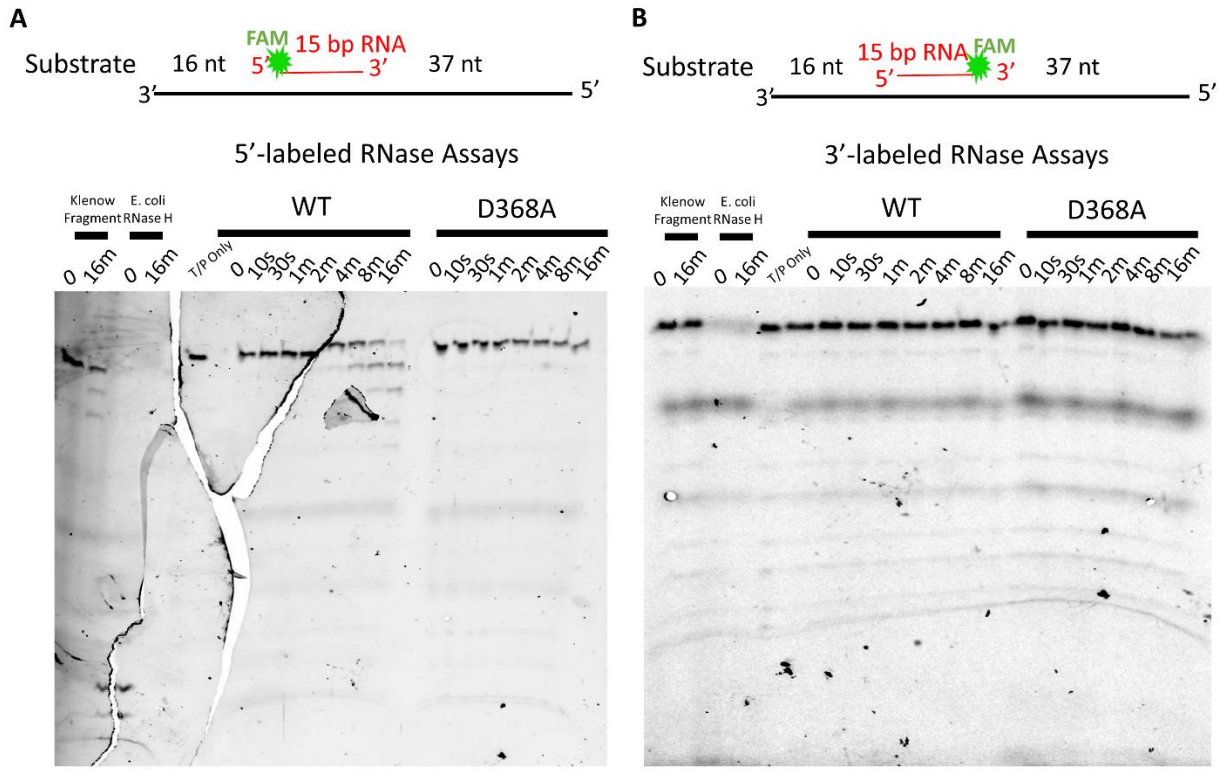

Figure B.9. Analysis of degradation of RNA annealed to a linear DNA oligonucleotide from either the 3' or 5' RNA end. Above the gel is a cartoon of the primer/template used in this experiment with the lengths of each section of the annealed linear P/T labeled. Below is the fluorescent image of two denaturing polyacrylamide gels loaded with equal amounts of each polymerase reaction over increasing time points at a 10:1 molar excess of enzyme to P/T (on the right). The enzyme used (WTΔN42 or D368A) is listed above the gel. Signal present in all lanes below the starting substrate band corresponds to background fluorescence from bromophenol blue in the loading dye that was later removed.

Appendix C

Temperature Sensitive HSV Pol Sequencing

In order to identify the substitutions present within previously generated temperature sensitive mutants of the herpes simplex virus-1 (HSV-1) strain KOS and herpes simplex virus-2 (HSV-2) strain HG52 left from Priscilla Schaffer's viral stocks, we grew the viruses on Vero cells, extracted the viral genomes, and sequenced the *pol* gene. As a positive control, we used the tsD9 mutant, which had been sequenced previously and reported to contain a single amino acid substitution, E597K (Gibbs et al., 1988). The other mutants had been previously mapped to various degrees, but none had been sequenced completely. The substitutions identified based on the sequencing we performed is found in Table C.1, and the location of the residues identified as being substituted in the sequences are shown in black in Figure C.1. Overall, these mutations agree with previous mapping based on regions of marker rescue (Chartrand, Wilkie, & Timbury, 1981; Coen et al., 1984; Schaffer, Aron, Biswal, & Benyesh-Melnick, 1973; Weller, Aschman, Sacks, Coen, & Schaffer, 1983). In particular, the tsC4 G314D but not the R895H substitution falls in the complementation region.

Overall, these substitutions are within the pre-NH_2-terminal domain, NH_2-terminal domain, 3'-5'exonuclease domain, and thumb domain. However, a majority fall within the area between the pre-NH_2-terminal domain and 3'-5' exonuclease or within the NH_2-terminal domain. Because we do not have activities assigned to either of the N-terminal domains, it is difficult to place a reason why these mutations in particular would generate temperature sensitive phenotypes. With further work, hopefully we can characterize these mutants and determine the effect of these substitutions on DNA synthesis and the functions associated with HSV Pol.

Table C.1. Mutations determined to be present within previously identified temperature sensitive mutants of HSV Pol from two HSV strains. The temperature sensitive viruses listed in the table were sequenced to identify mutations within the *pol* gene. The corresponding substitutions that were identified within the protein are listed on the right.

Strain	Temperature Sensitive Mutant	Substitutions Identified
HSV-1 KOS	tsD9	E597K
	tsC4	G314D, R895H
	tsC7	P124S
	284	A328V, S443N
HSV-2 HG52	ts6	L990S

Figure C.1. Location of substitutions identified in temperature sensitive HSV Pol mutants. The HSV Pol structure is colored and labeled by domain as in Figure 1.2. The residues found to be mutated are shown in black A) within the entire protein structure and B) close-up.

Figure C.1 (Continued)

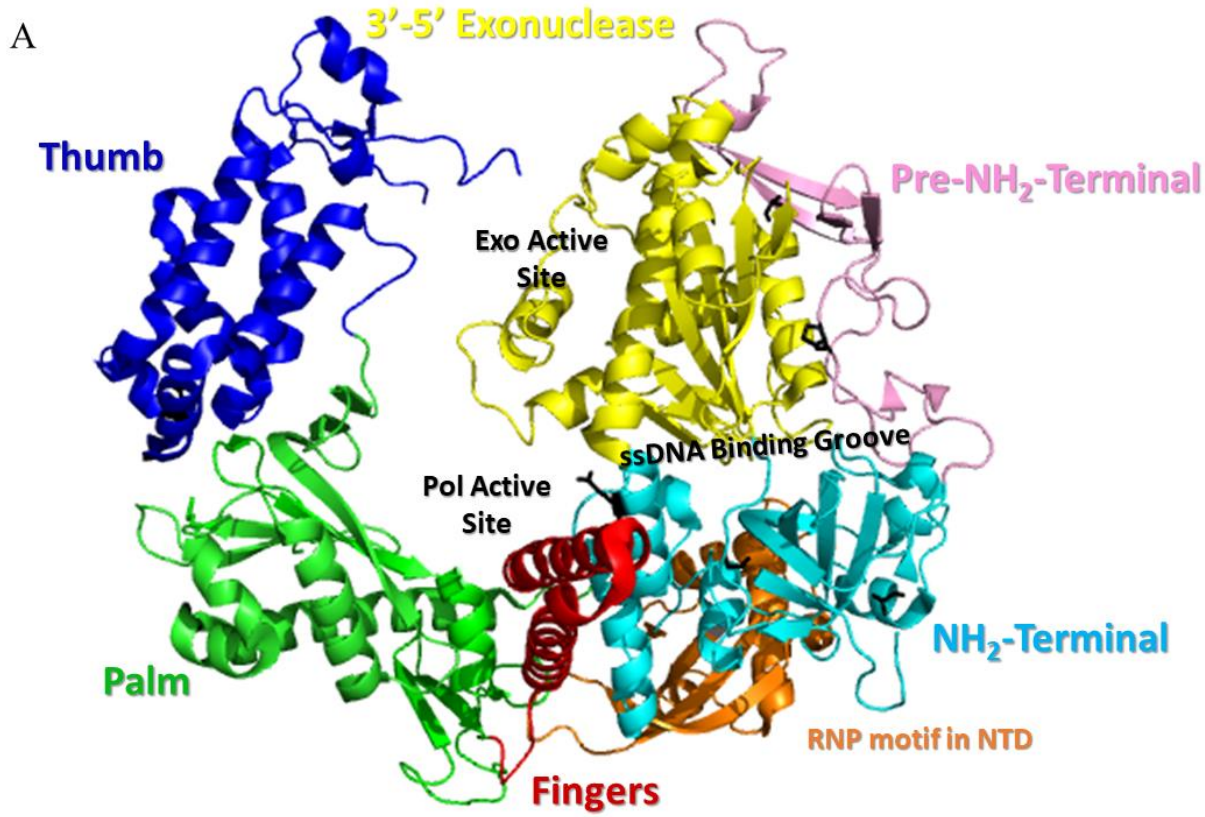

Figure C.1 (Continued)

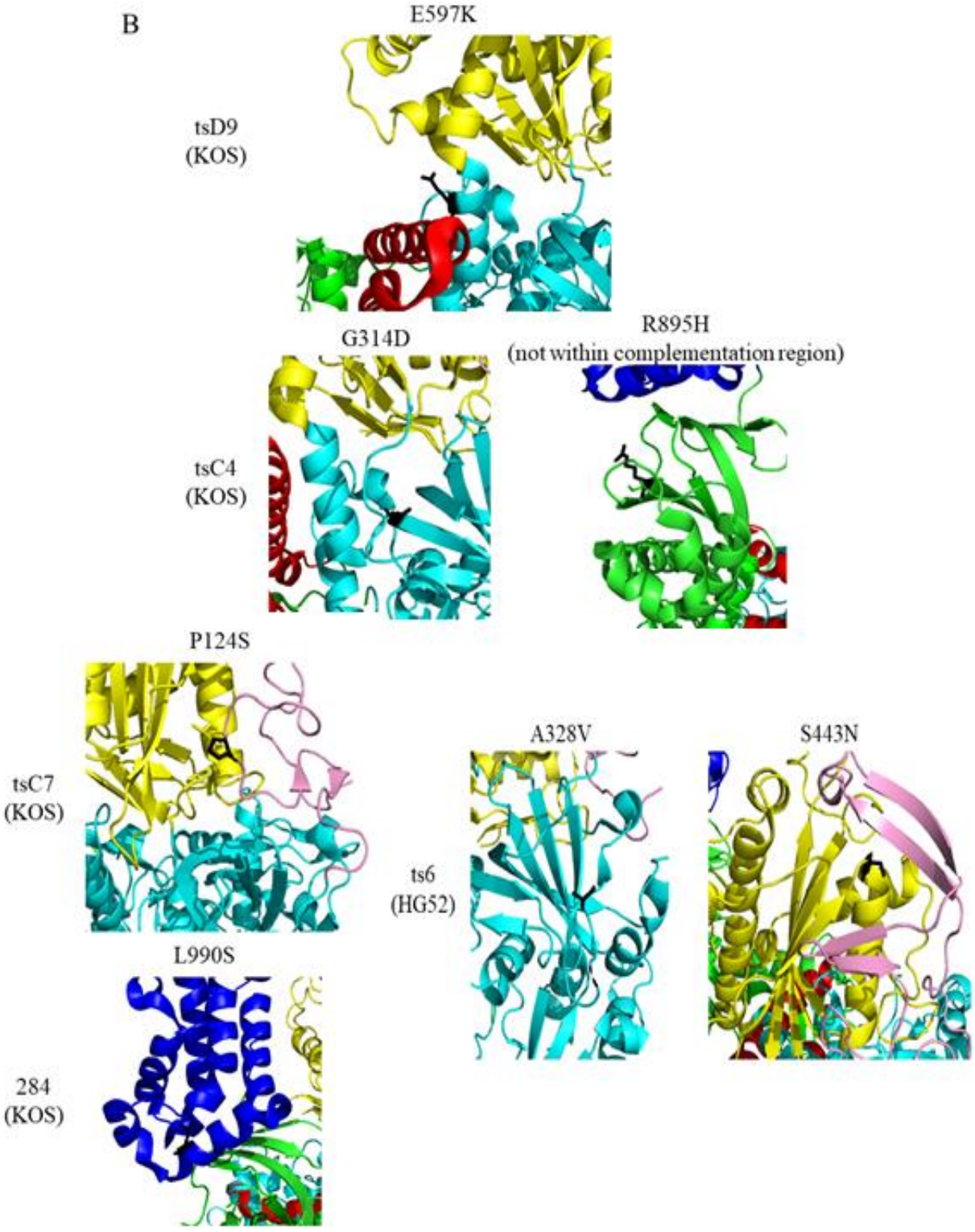

References

Alberts, B. M., Barry, J., Bedinger, P., Formosa, T., Jongeneel, C. V., & Kreuzer, K. N. (1983). Studies on DNA replication in the bacteriophage T4 in vitro system. *Cold Spring Harb Symp Quant Biol, 47 Pt 2*, 655-668.

Aslani, A., Olsson, M., & Elias, P. (2002). ATP-dependent unwinding of a minimal origin of DNA replication by the origin-binding protein and the single-strand DNA-binding protein ICP8 from herpes simplex virus type I. *J Biol Chem, 277*(43), 41204-41212. doi:10.1074/jbc.M208270200

Auer, T., Landre, P. A., & Myers, T. W. (1995). Properties of the 5'-->3' exonuclease/ribonuclease H activity of Thermus thermophilus DNA polymerase. *Biochemistry, 34*(15), 4994-5002.

Averett, D. R., Lubbers, C., Elion, G. B., & Spector, T. (1983). Ribonucleotide reductase induced by herpes simplex type 1 virus. Characterization of a distinct enzyme. *J Biol Chem, 258*(16), 9831-9838.

Ayyagari, R., Gomes, X. V., Gordenin, D. A., & Burgers, P. M. (2003). Okazaki fragment maturation in yeast. I. Distribution of functions between FEN1 AND DNA2. *J Biol Chem, 278*(3), 1618-1625. doi:10.1074/jbc.M209801200

Baker, R. O., & Hall, J. D. (1998). Impaired mismatch extension by a herpes simplex DNA polymerase mutant with an editing nuclease defect. *J Biol Chem, 273*(37), 24075-24082.

Balakrishnan, L., & Bambara, R. A. (2013). Okazaki fragment metabolism. *Cold Spring Harb Perspect Biol, 5*(2), a010173. doi:10.1101/cshperspect.a010173

Balasubramanian, N., Bai, P., Buchek, G., Korza, G., & Weller, S. K. (2010). Physical interaction between the herpes simplex virus type 1 exonuclease, UL12, and the DNA double-strand break-sensing MRN complex. *J Virol, 84*(24), 12504-12514. doi:10.1128/JVI.01506-10

Bandziulis, R. J., Swanson, M. S., & Dreyfuss, G. (1989). RNA-binding proteins as developmental regulators. *Genes Dev, 3*(4), 431-437.

Barnard, E. C., Brown, G., & Stow, N. D. (1997). Deletion mutants of the herpes simplex virus type 1 UL8 protein: effect on DNA synthesis and ability to interact with and influence the

intracellular localization of the UL5 and UL52 proteins. *Virology, 237*(1), 97-106. doi:10.1006/viro.1997.8763

Becker, Y., Asher, Y., Friedmann, A., & Kessler, E. (1978). Circular, circular-linear and branched herpes simplex virus DNA molecules from arginine deprived cells. *J Gen Virol, 41*(3), 629-633. doi:10.1099/0022-1317-41-3-629

Bermek, O., Willcox, S., & Griffith, J. D. (2015). DNA replication catalyzed by herpes simplex virus type 1 proteins reveals trombone loops at the fork. *J Biol Chem, 290*(5), 2539-2545. doi:10.1074/jbc.M114.623009

Bernad, A., Blanco, L., Lazaro, J. M., Martin, G., & Salas, M. (1989). A conserved 3'----5' exonuclease active site in prokaryotic and eukaryotic DNA polymerases. *Cell, 59*, 219-228.

Bhagwat, M., & Nossal, N. G. (2001). Bacteriophage T4 RNase H removes both RNA primers and adjacent DNA from the 5' end of lagging strand fragments. *J Biol Chem, 276*(30), 28516-28524. doi:10.1074/jbc.M103914200

Bigalke, J. M., Heuser, T., Nicastro, D., & Heldwein, E. E. (2014). Membrane deformation and scission by the HSV-1 nuclear egress complex. *Nat Commun, 5*, 4131. doi:10.1038/ncomms5131

Birney, E., Kumar, S., & Krainer, A. R. (1993). Analysis of the RNA-recognition motif and RS and RGG domains: conservation in metazoan pre-mRNA splicing factors. *Nucleic Acids Res, 21*(25), 5803-5816.

Bjornberg, O., Bergman, A. C., Rosengren, A. M., Persson, R., Lehman, I. R., & Nyman, P. O. (1993). dUTPase from herpes simplex virus type 1; purification from infected green monkey kidney (Vero) cells and from an overproducing Escherichia coli strain. *Protein Expr Purif, 4*(2), 149-159. doi:10.1006/prep.1993.1021

Blumel, J., & Matz, B. (1995). Thermosensitive UL9 gene function is required for early stages of herpes simplex virus type 1 DNA synthesis. *J Gen Virol, 76 (Pt 12)*, 3119-3124. doi:10.1099/0022-1317-76-12-3119

Boehmer, P. E., & Lehman, I. R. (1993a). Herpes simplex virus type 1 ICP8: helix-destabilizing properties. *J Virol, 67*(2), 711-715.

Boehmer, P. E., & Lehman, I. R. (1993b). Physical interaction between the herpes simplex virus 1 origin-binding protein and single-stranded DNA-binding protein ICP8. *Proc Natl Acad Sci U S A, 90*(18), 8444-8448.

Boehmer, P. E., & Lehman, I. R. (1997). Herpes simplex virus DNA replication. *Annu Rev Biochem, 66*, 347-384. doi:10.1146/annurev.biochem.66.1.347

Bogani, F., & Boehmer, P. E. (2008). The replicative DNA polymerase of herpes simplex virus 1 exhibits apurinic/apyrimidinic and 5'-deoxyribose phosphate lyase activities. *Proc Natl Acad Sci U S A, 105*(33), 11709-11714. doi:10.1073/pnas.0806375105

Bridges, K. G., Hua, Q., Brigham-Burke, M. R., Martin, J. D., Hensley, P., Dahl, C. E., . . . Coen, D. M. (2000). Secondary structure and structure-activity relationships of peptides corresponding to the subunit interface of herpes simplex virus DNA polymerase. *J Biol Chem, 275*(1), 472-478.

Brown, D. G., Visse, R., Sandhu, G., Davies, A., Rizkallah, P. J., Melitz, C., . . . Sanderson, M. R. (1995). Crystal structures of the thymidine kinase from herpes simplex virus type-1 in complex with deoxythymidine and ganciclovir. *Nat Struct Biol, 2*(10), 876-881.

Bryant, K. F., & Coen, D. M. (2008). Inhibition of translation by a short element in the 5' leader of the herpes simplex virus 1 DNA polymerase transcript. *J Virol, 82*(1), 77-85. doi:10.1128/JVI.01484-07

Caradonna, S. J., & Adamkiewicz, D. M. (1984). Purification and properties of the deoxyuridine triphosphate nucleotidohydrolase enzyme derived from HeLa S3 cells. Comparison to a distinct dUTP nucleotidohydrolase induced in herpes simplex virus-infected HeLa S3 cells. *J Biol Chem, 259*(9), 5459-5464.

Caradonna, S. J., & Cheng, Y. C. (1981). Induction of uracil-DNA glycosylase and dUTP nucleotidohydrolase activity in herpes simplex virus-infected human cells. *J Biol Chem, 256*(19), 9834-9837.

Carrington-Lawrence, S. D., & Weller, S. K. (2003). Recruitment of polymerase to herpes simplex virus type 1 replication foci in cells expressing mutant primase (UL52) proteins. *J Virol, 77*(7), 4237-4247.

Cavanaugh, N. A., & Kuchta, R. D. (2009). Initiation of new DNA strands by the herpes simplex virus-1 primase-helicase complex and either herpes DNA polymerase or human DNA polymerase alpha. *J Biol Chem, 284*(3), 1523-1532. doi:10.1074/jbc.M805476200

Ceska, T. A., & Sayers, J. R. (1998). Structure-specific DNA cleavage by 5' nucleases. *Trends Biochem Sci, 23*(9), 331-336.

Challberg, M. D., & Kelly, T. J. (1982). Eukaryotic DNA replication: viral and plasmid model systems. *Annu Rev Biochem, 51*, 901-934. doi:10.1146/annurev.bi.51.070182.004345

Chartrand, P., Wilkie, N. M., & Timbury, M. C. (1981). Physical mapping of temperature-sensitive mutations of herpes simplex virus type 2 by marker rescue. *J Gen Virol, 52*(Pt 1), 121-133. doi:10.1099/0022-1317-52-1-121

Chattopadhyay, S., & Weller, S. K. (2006). DNA binding activity of the herpes simplex virus type 1 origin binding protein, UL9, can be modulated by sequences in the N terminus: correlation between transdominance and DNA binding. *J Virol, 80*(9), 4491-4500. doi:10.1128/JVI.80.9.4491-4500.2006

Chaudhuri, M., Song, L., & Parris, D. S. (2003). The herpes simplex virus type 1 DNA polymerase processivity factor increases fidelity without altering pre-steady-state rate constants for polymerization or excision. *J Biol Chem, 278*(11), 8996-9004. doi:10.1074/jbc.M210023200

Chelbi-Alix, M. K., & de The, H. (1999). Herpes virus induced proteasome-dependent degradation of the nuclear bodies-associated PML and Sp100 proteins. *Oncogene, 18*(4), 935-941. doi:10.1038/sj.onc.1202366

Chen, H., Beardsley, G. P., & Coen, D. M. (2014). Mechanism of ganciclovir-induced chain termination revealed by resistant viral polymerase mutants with reduced exonuclease activity. *Proc Natl Acad Sci U S A, 111*(49), 17462-17467. doi:10.1073/pnas.1405981111

Chen, M. S., Summers, W. P., Walker, J., Summers, W. C., & Prusoff, W. H. (1979). Characterization of pyrimidine deoxyribonucleoside kinase (thymidine kinase) and thymidylate kinase as a multifunctional enzyme in cells transformed by herpes simplex virus type 1 and in cells infected with mutant strains of herpes simplex virus. *J Virol, 30*(3), 942-945.

Chen, Y., Bai, P., Mackay, S., Korza, G., Carson, J. H., Kuchta, R. D., & Weller, S. K. (2011). Herpes simplex virus type 1 helicase-primase: DNA binding and consequent protein oligomerization and primase activation. *J Virol, 85*(2), 968-978. doi:10.1128/JVI.01690-10

Clark, J. M., Joyce, C. M., & Beardsley, G. P. (1987). Novel blunt-end addition reactions catalyzed by DNA polymerase I of Escherichia coli. *J Mol Biol, 198*(1), 123-127.

Coen, D. M. (2009). Antiherpesviral DNA polymerase inhibitors. In R. L. LaFemina & A. S. f. Microbiology (Eds.), *Antiviral Research: Strategies in Antiviral Drug Discovery* (pp. 1-18): ASM Press.

Coen, D. M., Aschman, D. P., Gelep, P. T., Retondo, M. J., Weller, S. K., & Schaffer, P. A. (1984). Fine mapping and molecular cloning of mutations in the herpes simplex virus DNA polymerase locus. *J Virol, 49*(1), 236-247.

Coen, D. M., & Schaffer, P. A. (2003). Antiherpesvirus drugs: a promising spectrum of new drugs and drug targets. *Nat Rev Drug Discov, 2*(4), 278-288. doi:10.1038/nrd1065

Coloma, J., Johnson, R. E., Prakash, L., Prakash, S., & Aggarwal, A. K. (2016). Human DNA polymerase alpha in binary complex with a DNA:DNA template-primer. *Sci Rep, 6*, 23784. doi:10.1038/srep23784

Crute, J. J., & Lehman, I. R. (1989). Herpes simplex-1 DNA polymerase. Identification of an intrinsic 5'----3' exonuclease with ribonuclease H activity. *J Biol Chem, 264*(32), 19266-19270.

Crute, J. J., & Lehman, I. R. (1991). Herpes simplex virus-1 helicase-primase. Physical and catalytic properties. *J Biol Chem, 266*(7), 4484-4488.

Crute, J. J., Mocarski, E. S., & Lehman, I. R. (1988). A DNA helicase induced by herpes simplex virus type 1. *Nucleic Acids Res, 16*(14A), 6585-6596.

Crute, J. J., Tsurumi, T., Zhu, L. A., Weller, S. K., Olivo, P. D., Challberg, M. D., . . . Lehman, I. R. (1989). Herpes simplex virus 1 helicase-primase: a complex of three herpes-encoded gene products. *Proc Natl Acad Sci U S A, 86*(7), 2186-2189.

Darwish, A. S., Grady, L. M., Bai, P., & Weller, S. K. (2015). ICP8 Filament Formation Is Essential for Replication Compartment Formation during Herpes Simplex Virus Infection. *J Virol, 90*(5), 2561-2570. doi:10.1128/JVI.02854-15

Davison, A. J., & Wilkie, N. M. (1983). Inversion of the two segments of the herpes simplex virus genome in intertypic recombinants. *J Gen Virol, 64 (Pt 1)*, 1-18. doi:10.1099/0022-1317-64-1-1

de Bruyn Kops, A., & Knipe, D. M. (1988). Formation of DNA replication structures in herpes virus-infected cells requires a viral DNA binding protein. *Cell, 55*(5), 857-868.

de Bruyn Kops, A., Uprichard, S. L., Chen, M., & Knipe, D. M. (1998). Comparison of the intranuclear distributions of herpes simplex virus proteins involved in various viral functions. *Virology, 252*(1), 162-178. doi:10.1006/viro.1998.9450

De Clercq, E. (2008). The discovery of antiviral agents: ten different compounds, ten different stories. *Med Res Rev, 28*(6), 929-953. doi:10.1002/med.20128

De Clercq, E., & Holy, A. (2005). Acyclic nucleoside phosphonates: a key class of antiviral drugs. *Nat Rev Drug Discov, 4*(11), 928-940. doi:10.1038/nrd1877

De Lucia, P., & Cairns, J. (1969). Isolation of an E. coli strain with a mutation affecting DNA polymerase. *Nature, 224*(5225), 1164-1166.

Digard, P., Bebrin, W. R., Weisshart, K., & Coen, D. M. (1993). The extreme C terminus of herpes simplex virus DNA polymerase is crucial for functional interaction with processivity factor UL42 and for viral replication. *J Virol, 67*(1), 398-406.

Digard, P., Chow, C. S., Pirrit, L., & Coen, D. M. (1993). Functional analysis of the herpes simplex virus UL42 protein. *J Virol, 67*(3), 1159-1168.

Dorsky, D. I., & Crumpacker, C. S. (1988). Expression of herpes simplex virus type 1 DNA polymerase gene by in vitro translation and effects of gene deletions on activity. *J Virol, 62*, 3224-3232.

Doublie, S., & Zahn, K. E. (2014). Structural insights into eukaryotic DNA replication. *Front Microbiol, 5*, 444. doi:10.3389/fmicb.2014.00444

Dracheva, S., Koonin, E. V., & Crute, J. J. (1995). Identification of the primase active site of the herpes simplex virus type 1 helicase-primase. *J Biol Chem, 270*(23), 14148-14153.

Edgar, R. C. (2004a). MUSCLE: a multiple sequence alignment method with reduced time and space complexity. *BMC Bioinformatics, 5*, 113. doi:10.1186/1471-2105-5-113

Edgar, R. C. (2004b). MUSCLE: multiple sequence alignment with high accuracy and high throughput. *Nucleic Acids Res, 32*(5), 1792-1797. doi:10.1093/nar/gkh340

Elias, P., & Lehman, I. R. (1988). Interaction of origin binding protein with an origin of replication of herpes simplex virus 1. *Proc Natl Acad Sci U S A, 85*(9), 2959-2963.

Everett, R. D. (2006). Interactions between DNA viruses, ND10 and the DNA damage response. *Cell Microbiol, 8*(3), 365-374. doi:10.1111/j.1462-5822.2005.00677.x

Everett, R. D., Freemont, P., Saitoh, H., Dasso, M., Orr, A., Kathoria, M., & Parkinson, J. (1998). The disruption of ND10 during herpes simplex virus infection correlates with the Vmw110- and proteasome-dependent loss of several PML isoforms. *J Virol, 72*(8), 6581-6591.

Everett, R. D., & Murray, J. (2005). ND10 components relocate to sites associated with herpes simplex virus type 1 nucleoprotein complexes during virus infection. *J Virol, 79*(8), 5078-5089. doi:10.1128/JVI.79.8.5078-5089.2005

Falkenberg, M., Bushnell, D. A., Elias, P., & Lehman, I. R. (1997). The UL8 subunit of the heterotrimeric herpes simplex virus type 1 helicase-primase is required for the unwinding of single strand DNA-binding protein (ICP8)-coated DNA substrates. *J Biol Chem, 272*(36), 22766-22770.

Falkenberg, M., Lehman, I. R., & Elias, P. (2000). Leading and lagging strand DNA synthesis in vitro by a reconstituted herpes simplex virus type 1 replisome. *Proc Natl Acad Sci U S A, 97*(8), 3896-3900.

Fanning, E., & Zhao, K. (2009). SV40 DNA replication: from the A gene to a nanomachine. *Virology, 384*(2), 352-359. doi:10.1016/j.virol.2008.11.038

Franklin, M. C., Wang, J., & Steitz, T. A. (2001). Structure of the replicating complex of a pol alpha family DNA polymerase. *Cell, 105*(5), 657-667.

Friedmann, A., Shlomai, J., & Becker, Y. (1977). Electron microscopy of herpes simplex virus DNA molecules isolated from infected cells by centrifugation in CsCl density gradients. *J Gen Virol, 34*(3), 507-522. doi:10.1099/0022-1317-34-3-507

Fuentes, G. M., Rodriguez-Rodriguez, L., Palaniappan, C., Fay, P. J., & Bambara, R. A. (1996). Strand displacement synthesis of the long terminal repeats by HIV reverse transcriptase. *J Biol Chem, 271*(4), 1966-1971.

Fukushima, S., Itaya, M., Kato, H., Ogasawara, N., & Yoshikawa, H. (2007). Reassessment of the in vivo functions of DNA polymerase I and RNase H in bacterial cell growth. *J Bacteriol, 189*(23), 8575-8583. doi:10.1128/JB.00653-07

Garber, D. A., Beverley, S. M., & Coen, D. M. (1993). Demonstration of circularization of herpes simplex virus DNA following infection using pulsed field gel electrophoresis. *Virology, 197*(1), 459-462. doi:10.1006/viro.1993.1612

Gentry, G. A. (1992). Viral thymidine kinases and their relatives. *Pharmacol Ther, 54*(3), 319-355.

Gibbs, J. S., Chiou, H. C., Bastow, K. F., Cheng, Y. C., & Coen, D. M. (1988). Identification of amino acids in herpes simplex virus DNA polymerase involved in substrate and drug recognition. *Proc Natl Acad Sci U S A, 85*(18), 6672-6676.

Gibbs, J. S., Weisshart, K., Digard, P., deBruynKops, A., Knipe, D. M., & Coen, D. M. (1991). Polymerization activity of an alpha-like DNA polymerase requires a conserved 3'-5' exonuclease active site. *Mol Cell Biol, 11*, 4786-4795.

Gilbert, C., Bestman-Smith, J., & Boivin, G. (2002). Resistance of herpesviruses to antiviral drugs: clinical impacts and molecular mechanisms. *Drug Resist Updat, 5*(2), 88-114.

Goldstein, J. N., & Weller, S. K. (1998). In vitro processing of herpes simplex virus type 1 DNA replication intermediates by the viral alkaline nuclease, UL12. *J Virol, 72*(11), 8772-8781.

Gottlieb, J., Marcy, A. I., Coen, D. M., & Challberg, M. D. (1990). The herpes simplex virus type 1 UL42 gene product: a subunit of DNA polymerase that functions to increase processivity. *J Virol, 64*(12), 5976-5987.

Grady, L. M., Szczepaniak, R., Murelli, R. P., Masaoka, T., Le Grice, S. F. J., Wright, D. L., & Weller, S. K. (2017). The exonuclease activity of HSV-1 UL12 is required for the production of viral DNA that can be packaged to produce infectious virus. *J Virol*. doi:10.1128/JVI.01380-17

Grinde, B. (2013). Herpesviruses: latency and reactivation - viral strategies and host response. *J Oral Microbiol, 5*. doi:10.3402/jom.v5i0.22766

Gu, H., & Roizman, B. (2003). The degradation of promyelocytic leukemia and Sp100 proteins by herpes simplex virus 1 is mediated by the ubiquitin-conjugating enzyme UbcH5a. *Proc Natl Acad Sci U S A, 100*(15), 8963-8968. doi:10.1073/pnas.1533420100

Haarr, L., & Skulstad, S. (1994). The herpes simplex virus type 1 particle: structure and molecular functions. Review article. *APMIS, 102*(5), 321-346.

Haffey, M. L., Novotny, J., Bruccoleri, R. E., Carroll, R. D., Stevens, J. T., & Matthews, J. T. (1990). Structure-function studies of the herpes simplex virus type 1 DNA polymerase. *J Virol, 64*, 5008-5018.

Hall, J. D., Orth, K. L., & Claus-Walker, D. (1996). Evidence that the nuclease activities associated with the herpes simplex type 1 DNA polymerase are due to the 3'-5' exonuclease. *J Virol, 70*(7), 4816-4818.

Hall, J. D., Orth, K. L., Sander, K. L., Swihart, B. M., & Senese, R. A. (1995). Mutations within conserved motifs in the 3'-5' exonuclease domain of herpes simplex virus DNA polymerase. *J Gen Virol, 76*, 2999-3008.

Hamatake, R. K., Bifano, M., Hurlburt, W. W., & Tenney, D. J. (1997). A functional interaction of ICP8, the herpes simplex virus single-stranded DNA-binding protein, and the helicase-primase complex that is dependent on the presence of the UL8 subunit. *J Gen Virol, 78 (Pt 4)*, 857-865. doi:10.1099/0022-1317-78-4-857

He, X., & Lehman, I. R. (2001). An initial ATP-independent step in the unwinding of a herpes simplex virus type I origin of replication by a complex of the viral origin-binding protein and single-strand DNA-binding protein. *Proc Natl Acad Sci U S A, 98*(6), 3024-3028. doi:10.1073/pnas.061028298

Heming, J. D., Huffman, J. B., Jones, L. M., & Homa, F. L. (2014). Isolation and characterization of the herpes simplex virus 1 terminase complex. *J Virol, 88*(1), 225-236. doi:10.1128/JVI.02632-13

Henaff, D., Radtke, K., & Lippe, R. (2012). Herpesviruses exploit several host compartments for envelopment. *Traffic, 13*(11), 1443-1449. doi:10.1111/j.1600-0854.2012.01399.x

Hernandez, T. R., & Lehman, I. R. (1990). Functional interaction between the herpes simplex-1 DNA polymerase and UL42 protein. *J Biol Chem, 265*(19), 11227-11232.

Hirsch, I., Cabral, G., Patterson, M., & Biswal, N. (1977). Studies on the intracellular replicating DNA of herpes simplex virus type 1. *Virology, 81*(1), 48-61.

Homa, F. L., & Brown, J. C. (1997). Capsid assembly and DNA packaging in herpes simplex virus. *Rev Med Virol, 7*(2), 107-122.

Hong, X., & Kogoma, T. (1993). Absence of a direct role for RNase HI in initiation of DNA replication at the oriC site on the Escherichia coli chromosome. *J Bacteriol, 175*(20), 6731-6734.

Huang, L., Ishii, K. K., Zuccola, H., Gehring, A. M., Hwang, C. B., Hogle, J., & Coen, D. M. (1999). The enzymological basis for resistance of herpesvirus DNA polymerase mutants to acyclovir: relationship to the structure of alpha-like DNA polymerases. *Proc Natl Acad Sci U S A, 96*(2), 447-452.

Hubscher, U., Maga, G., & Spadari, S. (2002). Eukaryotic DNA polymerases. *Annu Rev Biochem, 71*, 133-163. doi:10.1146/annurev.biochem.71.090501.150041

Hughes, M. B., Yee, A. M., Dawson, M., & Karam, J. (1987). Genetic mapping of the amino-terminal domain of bacteriophage T4 DNA polymerase. *Genetics, 115*(3), 393-403.

Huszar, D., & Bacchetti, S. (1981). Partial purification and characterization of the ribonucleotide reductase induced by herpes simplex virus infection of mammalian cells. *J Virol, 37*(2), 580-588.

Hwang, Y. T., Liu, B. Y., Coen, D. M., & Hwang, C. B. (1997). Effects of mutations in the Exo III motif of the herpes simplex virus DNA polymerase gene on enzyme activities, viral replication, and replication fidelity. *J Virol, 71*(10), 7791-7798.

Hwang, Y. T., Smith, J. F., Gao, L., & Hwang, C. B. (1998). Mutations in the Exo III motif of the herpes simplex virus DNA polymerase gene can confer altered drug sensitivities. *Virology, 246*(2), 298-305. doi:10.1006/viro.1998.9201

Itaya, M., Omori, A., Kanaya, S., Crouch, R. J., Tanaka, T., & Kondo, K. (1999). Isolation of RNase H genes that are essential for growth of Bacillus subtilis 168. *J Bacteriol, 181*(7), 2118-2123.

Iwasaki, H., Ishino, Y., Toh, H., Nakata, A., & Shinagawa, H. (1991). Escherichia coli DNA polymerase II is homologous to alpha-like DNA polymerases. *Mol Gen Genet, 226*(1-2), 24-33.

Jacob, R. J., Morse, L. S., & Roizman, B. (1979). Anatomy of herpes simplex virus DNA. XII. Accumulation of head-to-tail concatemers in nuclei of infected cells and their role in the generation of the four isomeric arrangements of viral DNA. *J Virol, 29*(2), 448-457.

Jacob, R. J., & Roizman, B. (1977). Anatomy of herpes simplex virus DNA VIII. Properties of the replicating DNA. *J Virol, 23*(2), 394-411.

Jain, R., Rajashankar, K. R., Buku, A., Johnson, R. E., Prakash, L., Prakash, S., & Aggarwal, A. K. (2014). Crystal structure of yeast DNA polymerase epsilon catalytic domain. *PLoS One, 9*(4), e94835. doi:10.1371/journal.pone.0094835

Jarvis, T. C., Paul, L. S., Hockensmith, J. W., & von Hippel, P. H. (1989). Structural and enzymatic studies of the T4 DNA replication system. II. ATPase properties of the polymerase accessory protein complex. *J Biol Chem, 264*(21), 12717-12729.

Jiang, C., Hwang, Y. T., Randell, J. C., Coen, D. M., & Hwang, C. B. (2007). Mutations that decrease DNA binding of the processivity factor of the herpes simplex virus DNA polymerase reduce viral yield, alter the kinetics of viral DNA replication, and decrease the fidelity of DNA replication. *J Virol, 81*(7), 3495-3502. doi:10.1128/JVI.02359-06

Jiang, C., Hwang, Y. T., Wang, G., Randell, J. C., Coen, D. M., & Hwang, C. B. (2007). Herpes simplex virus mutants with multiple substitutions affecting DNA binding of UL42 are impaired for viral replication and DNA synthesis. *J Virol, 81*(21), 12077-12079. doi:10.1128/JVI.01133-07

Jiang, Y. C., Feng, H., Lin, Y. C., & Guo, X. R. (2016). New strategies against drug resistance to herpes simplex virus. *Int J Oral Sci, 8*(1), 1-6. doi:10.1038/ijos.2016.3

Jin, Y. H., Ayyagari, R., Resnick, M. A., Gordenin, D. A., & Burgers, P. M. (2003). Okazaki fragment maturation in yeast. II. Cooperation between the polymerase and 3'-5'-exonuclease activities of Pol delta in the creation of a ligatable nick. *J Biol Chem, 278*(3), 1626-1633. doi:10.1074/jbc.M209803200

Jongeneel, C. V., & Bachenheimer, S. L. (1981). Structure of replicating herpes simplex virus DNA. *J Virol, 39*(2), 656-660.

Jozwiakowski, S. K., Keith, B. J., Gilroy, L., Doherty, A. J., & Connolly, B. A. (2014). An archaeal family-B DNA polymerase variant able to replicate past DNA damage: occurrence of replicative and translesion synthesis polymerases within the B family. *Nucleic Acids Res, 42*(15), 9949-9963. doi:10.1093/nar/gku683

Kathera, C., Zhang, J., Janardhan, A., Sun, H., Ali, W., Zhou, X., . . . Guo, Z. (2017). Interacting partners of FEN1 and its role in the development of anticancer therapeutics. *Oncotarget, 8*(16), 27593-27602. doi:10.18632/oncotarget.15176

Kieff, E. D., Bachenheimer, S. L., & Roizman, B. (1971). Size, composition, and structure of the deoxyribonucleic acid of herpes simplex virus subtypes 1 and 2. *J Virol, 8*(2), 125-132.

Klinedinst, D. K., & Challberg, M. D. (1994). Helicase-primase complex of herpes simplex virus type 1: a mutation in the UL52 subunit abolishes primase activity. *J Virol, 68*(6), 3693-3701.

Knopf, C. W., & Weisshart, K. (1988). The herpes simplex virus DNA polymerase: analysis of the functional domains. *Biochim Biophys Acta, 951*, 298-314.

Knopf, C. W., & Weisshart, K. (1990). Comparison of exonucleolytic activities of herpes simplex virus type-1 DNA polymerase and DNase. *Eur J Biochem, 191*(2), 263-273.

Knopf, K. W. (1979). Properties of herpes simplex virus DNA polymerase and characterization of its associated exonuclease activity. *Eur J Biochem, 98*(1), 231-244.

Koc, K. N., Stodola, J. L., Burgers, P. M., & Galletto, R. (2015). Regulation of yeast DNA polymerase delta-mediated strand displacement synthesis by 5'-flaps. *Nucleic Acids Res, 43*(8), 4179-4190. doi:10.1093/nar/gkv260

Komazin-Meredith, G., Mirchev, R., Golan, D. E., van Oijen, A. M., & Coen, D. M. (2008). Hopping of a processivity factor on DNA revealed by single-molecule assays of diffusion. *Proc Natl Acad Sci U S A, 105*(31), 10721-10726. doi:10.1073/pnas.0802676105

Komazin-Meredith, G., Santos, W. L., Filman, D. J., Hogle, J. M., Verdine, G. L., & Coen, D. M. (2008). The positively charged surface of herpes simplex virus UL42 mediates DNA binding. *J Biol Chem, 283*(10), 6154-6161. doi:10.1074/jbc.M708691200

Kong, X. P., Onrust, R., O'Donnell, M., & Kuriyan, J. (1992). Three-dimensional structure of the beta subunit of E. coli DNA polymerase III holoenzyme: a sliding DNA clamp. *Cell, 69*(3), 425-437.

Kornberg, A., & Baker, T. A. (1992). *DNA replication*: Wh Freeman San Francisco.

Krishna, T. S., Kong, X. P., Gary, S., Burgers, P. M., & Kuriyan, J. (1994). Crystal structure of the eukaryotic DNA polymerase processivity factor PCNA. *Cell, 79*(7), 1233-1243.

Kuhn, F. J., & Knopf, C. W. (1996). Herpes simplex virus type 1 DNA polymerase. Mutational analysis of the 3'-5'-exonuclease domain. *J Biol Chem, 271*(46), 29245-29254.

Lamberti, C., & Weller, S. K. (1998). The herpes simplex virus type 1 cleavage/packaging protein, UL32, is involved in efficient localization of capsids to replication compartments. *J Virol, 72*(3), 2463-2473.

Lawler, J. L., Mukherjee, P., & Coen, D. M. (2018). HSV-1 DNA Polymerase RNase H Activity Acts in a 3' -5' Direction and is Dependent on the 3' -5' Exonuclease Active Site. *J Virol, 92*, e01813-01817. doi:10.1128/JVI.01813-17

Lee, C. K., & Knipe, D. M. (1985). An immunoassay for the study of DNA-binding activities of herpes simplex virus protein ICP8. *J Virol, 54*(3), 731-738.

Lehman, I. R., & Kaguni, L. S. (1989). DNA polymerase alpha. *J Biol Chem, 264*(8), 4265-4268.

Li, V., Hogg, M., & Reha-Krantz, L. J. (2010). Identification of a new motif in family B DNA polymerases by mutational analyses of the bacteriophage t4 DNA polymerase. *J Mol Biol, 400*(3), 295-308. doi:10.1016/j.jmb.2010.05.030

Lilley, C. E., Chaurushiya, M. S., & Weitzman, M. D. (2010). Chromatin at the intersection of viral infection and DNA damage. *Biochim Biophys Acta, 1799*(3-4), 319-327. doi:10.1016/j.bbagrm.2009.06.007

Liptak, L. M., Uprichard, S. L., & Knipe, D. M. (1996). Functional order of assembly of herpes simplex virus DNA replication proteins into prereplicative site structures. *J Virol, 70*(3), 1759-1767.

Liu, F., & Zhou, Z. H. (2007). Comparative virion structures of human herpesviruses. In A. Arvin, G. Campadelli-Fiume, E. Mocarski, P. S. Moore, B. Roizman, R. Whitley, & K. Yamanishi (Eds.), *Human Herpesviruses: Biology, Therapy, and Immunoprophylaxis*. Cambridge.

Liu, S., Knafels, J. D., Chang, J. S., Waszak, G. A., Baldwin, E. T., Deibel, M. R., Jr., . . . Seddon, A. P. (2006). Crystal structure of the herpes simplex virus 1 DNA polymerase. *J Biol Chem, 281*(26), 18193-18200. doi:10.1074/jbc.M602414200

Livingston, C. M., DeLuca, N. A., Wilkinson, D. E., & Weller, S. K. (2008). Oligomerization of ICP4 and rearrangement of heat shock proteins may be important for herpes simplex virus type 1 prereplicative site formation. *J Virol, 82*(13), 6324-6336. doi:10.1128/JVI.00455-08

Livingston, C. M., Ifrim, M. F., Cowan, A. E., & Weller, S. K. (2009). Virus-Induced Chaperone-Enriched (VICE) domains function as nuclear protein quality control centers during HSV-1 infection. *PLoS Pathog, 5*(10), e1000619. doi:10.1371/journal.ppat.1000619

Lukonis, C. J., & Weller, S. K. (1996). Characterization of nuclear structures in cells infected with herpes simplex virus type 1 in the absence of viral DNA replication. *J Virol, 70*(3), 1751-1758.

Lukonis, C. J., & Weller, S. K. (1997). Formation of herpes simplex virus type 1 replication compartments by transfection: requirements and localization to nuclear domain 10. *J Virol, 71*(3), 2390-2399.

Lye, M. F., Wilkie, A. R., Filman, D. J., Hogle, J. M., & Coen, D. M. (2017). Getting to and through the inner nuclear membrane during herpesvirus nuclear egress. *Curr Opin Cell Biol, 46*, 9-16. doi:10.1016/j.ceb.2016.12.007

Lyman, M. G., & Enquist, L. W. (2009). Herpesvirus interactions with the host cytoskeleton. *J Virol, 83*(5), 2058-2066. doi:10.1128/JVI.01718-08

Macao, B., Olsson, M., & Elias, P. (2004). Functional properties of the herpes simplex virus type I origin-binding protein are controlled by precise interactions with the activated form of the origin of DNA replication. *J Biol Chem, 279*(28), 29211-29217. doi:10.1074/jbc.M400371200

Maga, G., Villani, G., Tillement, V., Stucki, M., Locatelli, G. A., Frouin, I., . . . Hubscher, U. (2001). Okazaki fragment processing: modulation of the strand displacement activity of DNA polymerase delta by the concerted action of replication protein A, proliferating cell nuclear antigen, and flap endonuclease-1. *Proc Natl Acad Sci U S A, 98*(25), 14298-14303. doi:10.1073/pnas.251193198

Makhov, A. M., Boehmer, P. E., Lehman, I. R., & Griffith, J. D. (1996). The herpes simplex virus type 1 origin-binding protein carries out origin specific DNA unwinding and forms stem-loop structures. *EMBO J, 15*(7), 1742-1750.

Marcy, A. I., Olivo, P. D., Challberg, M. D., & Coen, D. M. (1990). Enzymatic activities of overexpressed herpes simplex virus DNA polymerase purified from recombinant baculovirus-infected insect cells. *Nucleic Acids Res, 18*(5), 1207-1215.

Marcy, A. I., Yager, D. R., & Coen, D. M. (1990). Isolation and characterization of herpes simplex virus mutants containing engineered mutations at the DNA polymerase locus. *J Virol, 64*(5), 2208-2216.

Marsden, H. S., Cross, A. M., Francis, G. J., Patel, A. H., MacEachran, K., Murphy, M., . . . Stow, N. D. (1996). The herpes simplex virus type 1 UL8 protein influences the intracellular localization of the UL52 but not the ICP8 or POL replication proteins in virus-infected cells. *J Gen Virol, 77 (Pt 9)*, 2241-2249. doi:10.1099/0022-1317-77-9-2241

Matsui, E., Abe, J., Yokoyama, H., & Matsui, I. (2004). Aromatic residues located close to the active center are essential for the catalytic reaction of flap endonuclease-1 from hyperthermophilic archaeon Pyrococcus horikoshii. *J Biol Chem, 279*(16), 16687-16696. doi:10.1074/jbc.M313695200

McGeoch, D. J., Dalrymple, M. A., Dolan, A., McNab, D., Perry, L. J., Taylor, P., & Challberg, M. D. (1988). Structures of herpes simplex virus type 1 genes required for replication of virus DNA. *J Virol, 62*(2), 444-453.

McLean, G. W., Abbotts, A. P., Parry, M. E., Marsden, H. S., & Stow, N. D. (1994). The herpes simplex virus type 1 origin-binding protein interacts specifically with the viral UL8 protein. *J Gen Virol, 75 (Pt 10)*, 2699-2706. doi:10.1099/0022-1317-75-10-2699

Meier, E., Harmison, G. G., & Schubert, M. (1987). Homotypic and heterotypic exclusion of vesicular stomatitis virus replication by high levels of recombinant polymerase protein L. *J Virol, 61*(10), 3133-3142.

Mettenleiter, T. C. (2002). Herpesvirus assembly and egress. *J Virol, 76*(4), 1537-1547.

Mocarski Jr, E. S. (2007). Comparative analysis of herpesvirus-common proteins. In A. Arvin, G. Campadelli-Fiume, E. Mocarski, P. S. Moore, B. Roizman, R. Whitley, & K. Yamanishi (Eds.), *Human Herpesviruses: Biology, Therapy, and Immunoprophylaxis*. Cambridge.

Monier, K., Armas, J. C., Etteldorf, S., Ghazal, P., & Sullivan, K. F. (2000). Annexation of the interchromosomal space during viral infection. *Nat Cell Biol, 2*(9), 661-665. doi:10.1038/35023615

O'Donnell, M., Langston, L., & Stillman, B. (2013). Principles and concepts of DNA replication in bacteria, archaea, and eukarya. *Cold Spring Harb Perspect Biol, 5*(7). doi:10.1101/cshperspect.a010108

O'Donnell, M. E., Elias, P., & Lehman, I. R. (1987). Processive replication of single-stranded DNA templates by the herpes simplex virus-induced DNA polymerase. *J Biol Chem, 262*(9), 4252-4259.

Okazaki, R., Okazaki, T., Sakabe, K., Sugimoto, K., & Sugino, A. (1968). Mechanism of DNA chain growth. I. Possible discontinuity and unusual secondary structure of newly synthesized chains. *Proc Natl Acad Sci U S A, 59*(2), 598-605.

Okazaki, T. (2002). [Okazaki furaguments and discontinuous replication]. *Seikagaku, 74*(2), 103-117.

Olsson, M., Tang, K. W., Persson, C., Wilhelmsson, L. M., Billeter, M., & Elias, P. (2009). Stepwise evolution of the herpes simplex virus origin binding protein and origin of replication. *J Biol Chem, 284*(24), 16246-16255. doi:10.1074/jbc.M807551200

Pandey, M., Syed, S., Donmez, I., Patel, G., Ha, T., & Patel, S. S. (2009). Coordinating DNA replication by means of priming loop and differential synthesis rate. *Nature, 462*(7275), 940-943. doi:10.1038/nature08611

Pavlov, A. R., & Karam, J. D. (1994). Binding specificity of T4 DNA polymerase to RNA. *J Biol Chem, 269*(17), 12968-12972.

Pellett, P. E., & Roizman, B. (2013). Herpesviridae. In D. M. Knipe & P. M. Howley (Eds.), *Fields virology* (6th ed., pp. 1802-1822). Philadelphia: Wolters Kluwer Health/Lippincott Williams & Wilkins.

Perera, R. L., Torella, R., Klinge, S., Kilkenny, M. L., Maman, J. D., & Pellegrini, L. (2013). Mechanism for priming DNA synthesis by yeast DNA polymerase alpha. *Elife, 2*, e00482. doi:10.7554/eLife.00482

Petrov, V. M., Ng, S. S., & Karam, J. D. (2002). Protein determinants of RNA binding by DNA polymerase of the T4-related bacteriophage RB69. *J Biol Chem, 277*(36), 33041-33048. doi:10.1074/jbc.M204754200

Piret, J., & Boivin, G. (2011). Resistance of herpes simplex viruses to nucleoside analogues: mechanisms, prevalence, and management. *Antimicrob Agents Chemother, 55*(2), 459-472. doi:10.1128/AAC.00615-10

Placek, B. J., & Berger, S. L. (2010). Chromatin dynamics during herpes simplex virus-1 lytic infection. *Biochim Biophys Acta, 1799*(3-4), 223-227. doi:10.1016/j.bbagrm.2010.01.012

Poffenberger, K. L., & Roizman, B. (1985). A noninverting genome of a viable herpes simplex virus 1: presence of head-to-tail linkages in packaged genomes and requirements for circularization after infection. *J Virol, 53*(2), 587-595.

Ponce de Leon, M., Eisenberg, R. J., & Cohen, G. H. (1977). Ribonucleotide reductase from herpes simplex virus (types 1 and 2) infected and uninfected KB cells: properties of the partially purified enzymes. *J Gen Virol, 36*(1), 163-173. doi:10.1099/0022-1317-36-1-163

Powell, K. L., & Purifoy, D. J. (1977). Nonstructural proteins of herpes simplex virus. I. Purification of the induced DNA polymerase. *J Virol, 24*(2), 618-626.

Prindle, M. J., Schmitt, M. W., Parmeggiani, F., & Loeb, L. A. (2013). A substitution in the fingers domain of DNA polymerase delta reduces fidelity by altering nucleotide discrimination in the catalytic site. *J Biol Chem, 288*(8), 5572-5580. doi:10.1074/jbc.M112.436410

Purifoy, D. J., Lewis, R. B., & Powell, K. L. (1977). Identification of the herpes simplex virus DNA polymerase gene. *Nature, 269*(5629), 621-623.

Quinlan, M. P., Chen, L. B., & Knipe, D. M. (1984). The intranuclear location of a herpes simplex virus DNA-binding protein is determined by the status of viral DNA replication. *Cell, 36*(4), 857-868.

Rabkin, S. D., & Hanlon, B. (1990). Herpes simplex virus DNA synthesis at a preformed replication fork in vitro. *J Virol, 64*(10), 4957-4967.

Randell, J. C., & Coen, D. M. (2004). The herpes simplex virus processivity factor, UL42, binds DNA as a monomer. *J Mol Biol, 335*(2), 409-413.

Randell, J. C., Komazin, G., Jiang, C., Hwang, C. B., & Coen, D. M. (2005). Effects of substitutions of arginine residues on the basic surface of herpes simplex virus UL42 support a role for DNA binding in processive DNA synthesis. *J Virol, 79*(18), 12025-12034. doi:10.1128/JVI.79.18.12025-12034.2005

Reha-Krantz, L. (1994). In K. J. D., D. J. W., K. K. N., M. G., H. D. W., E. F. A., B. L. W., S. E. K., K. E., C. K., & M. E. S. (Eds.), *Molecular biology of bacteriophage T4* (pp. 307-312). Washington D.C.: American Society for Microbiology.

Rivas, H. G., Schmaling, S. K., & Gaglia, M. M. (2016). Shutoff of Host Gene Expression in Influenza A Virus and Herpesviruses: Similar Mechanisms and Common Themes. *Viruses, 8*(4), 102. doi:10.3390/v8040102

Rodriguez, A. C., Park, H. W., Mao, C., & Beese, L. S. (2000). Crystal structure of a pol alpha family DNA polymerase from the hyperthermophilic archaeon Thermococcus sp. 9 degrees N-7. *J Mol Biol, 299*(2), 447-462. doi:10.1006/jmbi.2000.3728

Roizman, B., Knipe, D. M., & Whitley, R. (2013). Herpes Simplex Viruses. In D. M. Knipe & P. M. Howley (Eds.), *Fields virology* (pp. 1824-1897). Philadelphia: Wolters Kluwer Health/Lippincott Williams & Wilkins.

Ruyechan, W. T., & Weir, A. C. (1984). Interaction with nucleic acids and stimulation of the viral DNA polymerase by the herpes simplex virus type 1 major DNA-binding protein. *J Virol, 52*(3), 727-733.

Sakabe, K., & Okazaki, R. (1966). A unique property of the replicating region of chromosomal DNA. *Biochim Biophys Acta, 129*(3), 651-654.

Salmon, B., & Baines, J. D. (1998). Herpes simplex virus DNA cleavage and packaging: association of multiple forms of U(L)15-encoded proteins with B capsids requires at least the U(L)6, U(L)17, and U(L)28 genes. *J Virol, 72*(4), 3045-3050.

Schaffer, P. A., Aron, G. M., Biswal, N., & Benyesh-Melnick, M. (1973). Temperature-sensitive mutants of herpes simplex virus type 1: isolation, complementation and partial characterization. *Virology, 52*(1), 57-71.

Schmid, M., Speiseder, T., Dobner, T., & Gonzalez, R. A. (2014). DNA virus replication compartments. *J Virol, 88*(3), 1404-1420. doi:10.1128/JVI.02046-13

Schumacher, A. J., Mohni, K. N., Kan, Y., Hendrickson, E. A., Stark, J. M., & Weller, S. K. (2012). The HSV-1 exonuclease, UL12, stimulates recombination by a single strand annealing mechanism. *PLoS Pathog, 8*(8), e1002862. doi:10.1371/journal.ppat.1002862

Severini, A., Scraba, D. G., & Tyrrell, D. L. (1996). Branched structures in the intracellular DNA of herpes simplex virus type 1. *J Virol, 70*(5), 3169-3175.

Shamoo, Y., Krueger, U., Rice, L. M., Williams, K. R., & Steitz, T. A. (1997). Crystal structure of the two RNA binding domains of human hnRNP A1 at 1.75 A resolution. *Nat Struct Biol, 4*(3), 215-222.

Shamoo, Y., & Steitz, T. A. (1999). Building a replisome from interacting pieces: sliding clamp complexed to a peptide from DNA polymerase and a polymerase editing complex. *Cell, 99*(2), 155-166.

Sherman, G., Gottlieb, J., & Challberg, M. D. (1992). The UL8 subunit of the herpes simplex virus helicase-primase complex is required for efficient primer utilization. *J Virol, 66*(8), 4884-4892.

Shlomai, J., Friedmann, A., & Becker, Y. (1976). Replication intermediates of herpes simplex virus DNA. *Virology, 69*(2), 647-659.

Simpson-Holley, M., Colgrove, R. C., Nalepa, G., Harper, J. W., & Knipe, D. M. (2005). Identification and functional evaluation of cellular and viral factors involved in the alteration of nuclear architecture during herpes simplex virus 1 infection. *J Virol, 79*(20), 12840-12851. doi:10.1128/JVI.79.20.12840-12851.2005

Skaliter, R., & Lehman, I. R. (1994). Rolling circle DNA replication in vitro by a complex of herpes simplex virus type 1-encoded enzymes. *Proc Natl Acad Sci U S A, 91*(22), 10665-10669.

Skaliter, R., Makhov, A. M., Griffith, J. D., & Lehman, I. R. (1996). Rolling circle DNA replication by extracts of herpes simplex virus type 1-infected human cells. *J Virol, 70*(2), 1132-1136.

Song, L., Chaudhuri, M., Knopf, C. W., & Parris, D. S. (2004). Contribution of the 3'- to 5'-exonuclease activity of herpes simplex virus type 1 DNA polymerase to the fidelity of DNA synthesis. *J Biol Chem, 279*(18), 18535-18543. doi:10.1074/jbc.M309848200

Spaete, R. R., & Frenkel, N. (1982). The herpes simplex virus amplicon: a new eucaryotic defective-virus cloning-amplifying vector. *Cell, 30*(1), 295-304.

Spicer, E. K., Rush, J., Fung, C., Reha-Krantz, L. J., Karam, J. D., & Konigsberg, W. H. (1988). Primary structure of T4 DNA polymerase. Evolutionary relatedness to eucaryotic and other procaryotic DNA polymerases. *J Biol Chem, 263*(16), 7478-7486.

Steitz, T. A. (1999). DNA polymerases: structural diversity and common mechanisms. *J Biol Chem, 274*(25), 17395-17398.

Stengel, G., & Kuchta, R. D. (2011). Coordinated leading and lagging strand DNA synthesis by using the herpes simplex virus 1 replication complex and minicircle DNA templates. *J Virol, 85*(2), 957-967. doi:10.1128/JVI.01688-10

Stow, N. D. (1982). Localization of an origin of DNA replication within the TRS/IRS repeated region of the herpes simplex virus type 1 genome. *EMBO J, 1*(7), 863-867.

Stow, N. D., McMonagle, E. C., & Davison, A. J. (1983). Fragments from both termini of the herpes simplex virus type 1 genome contain signals required for the encapsidation of viral DNA. *Nucleic Acids Res, 11*(23), 8205-8220.

Strang, B. L., & Stow, N. D. (2005). Circularization of the herpes simplex virus type 1 genome upon lytic infection. *J Virol, 79*(19), 12487-12494. doi:10.1128/JVI.79.19.12487-12494.2005

Strick, R., Hansen, J., Bracht, R., Komitowski, D., & Knopf, C. W. (1997). Epitope mapping and functional characterization of monoclonal antibodies specific for herpes simplex virus type I DNA polymerase. *Intervirology, 40*(1), 41-49.

Swan, M. K., Johnson, R. E., Prakash, L., Prakash, S., & Aggarwal, A. K. (2009). Structural basis of high-fidelity DNA synthesis by yeast DNA polymerase delta. *Nat Struct Mol Biol, 16*(9), 979-986. doi:10.1038/nsmb.1663

Tadokoro, T., & Kanaya, S. (2009). Ribonuclease H: molecular diversities, substrate binding domains, and catalytic mechanism of the prokaryotic enzymes. *FEBS J, 276*(6), 1482-1493. doi:10.1111/j.1742-4658.2009.06907.x

Tanguy Le Gac, N., Villani, G., Hoffmann, J. S., & Boehmer, P. E. (1996). The UL8 subunit of the herpes simplex virus type-1 DNA helicase-primase optimizes utilization of DNA templates covered by the homologous single-strand DNA-binding protein ICP8. *J Biol Chem, 271*(35), 21645-21651.

Tavalai, N., & Stamminger, T. (2009). Interplay between Herpesvirus Infection and Host Defense by PML Nuclear Bodies. *Viruses, 1*(3), 1240-1264. doi:10.3390/v1031240

Taylor, T. J., McNamee, E. E., Day, C., & Knipe, D. M. (2003). Herpes simplex virus replication compartments can form by coalescence of smaller compartments. *Virology, 309*(2), 232-247.

Tenney, D. J., Hurlburt, W. W., Micheletti, P. A., Bifano, M., & Hamatake, R. K. (1994). The UL8 component of the herpes simplex virus helicase-primase complex stimulates primer synthesis by a subassembly of the UL5 and UL52 components. *J Biol Chem, 269*(7), 5030-5035.

Tenney, D. J., Sheaffer, A. K., Hurlburt, W. W., Bifano, M., & Hamatake, R. K. (1995). Sequence-dependent primer synthesis by the herpes simplex virus helicase-primase complex. *J Biol Chem, 270*(16), 9129-9136.

Terrell, S. L., & Coen, D. M. (2012). The pre-NH(2)-terminal domain of the herpes simplex virus 1 DNA polymerase catalytic subunit is required for efficient viral replication. *J Virol, 86*, 11057-11065. doi:10.1128/JVI.01034-12

Terrell, S. L., Pesola, J. M., & Coen, D. M. (2014). Roles of conserved residues within the pre-NH2-terminal domain of herpes simplex virus 1 DNA polymerase in replication and latency in mice. *J Gen Virol, 95*(Pt 4), 940-947. doi:10.1099/vir.0.061903-0

Tischer, B. K., Smith, G. A., & Osterrieder, N. (2010). En passant mutagenesis: a two step markerless red recombination system. *Methods Mol Biol, 634*, 421-430. doi:10.1007/978-1-60761-652-8_30

Tischer, B. K., von Einem, J., Kaufer, B., & Osterrieder, N. (2006). Two-step red-mediated recombination for versatile high-efficiency markerless DNA manipulation in Escherichia coli. *Biotechniques, 40*, 191-197.

Tuerk, C., Eddy, S., Parma, D., & Gold, L. (1990). Autogenous translational operator recognized by bacteriophage T4 DNA polymerase. *J Mol Biol, 213*(4), 749-761. doi:10.1016/S0022-2836(05)80261-X

Villani, G., Tanguy Le Gac, N., Wasungu, L., Burnouf, D., Fuchs, R. P., & Boehmer, P. E. (2002). Effect of manganese on in vitro replication of damaged DNA catalyzed by the herpes simplex virus type-1 DNA polymerase. *Nucleic Acids Res, 30*(15), 3323-3332.

Villarreal, E. C. (2003). Current and potential therapies for the treatment of herpes-virus infections. *Prog Drug Res, 60*, 263-307.

Wadsworth, S., Hayward, G. S., & Roizman, B. (1976). Anatomy of herpes simplex virus DNA. V. Terminally repetitive sequences. *J Virol, 17*(2), 503-512.

Wald, A., & Corey, L. (2007). Persistence in the population: epidemiology, transmission. In A. Arvin, G. Campadelli-Fiume, E. Mocarski, P. S. Moore, B. Roizman, R. Whitley, & K. Yamanishi (Eds.), *Human Herpesviruses: Biology, Therapy, and Immunoprophylaxis*. Cambridge.

Wang, C. C., Pavlov, A., & Karam, J. D. (1997). Evolution of RNA-binding specificity in T4 DNA polymerase. *J Biol Chem, 272*(28), 17703-17710.

Wang, J., Sattar, A. K., Wang, C. C., Karam, J. D., Konigsberg, W. H., & Steitz, T. A. (1997). Crystal structure of a pol alpha family replication DNA polymerase from bacteriophage RB69. *Cell, 89*(7), 1087-1099.

Wang, J., Yu, P., Lin, T. C., Konigsberg, W. H., & Steitz, T. A. (1996). Crystal structures of an NH2-terminal fragment of T4 DNA polymerase and its complexes with single-stranded DNA and with divalent metal ions. *Biochemistry, 35*(25), 8110-8119. doi:10.1021/bi960178r

Wang, M., Xia, S., Blaha, G., Steitz, T. A., Konigsberg, W. H., & Wang, J. (2011). Insights into base selectivity from the 1.8 A resolution structure of an RB69 DNA polymerase ternary complex. *Biochemistry, 50*(4), 581-590. doi:10.1021/bi101192f

Wang, T. S., Wong, S. W., & Korn, D. (1989). Human DNA polymerase alpha: predicted functional domains and relationships with viral DNA polymerases. *FASEB J, 3*, 14-21.

Weissbach, A., Hong, S. C., Aucker, J., & Muller, R. (1973). Characterization of herpes simplex virus-induced deoxyribonucleic acid polymerase. *J Biol Chem, 248*(18), 6270-6277.

Weisshart, K., Kuo, A. A., Hwang, C. B., Kumura, K., & Coen, D. M. (1994). Structural and functional organization of herpes simplex virus DNA polymerase investigated by limited proteolysis. *J Biol Chem, 269*, 22788-22796.

Weitzman, M. D., & Weller, S. K. (2011). Interactions between HSV-1 and the DNA damage response. In S. K. Weller (Ed.), *Alphaherpesviruses: Molecular Virology* (pp. 89-112): Caister Academic Press.

Weller, S. K. (2010). Herpes simplex virus reorganizes the cellular DNA repair and protein quality control machinery. *PLoS Pathog, 6*(11), e1001105. doi:10.1371/journal.ppat.1001105

Weller, S. K., Aschman, D. P., Sacks, W. R., Coen, D. M., & Schaffer, P. A. (1983). Genetic analysis of temperature-sensitive mutants of HSV-1: the combined use of complementation and physical mapping for cistron assignment. *Virology, 130*(2), 290-305.

Weller, S. K., & Coen, D. M. (2006). Herpes Simplex Virus. In M. L. DePamphilis (Ed.), *DNA Replication and Human Disease* (pp. 663-686): Cold Spring Harbor Laboratory Press.

Weller, S. K., & Coen, D. M. (2012). Herpes simplex viruses: mechanisms of DNA replication. *Cold Spring Harb Perspect Biol, 4*(9), a013011. doi:10.1101/cshperspect.a013011

Weller, S. K., & Kuchta, R. D. (2013). The DNA helicase-primase complex as a target for herpes viral infection. *Expert Opin Ther Targets, 17*(10), 1119-1132. doi:10.1517/14728222.2013.827663

Weller, S. K., Spadaro, A., Schaffer, J. E., Murray, A. W., Maxam, A. M., & Schaffer, P. A. (1985). Cloning, sequencing, and functional analysis of oriL, a herpes simplex virus type 1 origin of DNA synthesis. *Mol Cell Biol, 5*(5), 930-942.

Whitley, R., Kimberlin, D. W., & Prober, C. G. (2007). Pathogenesis and disease. In A. Arvin, G. Campadelli-Fiume, E. Mocarski, P. S. Moore, B. Roizman, R. Whitley, & K. Yamanishi (Eds.), *Human Herpesviruses: Biology, Therapy, and Immunoprophylaxis*. Cambridge.

Wilkins, M. R., Gasteiger, E., Bairoch, A., Sanchez, J. C., Williams, K. L., Appel, R. D., & Hochstrasser, D. F. (1999). Protein identification and analysis tools in the ExPASy server. *Methods Mol Biol, 112*, 531-552.

Wilkinson, D. E., & Weller, S. K. (2003). The role of DNA recombination in herpes simplex virus DNA replication. *IUBMB Life, 55*(8), 451-458. doi:10.1080/15216540310001612237

Williams, M. V. (1984). Deoxyuridine triphosphate nucleotidohydrolase induced by herpes simplex virus type 1. Purification and characterization of induced enzyme. *J Biol Chem, 259*(16), 10080-10084.

Wobbe, K. K., Digard, P., Staknis, D., & Coen, D. M. (1993). Unusual regulation of expression of the herpes simplex virus DNA polymerase gene. *J Virol, 67*(9), 5419-5425.

Wu, C. A., Nelson, N. J., McGeoch, D. J., & Challberg, M. D. (1988). Identification of herpes simplex virus type 1 genes required for origin-dependent DNA synthesis. *J Virol, 62*(2), 435-443.

Xia, S., & Konigsberg, W. H. (2014). RB69 DNA polymerase structure, kinetics, and fidelity. *Biochemistry, 53*(17), 2752-2767. doi:10.1021/bi4014215

Xiaofei, E., & Kowalik, T. F. (2014). The DNA damage response induced by infection with human cytomegalovirus and other viruses. *Viruses, 6*(5), 2155-2185. doi:10.3390/v6052155

Yager, D. R., & Coen, D. M. (1988). Analysis of the transcript of the herpes simplex virus DNA polymerase gene provides evidence that polymerase expression is inefficient at the level of translation. *J Virol, 62*(6), 2007-2015.

Yager, D. R., Marcy, A. I., & Coen, D. M. (1990). Translational regulation of herpes simplex virus DNA polymerase. *J Virol, 64*(5), 2217-2225.

Zhao, Y., Jeruzalmi, D., Moarefi, I., Leighton, L., Lasken, R., & Kuriyan, J. (1999). Crystal structure of an archaebacterial DNA polymerase. *Structure, 7*(10), 1189-1199.

Zheng, L., & Shen, B. (2011). Okazaki fragment maturation: nucleases take centre stage. *J Mol Cell Biol, 3*(1), 23-30. doi:10.1093/jmcb/mjq048

Zhu, L. A., & Weller, S. K. (1992a). The six conserved helicase motifs of the UL5 gene product, a component of the herpes simplex virus type 1 helicase-primase, are essential for its function. *J Virol, 66*(1), 469-479.

Zhu, L. A., & Weller, S. K. (1992b). The UL5 gene of herpes simplex virus type 1: isolation of a lacZ insertion mutant and association of the UL5 gene product with other members of the helicase-primase complex. *J Virol, 66*(1), 458-468.

Zhu, Y., Stroud, J., Song, L., & Parris, D. S. (2010). Kinetic approaches to understanding the mechanisms of fidelity of the herpes simplex virus type 1 DNA polymerase. *J Nucleic Acids, 2010*, 631595. doi:10.4061/2010/631595

Zhu, Y., Trego, K. S., Song, L., & Parris, D. S. (2003). 3' to 5' exonuclease activity of herpes simplex virus type 1 DNA polymerase modulates its strand displacement activity. *J Virol, 77*(18), 10147-10153.

Zhu, Y., Wu, Z., Cardoso, M. C., & Parris, D. S. (2010). Processing of lagging-strand intermediates in vitro by herpes simplex virus type 1 DNA polymerase. *J Virol, 84*, 7459-7472. doi:10.1128/JVI.01875-09

Zuccola, H. J., Filman, D. J., Coen, D. M., & Hogle, J. M. (2000). The crystal structure of an unusual processivity factor, herpes simplex virus UL42, bound to the C terminus of its cognate polymerase. *Mol Cell, 5*(2), 267-278.